# Copernicus Atmosphere Monitoring Service - Regional Air Quality Production System v1.0

Augustin Colette[1], Gaëlle Collin[2], François Besson[2], Etienne Blot[2], Vincent Guidard[2,14], Frédérik Meleux[1], Adrien Royer[2], Valentin Petiot[2,14], Claire Miller[2], Oihana Fermond[2], Alizé Jeant[2], Mario Adani[5,16], Joaquim Arteta[14], Anna Benedictow[10], Robert Bergström[11], Dene Bowdalo[8], Jorgen Brandt[4], Gino Briganti[5], Ana. C. Carvalho[11], Jesper Heile Christensen[4], Florian Couvidat[1], Ilaria D'Elia[5], Massimo D'Isidoro[5], Hugo Denier van der Gon[12], Gaël Descombes[1], Enza Di Tomaso[3, 8], John Douros[13], Jeronimo Escribano[8], Henk Eskes[13], Hilde Fagerli[10], Yalda Fatahi[9], Johannes Flemming[3], Elmar Friese[6], Lise Frohn[4], Michael Gauss[10], Camilla. Geels[4], Guido Guarnieri[5], Marc Guevara[8], Antoine Guion[1], Jonathan Guth[14], Risto Hänninen[9], Kaj Hansen[4], Ulas Im[4], Ruud Janssen[12], Marine Jeoffrion[2], Mathieu Joly[14], Luke Jones[3], Oriol Jorba[8], Evgeni Kadantsev[9], Michael Kahnert[11], Jacek W. Kaminski[7], Rostislav Kouznetsov[9], Richard Kranenburg[12], Jeroen Kuenen[12], Anne Caroline Lange[6], Joachim Langner[11], Victor Lannuque[1], Francesca Macchia[8], Astrid Manders[12], Mihaela Mircea[5], Agnes Nyiri[10], Miriam Olid[8], Carlos Pérez García-Pando[8,15], Julia Palamarchuk[9], Antonio Piersanti[5], Blandine Raux[1], Miha Razinger[3], Lennard Robertson[11], Arjo Segers[12], Martijn Schaap[12], Pilvi Siljamo[9], David Simpson[10], Mikhail Sofiev[9], Anders Stangel[9], Joanna Struzewska[7], Carles Tena[8], Renske Timmermans[12], Thanos Tsikerdekis[13], Svetlana Tsyro[10], Svyatoslav Tyuryakov[9], Anthony Ung[1], Andreas Uppstu[9], Alvaro Valdebenito[10], Peter van Velthoven[13], Lina Vitali[5], Zhuyun Ye[4], Vincent-Henri Peuch[3], Laurence Rouïl[1, ^a]

[1]INERIS: Institut National de l'Environnement Industriel et des Risques, Verneuil en Halatte, 60550, France

[2]Météo-France, Saint-Mandé, 94165, France

[3]ECMWF: European Centre for Medium-Range Weather Forecasts, Reading, RG2 9AX, United Kingdom

[4]Aarhus University: Roskilde, 4000, Denmark

[5]ENEA: Italian National Agency for New Technologies, Energy and Sustainable Economic Development, Bologna, 40129, Italy

[6] Forschungszentrum Jülich GmbH, ICE-3, Institute of Climate and Energy Systems - Troposphere, 52428 Jülich, Germany

[7] IEP-NRI: Institute of Environmental Protection - National Research Institute, Warsaw, 00-001, Poland

[8]BSC: Barcelona Supercomputing Center, Barcelona, 08034, Spain

[9]FMI, Finnish Meteorological Institute, Helsinki, 00-001, Finland

[10]MET Norway: Norwegian Meteorological Institute, Oslo, 0372, Norway

[11]SMHI: Swedish Meteorological and Hydrological Institute. Norrköping, SE-601 76, Sweden

[12]TNO: Netherlands Organisation for applied scientific research, Utrecht, 3584, The Netherlands

[13] KNMI: Royal Netherlands Meteorological Institute, De Bilt, 3730, The Netherlands

[14]: Centre National de Recherches Météorologiques - UMR 3589 CNRS/Météo-France, Toulouse, 31000, France

[15]. Catalan Institution for Research and Advanced Studies (ICREA), 08010, Barcelona, Spain

[16] Centro Euro-Mediterraneo sui Cambiamenti Climatici, 40127 Bologna, Italy

^a: now at: ECMWF: European Centre for Medium-Range Weather Forecasts, Reading, RG2 9AX, United Kingdom

*Correspondence to*: Augustin Colette (augustin.colette@ineris.fr)

**Abstract**

The Copernicus Atmosphere Monitoring Service (CAMS) delivers a wide range of ~~full,~~ free and open products in relation to atmospheric composition at global and regional scales. The CAMS Regional Service produces daily forecasts, analyses, and reanalyses of air quality in Europe. This Service relies on a distributed modelling production by eleven teams in ten European countries: CHIMERE (France), DEHM (Denmark), EMEP (Norway), EURAD-IM (Germany), GEM-AQ (Poland), LOTOS-EUROS (The Netherlands), MATCH (Sweden), MINNI (Italy), MOCAGE (France), MONARCH (Spain), and SILAM (Finland). The project management and coordination of the service is devoted to a Centralised Regional Production Unit. Each model produces every day 24h analyses for the previous day and 97h forecasts for 19 chemical species over a spatial domain at 0.1x0.1~~.~~ degree resolution (approximately 10km x 10km) with 420 points in latitude and 700 in longitude and 10 vertical levels. Six pollen species are also delivered for the surface forecasts. The eleven individual models are then combined into an ENSEMBLE median. In total, more than 82 billion data points are made available for public use on a daily basis.

The design of the system follows clear technical requirements in terms of consistency in the model setup and forcing fields (meteorology, surface anthropogenic emission fluxes, and chemical boundary conditions). But it also benefits from a diversity ~~of~~ in the description of atmospheric processes through the design of the eleven European Chemistry Transport Model~~s~~ (CTM) involved.

The present article aims to provide a comprehensive technical documentation, both for the setup as well as for the diversity of CTMs involved in the Service. We also include an overview of the main output products, their public dissemination and the related evaluation and quality control strategy.

## 1 Introduction

The Copernicus Atmosphere Monitoring Service (CAMS, atmosphere.copernicus.eu/) is the core global and regional atmospheric environmental service operated by the European Centre for Medium-Range Weather Forecast (ECMWF) within the European Union Copernicus Earth Observation Programme. It provides a wide range of ~~full,~~ free, open, and quality assured products in relation to global and regional air quality, inventory-based emissions, observation-based surface fluxes of greenhouse gases and from biomass burning, solar energy, ozone and UV radiation, and climate forcings (Peuch et al., 2022).

We focus here on the regional production service (https://atmosphere.copernicus.eu/european-air-quality-forecast-plots/) which provides daily 4-day forecasts of the main air quality species and analyses of the day before, as well as posterior re-analyses using the latest observation datasets available for assimilation. It constitutes today the reference air quality forecasting system at European scale by building upon a distributed production of eleven chemistry transport models operated in ten European countries, with a Centralised Regional Production Unit to ensure a consistent implementation. Such a comprehensive air quality forecasting system operated at continental scale has no equivalent in the world.

Air quality monitoring and forecasting constitute an essential activity to improve the knowledge of atmospheric composition and air pollution patterns and identify short and long-term mitigation strategies. In the European legislation, the Directive (Ec, 2008) on ambient air quality and cleaner air for Europe of the European Parliament and of the European Council, defines limit and target values for regulatory ambient air concentrations and improvement of ambient air quality to avoid, prevent or reduce harmful effects on human health and the environment. To this end, it sets out the methodological requirements for the assessment of ambient air quality in Member States which are based on the implementation of adequate monitoring systems, typically relying on reference and standardised instruments operated at air quality monitoring stations whose data are reported to the Air Quality e-reporting database maintained by the European Environment Agency (which subsequently makes the data publicly available). A revision of the Ambient Air Quality Directive was adopted by the European Council in October 2024, the revision includes amongst other features, a stronger emphasis on the use of air quality models as well as an explicit reference to the Copernicus Atmosphere Monitoring Service as a trusted source of information products and supplementary tools to support reporting activities in relation to forecasting and management of air pollution episodes.

Modelling comes as a complementary information on ambient air quality. Fitness for forecasting purposes of air quality modelling has been widely documented (Zhang et al., 2012a, b), but air quality models are also essential to produce exposure maps through data assimilation or data fusion. In such processes, the prior modelled estimates of surface air concentrations of the main air pollutants are combined with in situ or remote sensing observations to produce improved mapping of air pollution, typically for use in health impact assessment or epidemiological studies (Shaddick et al., 2020). Air quality modelling and reanalyses are also typically used to anticipate ex-ante and assess ex-post the effectiveness of policy mitigation strategies. The

projections and hindcasts performed in the framework of the Convention on Long Range Transboundary Air Pollution (CLRTAP) of the United Nations Economic Commission for Europe Geneva Air Convention and its Gothenburg Protocol constitute a good example of atmospheric modelling activities in support of policy decisions at European scale (Maas and Grennfelt 2016).

Whereas several European countries or selected metropolitan areas operate their own air quality modelling system, there is also a need to produce air quality forecasts and analyses over the whole European continent: to provide background data for those local systems (chemical boundary conditions), for the areas not covered by any national system, or just as complementary information. The Copernicus Atmosphere Monitoring Service has played that role since 2015. It builds upon the earlier research and development phases initiated since 2005 through European collaborative research and innovation projects: GEMS (Hollingsworth, 2008) and MACC, MACC-II, and MACC-III (Marécal et al., 2015; Peuch et al., 2014).

The unique setup of the system allows it to reach an unprecedented level of quality and robustness by relying on a set of stringent common requirements combined with a large variety of Chemistry-Transport Models (CTMs). Since 2022, an ensemble of eleven CTMs have been used: CHIMERE (INERIS, France), DEHM (Aarhus Univ., Denmark), EMEP (Met Norway), EURAD-IM (Forschungszentrum Juelich, Germany), GEM-AQ (IEP-NRI, Poland), LOTOS-EUROS (TNO and KNMI, The Netherlands), MATCH (SMHI, Sweden), MINNI (ENEA, Italy), MOCAGE (Météo-France, France), MONARCH (BSC, Spain), and SILAM (FMI, Finland). Using an ensemble of CTMs allows at the same time to minimize the risk of failure in the daily operational production, and to increase the skill of the forecast (Galmarini et al., 2013). But consistency in the implementation is key to ensure the continuous improvement of the system, hence the crucial role of the CAMS Regional Central Production Unit led by Météo-France and INERIS.

Each model delivers every day 24h analyses and 97h forecast for 19 chemical species over a spatial domain at 0.1x0.1 degree resolution (approximately 10km x 10km) with 420 points in latitude and 700 in longitude and 10 vertical levels. Additionally, surface forecasts of six pollen species are delivered. With the 11 individual models and one ENSEMBLE median, it is a total of almost 82 billion data point made available for public use every day.

The results of the CAMS Regional Service are made publicly available as quick looks on the website atmosphere.copernicus.eu/european-air-quality-forecast-plots and the numerical outputs are disseminated on the Copernicus Atmosphere Data Store (ADS): ads.atmosphere.copernicus.eu. The typical use of the forecasts is as background information used by national and local air quality agencies, in addition to their knowledge about specific local air pollution sources. This can be done either qualitatively by the consultation of available online viewers, or by using the numerical data to feed downstream chemistry-transport, gaussian, or machine-learning models. The use of reanalyses is rather for policy applications

(for regulatory reporting obligations or to assess the impact policy interventions through trends analyses) or exposure assessment in health impact studies.

The aim of the present article is to provide a transparent and detailed documentation to serve as a reference for the user of CAMS Regional Air quality Products. It constitutes an update of the previous similar article devoted to the MACC regional forecast system (Marécal et al., 2015), whereas the system was still in research mode at the time and not fully operational. A focus on regional activities within the overall CAMS portfolio was also described in (Peuch et al., 2022). The CAMS Regional production system has evolved continuously over the past. In the present article, we provide a detailed description of the system as it stands in 2024. But since the near real time production of forecast and analysis remains available for public use with a 3-year retention time, and reanalysis data remain available since the beginning of the production, we also provide some information about the major evolutions in the recent past.

The main characteristics of the centralised production system are introduced in Section 2. This section covers the overall production workflow, but also the common features and requirements which apply to the distributed production of individual modelling teams such as the common external forcing data. Since the use of an ensemble of eleven different chemistry transport models is an important specificity of the service, we devote a large part of the paper in Section 3 to summarize the formulation of each model and how they adapt specifically to the requirement of the CAMS Regional Production System. The post-processing as well as some elements regarding the evaluation and quality control or the main uses of the production are presented in Section 4. In the conclusion (Section 5) we refer to the short and long-term development priorities to ensure the performance and sustainability of the system over the long term.

# 2 Centralised Regional Production Unit

## 2.1 Organisation of the production system

The CAMS regional production relies on a quite unique ensemble of 11 individual models whose daily operation is distributed amongst 11 modelling centres in ten European countries. The coordination is handled by the Central Regional Production Unit (CRPU) which is led by Météo-France, with the support of INERIS for model development matters and reanalysis production (Figure 1).

The CRPU defines the design of the regional production system under the auspices of ECMWF. This includes setting the guidance and requirements for the implementation of individual models as well as continuous evolution in order to maintain the system within the state of the art. The CRPU is also in charge of contractual matters and relations with the providers of input data as well as the delivery of model results to the Atmosphere Data Store for public use (Section 4.3).

In earlier MACC phases and the first CAMS regional project, only 7 models were contributing to the distributed operational production: CHIMERE, EMEP, EURAD-IM, LOTOS-EUROS, MATCH, MOCAGE, and SILAM. As of October 2019, DEHM and GEM-AQ joined the operational system. As of June 2022, MINNI and MONARCH joined the production.

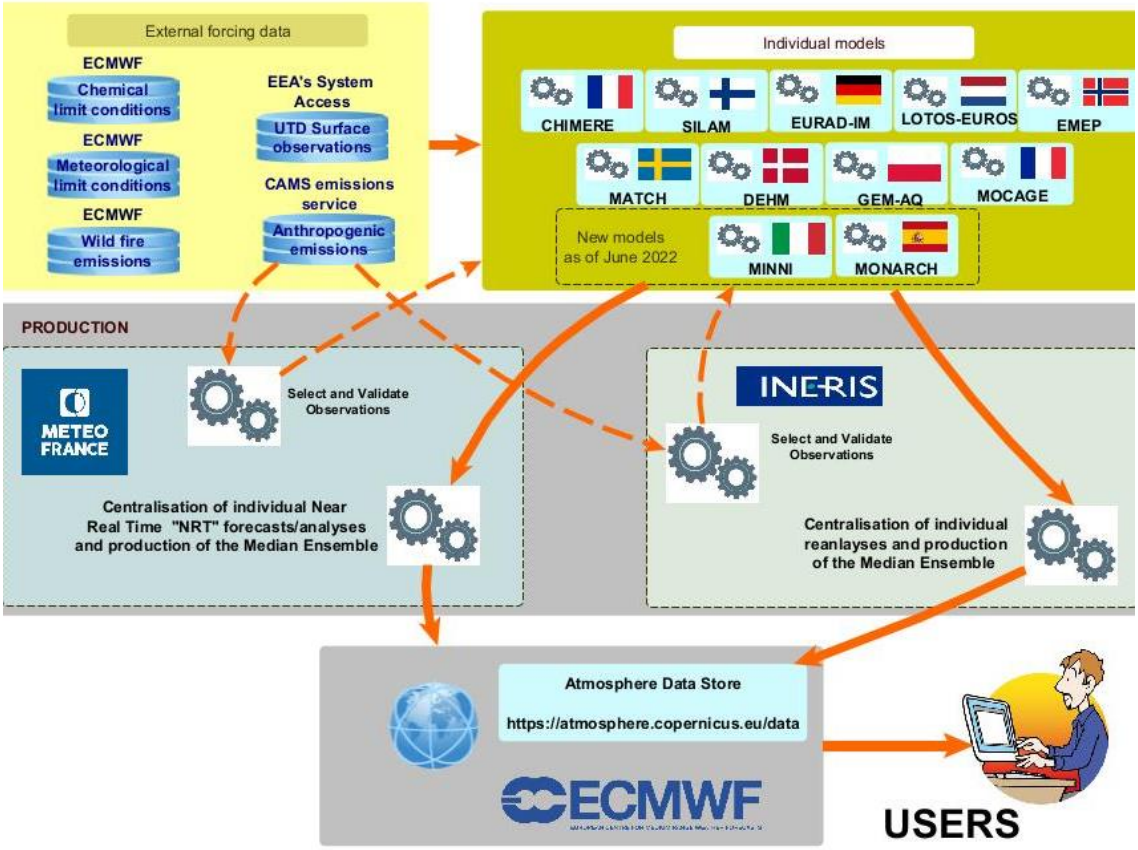


*Figure 1: Schematic of the CAMS Regional Production workflow. Top-left the external forcings (anthropogenic emissions, meteorology, boundary conditions) and in-situ observations for assimilation and evaluation. Top right: eleven regional chemistry-transport model operated in ten European countries. Middle: Meteo-France (for the near real time) and INERIS (for the reanalysis) centralise the individual productions. Bottom: the results are disseminated~~ing~~ to the Atmosphere Data Store.*

## 2.2 Modelling products

The CAMS regional system includes both daily 4-days forecasts and several analysis products. All of them are provided from both eleven individual CTMs results and an ENSEMBLE product which is constituted by the median of individual models at each grid point (See also Section 4 on post-processing).

Hourly near-real time forecasts (NRT/FC) are released every day with a 4 days horizon (from 0 to 96hrs forecasts). They rely on chemistry-transport outputs, some of which are initialised on the basis of the previous analysis (see details in Section 3). The ENSEMBLE NRT/FC fields are made available publicly each day at 08:00 UTC for forecast horizon 0 to 48hrs (day 1

and day 2), and at 10:00 UTC for forecast horizon 49 to 96hrs (day 3 and days 4). All the forecasts are initiated at 00 UTC, the differentiated timing for the 48hr or 96hr lead time is only to account for longer production times.

The list of output species has been expanding gradually over the years. The choice of selected species accounts for user requests, especially with regards to downstream modelling needs (in the case where the CAMS regional system is used as forcing boundary conditions for smaller scale nested models), understanding air pollution episodes, and availability of observation data for evaluation and quality control (which is essentially focusing on $PM_{10}$, $PM_{2.5}$, $NO_2$, $O_3$ and pollens at present, but research grade measurement of the EMEP Monitoring Programme or the ACTRIS European Research Infrastructure are consider to strengthen the quality control procedures).

As of ~~January~~ April 2025~~4~~, the list of species in the NRT/FC includes the following gases: ozone ($O_3$), nitrogen oxide (NO), nitrogen dioxide ($NO_2$), carbon monoxide (CO), sulphur dioxide ($SO_2$), glyoxal (CHOCHO), formaldehyde (HCHO), ammonia ($NH_3$), total Non-Methane Volatile Organic Compounds (NMVOC, defined as the sum of the mass of the carbon atoms of all the VOC species of the chemical scheme of the model, excluding the methane and PANs species, and expressed in unit $\mu g/m^3$ of carbon atoms), and total Peroxy-Acetyl Nitrates (PANs). Particulate matter (PM) are included as : $PM_{2.5}$ (smaller than 2.5µm), $PM_{10}$ (smaller than 10µm). The following tracers in the $PM_{2.5}$ fraction are also provided: sulphate ($SO_4^{2-}$), nitrate ($NO_3^-$), ammonium ($NH_4^+$), total secondary inorganic aerosols (SIA), total elemental carbon (EC), EC fraction related to residential emissions, total organic matter. In the $PM_{10}$ fraction, the tracers include desert dust, sea salt and wildfires. In addition, six pollen species are included: birch, olive, grass, alder, mugwort and ragweed.

Hourly near-real time analysis (NRT/AN) are released each day by 12:00 UTC for the previous day. Here, each individual model is corrected to minimise error with observed air pollutant concentrations over Europe. For the latest reanalysis available on the ADS as of January 2024 (covering the year 2021), the list of species is: for $O_3$, NO, $NO_2$, CO, $NH_3$, NMVOC, $PM_{10}$, $PM_{2.5}$, $PM_{10}$ wildfires, $PM_{10}$ dust, EC total, EC residential, PAN, SIA, $SO_2$. For earlier years, not all of these species are available, and in the future the list will continue expanding to catch up with the full species set in the daily forecast production. Note that observations are ~~not~~ available for assimilation only for $NO_2$, $O_3$, $PM_{10}$, and $PM_{2.5}$. ~~for all of those species, i~~Individual components contributing to the total $PM_{10}$ or $PM_{2.5}$ mass are scaled according to the assimilation of total $PM_{10}$ or $PM_{2.5}$ measurements, and pollen species are not assimilated.

The daily analyses products are supplemented by an interim reanalysis (IRA) and a validated reanalysis (VRA). Both rely on the same modelling tools as the NRT production, including assimilation strategy. But the observations taken into account differ. Acknowledging that for the NRT/AN production some observations can be missing or not validated, daily analyses are reproduced with a 20 days delay in the IRA. This time gap is considered sufficient to fix most failures in NRT data flows and maximise the number of available measurement data. The interim reanalysis is subsequently consolidated and delivered in the

first months of Y+1. Since all observations are only definitively validated by European member states by the end of the following year (Y+1), the full year Y is reprocessed in Y+2 to produce the VRA of the corresponding year. As for NRT, the production of IRA/VRA is also distributed across individual modelling teams which operate their own modelling system. The CRPU (INERIS in the case of reanalyses) defines the common requirements in terms of model setup, input data (meteorology, emissions, and assimilated observations) and centralised the verification and production of the ENSEMBLE product.

### 2.3 Air quality observations

The gathering, filtering and selection of observations is centralised by the CRPU and subsequently disseminated to individual modelling teams which apply different assimilation algorithms even though the exact same stations are assimilated by each model (see details in Section 3). All observation data are obtained from the Air Quality e-reporting database[1] maintained by the European Environment Agency where near real time "up-to-date" (UTD) and validated observations are reported, in particular for countries of the European Union which are expected to do so with respect to the European Directives.

An important step lies in the filtering and selection of data. For the NRT production (both FC and AN), the stations are clustered using ~~where~~ an objective classification which consists in building classes of stations which exhibit similar patterns of ~~is applied based upon the~~ temporal variability ~~patterns of the air pollutant concentrations~~ to differentiate background and proximity stations (Joly and Peuch, 2012). Originally (when the model had a resolution of approximately 20x20km2), only the stations corresponding broadly to suburban and rural typologies were included. But ~~Traffic and industrial sites are excluded from the assimilation strategy, but~~ since November 2020, all stations falling in classes 1-7 of the Joly & Peuch classification are included, which means broadly that urban background sites are taken into account while traffic and industrial sites are excluded~~, whereas earlier than November 2020, only suburban and rural sites were included~~. This way, even if the spatial resolution of the CAMS Regional Production is 10x10km, we ensure the relevance of the modelling setup to capture urban background air quality.

The design and use of this objective classification is particularly useful in NRT applications, which includes more outlying data than the reanalyses. Such NRT applications are also less used for regulatory applications for which reanalyses are preferred. This is why, the station classification in IRA and VRA follows the standard typology declared by the member states in their reporting (even if it is admitted that it is not exempt from misclassification). In VRA and IRA, stations labelled are traffic and industrial are strictly excluded and only background (urban, suburban, and rural) stations are included.

[1] https://www.eea.europa.eu/data-and-maps/data/aqereporting-9, last accessed 30/10/2024

Approximately 2-third of the stations' data are distributed by the CRPU for assimilation (both for NRT/AN and IRA&VRA), while the rest of the data are kept for evaluation (see Section 4.2).

This splitting is first performed using the station list used for VRA and IRA, therefore using only the sites for which member states declared the typology as "background" that are available for the previous years (year-1 for IRA (Y-1) and year-2 for VRA (Y-2)). Stations with less than 1 months of data are removed. The first prerequisite is to treat collocated stations together for the pollutant pairs $NO_2/O_3$ and $PM_{10}/PM_{2.5}$. This prevents, for example, having the same station for $NO_2$ assimilation and $O_3$ evaluation. The second prerequisite is to use a random selection process to ensure a good spatial coverage of stations in the two listings. However, the construction of the assimilation and validation station sets is not entirely random: evaluation stations are always selected near assimilation stations, while spatially isolated stations (typically in remote areas of Europe) are used for assimilation. This classification is revised on an annual basis for each new production cycle of IRA and VRA to take into account the evolution of the network.

The splitting obtained for the VRA and IRA production is subsequently translated for the NRT production. All the stations from classes 1 to 7 belonging to the set of evaluation of VRA/IRA are tagged for NRT evaluation and all the stations that do not belong to the evaluation of VRA/IRA are tagged for NRT assimilation (AN).

At present there is no centralisation of the dissemination of any satellite observation of atmospheric composition even if many individual modelling teams already assimilate satellite data, and this is expected to further develop in the coming years (See details in the presentation of individual models in Section 3).

### 2.4 Modelling domain

The modelling domain covers Europe within 25°W to 45°E longitude and 30°N to 72°N latitude at a 0.1°x0.1° resolution. Whereas in earlier phases of the project some individual models were operating at slightly lower resolution (about 0.2°), today all models operate on a native resolution of about 0.1°. Covering the whole region is a strong requirement, and all models deliver data over the entire domain, which means that some of them perform the forecast on a slightly larger domain in order to include a buffer area or cope with differing geographic projection (see details in Section 3). The spatial extent has evolved marginally in recent years, it was only reaching up to 70°N until June 2019.

The strategy for the vertical discretisation is left open for individual contributing models, but there is a common requirement in the delivery of model results on common vertical levels. As of January 2024, the complete list of vertical levels is: surface, 50m, 100m, 250m, 500m, 750m, 1000m, 2000m, 3000m, and 5000m above ground. This has evolved substantially in recent years, only surface concentrations were provided in the earlier phases of CAMS, and different lists of vertical levels have been archived in the past for near real time forecast, analyses, and reanalysis products.

## 2.5 Meteorology and chemical boundary conditions

The meteorological fields used to force the individual operational CTMs are from the European Centre for Medium-Range Weather Forecasts (ECMWF) operational ~~IFS (Integrated Forecasting System) daily~~ meteorological forecasts at high resolution based on the IFS model (Integrated Forecasting System).~~of the European Centre for Medium-Range Weather Forecasts (ECMWF).~~ The spatial resolution of the IFS forecast has increased in time, it is about 9km as of 2024. The exact list of meteorological parameters used to drive the individual CTMs differs depending on the models (see details in Section 3). Most of them use the forecast starting at 12:00 UTC on D–1 but there might also be some deviations to account for operational constraints.

The chemical boundary conditions are also obtained from ECMWF but using the configuration including chemistry of the IFS: IFS-COMPO referred to as CAMS-Global in this article ~~including chemistry~~ (Flemming et al., 2015; Rémy et al., 2019) operating at approximately 40km spatial resolution. CAMS-Global ~~This configuration of the IFS model~~ runs forecasts twice daily from 00 and 12 UTC and the data are available every hour (for surface fields) and every 3 hours (for above surface model- and pressure-level fields). The model results are made available for further use as boundary conditions of regional models through different dissemination routes including the MARS archive server of ECMWF, a dedicated ftp access for the regional CAMS operational models, and the atmosphere data store (ADS) of Copernicus.

The list of species used as boundary conditions for the regional CAMS models is given in Table 2. Further details are available through the CAMS User Support website[2] and (Morcrette et al., 2009). All aerosol species are provided as dry PM, except for sea salt, whose mass and size is provided at a relative humidity of 80%. The mass of the corresponding dry sea salt is 1/4.3 smaller and the radius is half of the sea salt at relative humidity of 80%.

## 2.6 Surface emissions

### 2.6.1 Anthropogenic emissions

Using identical anthropogenic emissions in all the eleven individual models is essential for the consistency of the CAMS Regional products. The so-called TNO-MACC-III (Kuenen et al., 2014) emission inventory was used for several years in the past. Since June 2019, it has been replaced by the CAMS-REG emissions inventory, which is regularly updated (Kuenen et al., 2022). The CAMS-REG inventory is based on official national totals of air pollutant emissions reported in compliance with the European Directive on National Emission Reduction Commitments (2016/2284/EU) and the Gothenburg Protocol of the LRTAP Convention. Additional processing is applied to ensure consistency in the dataset by making corrections and

[2] https://confluence.ecmwf.int/display/CKB/CAMS%3A+Global+atmospheric+composition+forecast+data+documentation (last accessed 30/10/2024)

performing some gap-filling where information is missing. A consistent spatial distribution for gridded emission datasets is applied at 0.05° × 0.1° resolution. Since June 2021, the CAMS Regional production has used an improved version of the CAMS-REG inventory which substituted national estimates of wood burning emission in order to cope with a well-established inconsistency in the reporting of condensable emissions (Denier Van Der Gon et al., 2015).

The use of officially reported emissions induces a subsequent delay in the successive updates of the emission datasets. The Emissions for year Y, are reported in March Y+2. Then they undergo verification, gap filling and spatialisation before being considered for implementation in the CAMS Regional production. The emissions being used for the day-to-day forecasts are thus generally based on national emissions reported about 3 years earlier. In order to cope with this limitation, the CAMS-REG emission inventory developed a methodology to extrapolate the officially reported emissions to the most recent historical year. The methodology basically consists in two steps. First, early available relevant activity data for different sectors are used to extrapolate the trend in the activity, which are used to adjust future emissions. Second, for the historical years for which emission data are available from CAMS-REG the trend in these is compared to the trend in the activities. If a significant trend is found (here defined as >3% per year) the trend in the implied emission factor is determined by taking the ratio of the trend in emissions and in activities, which is then projected into the future. The methodology has been validated for historical years and overall works well, but such a method has also limitations, for instance it is not possible to predict sudden events such as closure of power plants or industrial facilities, or implementation of emission reduction techniques in large facilities~~a proxy inventory for the recent years, still based on the officially reported emissions~~. This way, the emission implemented in late 2024~~3~~ in the regional production could be based on an estimate for the year 2023 (CAMS-REG v7.1)~~2~~.

The common requirement to use CAMS-REG emissions in all CTMs is strictly enforced for the forecast. For the analysis, in one of the models (Table 1) analysed concentrations are pulled away from the state that is physically related to the emissions and therefore will not be strictly relatable anymore to specified required emissions. But none of the models use inverse modelled emissions based on observation in the forecast.

Only the spatialised annual fluxes of $NO_x$, $SO_x$, ~~non-methane volatile organic compounds, (~~NMVOCs~~)~~, $NH_3$, CO, $PM_{10}$ and $PM_{2.5}$ emissions are prescribed for all models. The subsequent disaggregation required in CTMs in terms of (i) hourly/daily/weekly/monthly profiles, (ii) vertical injection height, and (iii) mapping towards model chemical species is left open for individual modelling teams. Default information is nevertheless provided regarding the temporal disaggregation (Guevara et al., 2021) as well as the ~~ventilation~~ speciation of total VOC or total PM on individual VOC species or aerosol species, respectively. NMVOC emissions in CAMS-REG are provided with year-, sector- and country-dependent speciation profiles to breakdown total NMVOC to the 25 Global Emission InitiAtive (GEIA) species, originally defined under the REanalysis of the TROpospheric chemical composition (RETRO) project {Schultz, 2007 #1528}. Each CAMS individual modelling team performs a remapping of the 25 GEIA NMVOC species to the species of their corresponding gas phase

chemical mechanism. Concerning PM, the default profiles provided in CAMS-REG allow splitting coarse and fine PM emissions to primary organic carbon, elemental carbon, sulphates, sodium and others.

### 2.6.2 Biogenic, natural and wildfire emissions

Biogenic emissions are left to the choice of individual operational models, most of which include their own online calculation of emissions from vegetation and other natural sources. They include soil emissions for (i) mineral dust resuspension, (ii) soil NOx or even (iii) sea salt within the European domain, but the agriculture related NH3 emissions are issued from the anthropogenic emission inventory.

The only coordination regarding ecosystem emissions concerns wildfires where all models are expected to use the Global Fire Assimilation System (GFAS) product (Kaiser et al., 2012) provided by CAMS. GFAS is based on fire radiative power retrievals from data of the Moderate Resolution Imaging Spectroradiometer (MODIS) instruments aboard the Terra and Aqua satellites. GFAS provides hourly emission data with a 8-hr delay compared to real time. Each individual modelling team retrieves GFAS emission when initiating their forecast. As the individual forecasts are initiated between 12:00 D-1 and 03:00 D+0 depending on the regional systems, the only full day where GFAS wildfire emissions are available is D-2, and some systems also include part of D-1 emissions. Each system therefore reconstructs a 24hr cycle of emission based either on D-2 only or also including part of D-1 emissions. This cycle is used by all models for their analysis of D-1. For the forecast, persistence of this daily cycle of emission is only maintained for D+0 and D+1 considering that the vast majority of wildfires in Europe are not persisting for longer time periods.

### 2.6.3 Pollen emission and dispersion

The following pollen species are included in the CAMS Regional production: birch, grass, olive, ragweed, alder, and mugwort. Their implementation in the individual operational CAMS models differ in terms of advection and deposition strategies, but as ~~is more uniform than~~ for the anthropogenic air pollutants, the emission terms are coordinated following ~~as they all rely on~~ the original documentation of (Sofiev et al., 2013) and subsequent updates for additional species. The pollen species differ in terms of their geographic distribution (source masks), total amount of available pollen grains, start and end date of the season (heatsum thresholds), and the shape of the season (source strength as function of time). The alder pollen emission model is similar to that of birch and olive, while the mugwort source is a variation of the grass source. However, mugwort is implemented as five different sub-species, each with its own spatially gridded start and end dates of the flowering season. Ragweed pollen follows the method described in (Prank et al., 2013).

Once emitted, pollen species are advected in the model in the same way as other chemically inert species and are subject to gravitational settling and wet scavenging over time.

# 3 Individual Model Description

## 3.1 CHIMERE

### 3.1.1 Model Overview

CHIMERE is a multi-scale CTM developed jointly by INERIS and CNRS (Menut et al., 2021). Its development was initiated in the early 2000s (Bessagnet et al., 2004; Vautard et al., 2005) and it has since then pioneered operational national air quality forecasting in France (Rouïl et al., 2009). It is also extensively used for long-term simulations for emission control scenarios (Colette et al., 2013; Meleux et al., 2007; Colette et al., 2015). It runs over a range of spatial scale from the hemispheric to the urban scale, with resolutions from 100km to 1km (Colette et al., 2014; Bessagnet et al., 2017). The exact model version used since June 2021 in the CAMS Regional Production is CHIMERE v2020r1.

### 3.1.2 Model geometry

For the CAMS regional forecasts, CHIMERE uses a regular latitude-longitude grid with a 0.1°x0.1° resolution which covers 25˚W to 45˚E and 30˚N to 72˚N and 9 vertical levels, extending from the surface up to 500 hPa, a lowermost layer about 20m deep and about 7 layers below 2 km. No vertical downscaling is applied and concentrations in the lowermost model layer are considered representative of the surface.

### 3.1.3 Forcing Meteorology

The forcing meteorology is retrieved from the IFS model vertical layers covering the CHIMERE vertical extent on a 0.12°x0.12° horizontal grid resolution with a temporal resolution of 3 hours. The forecast released at 00:00UTC of the previous days is used. The three-dimensional meteorological parameters included to force the CHIMERE forecast are horizontal wind components, temperature, specific humidity, orography, rain water/snow mixing ratios, cloud liquid and ice water contents. The 2D variables included are: surface temperature, surface pressure, large scale and convective precipitations, boundary layer height, sensible and latent heat fluxes at surface, surface solar radiation downwards, soil parameters (water and temperature) for 4 layers (0-7 cm, 7-28 cm, 28-100 cm, 100-255 cm), sea ice cover, and snow depth.

### 3.1.4 Chemical initial and boundary conditions

Lateral and top boundary conditions are taken from chemical species available in CAMS-Gthe global IFS forecast model of the previous day at 3hr temporal resolution. The full list of species used from CAMS-Global the IFS model is given in Table 2. The forecasts are initialised by the CHIMERE forecasts of the previous day.

### 3.1.5 Emissions

The common annual anthropogenic emissions CAMS-REG are implemented as explained in Section 2.5.1. Temporal disaggregation is based on TNO time profiles provided with CAMS-REG. Chemical disaggregation for VOCs is based on (Passant, 2002). PM components are speciated using the splits provided with the CAMS-REG database.

Biogenic VOC emissions are computed online with the MEGAN 2.10 algorithm (Guenther et al., 2012) implemented in CHIMERE and using high spatiotemporal data LAI (30 arcsec every 8 days) generated from MODIS (Yuan et al., 2011). Biogenic emission factors are estimated based on the 30 arcsec USGS (US Geophysical Survey) land-use database and the emission factors provided for each functional type by (Guenther et al., 2012).

The hourly GFAS wildfire emission for D-2 (i.e. the last full day available when launching the forecast system) are used for the analysis (D-1) and the first two days of the forecast (D+0 and D+1). Fire emissions are set to zero for the remainder of the forecast horizon.

Dust production within the European domain is included (Alfaro and Gomes, 2001). It is based on a scheme for saltation and a vertical flux estimate using cohesion kinetic energies scheme (Marticorena and Bergametti, 1995).

### 3.1.6 Solver, advection and mixing

The numerical time solver is based on a splitting operator which solves separately transport (including deposition and emissions), chemistry and aerosol formation.

Advection is based on the Piecewise Parabolic Method 3d order scheme (Colella and Woodward, 1984). Vertical turbulent mixing takes place only in the boundary layer. The formulation uses K-diffusion parameterisation (Troen and Mahrt, 1986), without counter-gradient term.

### 3.1.7 Deposition

Dry deposition of gaseous and particle species is parameterised as a downward flux out of the lowest model layer where the deposition velocity is described through a resistance analogy (Wesely, 1989). Wet deposition of particles and gases are computed by using a polydisperse distribution of rain droplets based on (Willis and Tattelman, 1989) and by computing the efficiency of the collision. Below-cloud scavenging of gases is assumed irreversible and is therefore only accounted for the most soluble compounds ($HNO_3$, $H_2O_2$, HCl, $SO_2$ and $NH_3$). In-cloud scavenging is accounted for all gases by computing the gaseous and aqueous phases partitioning based on Henry's law constants and the pH of the clouds. Scavenging by snow is also accounted for and is based on (Chang, 1984) for gases and on (Wang et al., 2014) for particles.

### 3.1.8 Chemistry and aerosols

In order to optimise computing time, the reduced MELCHIOR2 mechanism with 44 species and about 120 reactions is derived from the full mechanism MELCHIOR (Derognat et al., 2003). The sectional aerosol module accounts for 7 species and 10 bins from 10nm to 40µm (primary particle material, nitrate, sulphate, ammonium, biogenic secondary organic aerosol SOA, anthropogenic SOA and water). Photolytic rates are attenuated using liquid water and relative humidity. The aerosol module is described in great details in (Couvidat et al., 2018) and accounts for condensation, nucleation, and condensation/evaporation. Aerosol thermodynamic equilibrium is achieved using the ISORROPIA model version 2.1. The secondary organic aerosol formation mechanism used in the operational forecasting version of CHIMERE is described in (Bessagnet et al., 2008).

### 3.1.9 Assimilation system

The CHIMERE assimilation for operational purposes relies on a kriging based approach to assimilate hourly concentration values for correcting the raw model results. For the analysis period, linear regression between a selected set of observations (excluding mountain and proximity sites) and the raw CHIMERE model is performed (in moving neighbourhood). The experimental variogram of the regression residuals is then computed and a variogram model is fitted; the model adequacy is checked by cross validation. Ultimately, observations are kriged with the CHIMERE model as external drift (in moving neighbourhood). This method is applied for $O_3$ and $NO_2$. For $PM_{10}$ and $PM_{2.5}$, an ordinary co-kriging of the observations (main variable) and CHIMERE (secondary variable) is applied to ensure consistency between both pollutants. Only in-situ surface observations are used.

Further evolution of the CHIMERE assimilation system using an ensemble Kalman Filter approach is under development, in particular to pave the way for assimilation of satellite data. It is has however not yet demonstrated to provide better skill score than the geostatistical method.

## 3.2 DEHM

### 3.2.1 Model Overview

The Danish Eulerian Hemispheric Model (DEHM) is a 3-dimensional, offline, large-scale, Eulerian, atmospheric chemistry transport model developed to study long-range transport of air pollution in the Northern Hemisphere. DEHM was originally developed in the early 1990's in order to study the atmospheric transport of sulphur-dioxide and sulphate into the Arctic (Christensen, 1997; Heidam et al., 2004). The model has been modified, extended and updated continuously since then and now includes a flexible setup with the possibility for nested domains with higher resolutions over targeted areas (Brandt et al., 2012; Geels et al., 2021). Apart from standard air pollution components and pollen, the DEHM model also includes mercury (Christensen et al., 2004), $CO_2$ (Lansø et al., 2019) and POPs (Hansen et al., 2008).

### 3.2.2 Model geometry

The horizontal domain is defined on a regular latitude-longitude grid of 0.1° resolution with grid centre points covering longitude 24.95˚W to 44.95˚E and latitude 30.05˚N to 71.95˚N. The vertical discretization is defined on 29 terrain-following sigma levels up to about 100hPa. The 12 lowest layers are within the lowest 1 km of the atmosphere and the thickness of the lowest layer is about 20m. The model includes an option for downscaling to the surface, but this is not applied in the operational setup.

### 3.2.3 Forcing Meteorology

The forcing meteorology is retrieved from the IFS model vertical layers covering the DEHM vertical extent on a 0.2°x0.2° horizontal grid resolution with a temporal resolution of 3 hours. The forecast released at 12:00 UTC of the previous days is used. The meteorological parameters included to force the DEHM forecast are: 3D fields of the horizontal wind components (U,V), temperature, specific humidity, cloud liquid water contents, cloud ice water contents, rain water contents, snow water contents and fraction of cloud cover. The 2D fields are land-sea mask, surface pressure, geopotential height, skin temperature, Ustar, large scale and convective rain, snow depth, sensible heat flux, latent heat flux, net solar radiation, boundary layer height, 2 m temperature, 2 m dew point temperature, 10 m wind (U,V), albedo, sea ice area fraction and surface roughness.

### 3.2.4 Chemical initial and boundary conditions

Lateral and top boundary conditions are taken from chemical species available in CAMS-G~~the g~~lobal ~~IFS~~ forecast model of the previous day at 3 hr temporal resolution. The full list of species used from CAMS-Global ~~the IFS model~~ is given in Table 2. The DEHM forecasts are initialised by the DEHM forecasts of the previous day.

### 3.2.5 Emissions

The common annual anthropogenic emissions CAMS-REG are implemented as explained in Section 2.5.1. Originally the temporal disaggregation was based on the GENEMIS tables, using a GNFR to SNAP matrix. From 2021 the new CAMS-TEMPO (Guevara et al., 2021) profiles for annual, monthly, weekly and daily distribution of emissions have been included in the operational version of DEHM. PM components are speciated using the splits provided with the CAMS-REG emissions. The speciation of VOCs from the emission input of total non-methane VOCs is based on the global speciated NMVOC emission database EDGAR 4.3.2 (Huang et al., 2017).

Natural emissions of the Biogenic Volatile Organic Compounds (BVOCs) isoprene and monoterpenes are estimated in the DEHM model based on the MEGAN model (Zare et al., 2012). The production of sea salt aerosols at the ocean surface is based on two parameterisation schemes describing the bubble-mediated sea spray production of smaller and larger aerosols. In each time step, the production is calculated for 10 size bins and thereafter summed up to give an aggregated production of fine (with dry diameters <1.3 um) and coarse (with dry diameters ranging 1.3-6μ~~u~~m) aerosols (Soares et al., 2016). ~~Soil and lightning~~ NOx emissions from soil are based on data from the Global Emissions Inventory Activity (Yienger and Levy, 1995) and from lightning they are from (Price et al., 1997).

The hourly GFAS wildfire emissions are retrieved as soon as they are available (i.e. with a 8-hr delay from real time) in order to obtain a recent 24hr cycle spanning over D-2 and D-1. This cycle is used for the analysis (D-1) and the first two days of the forecast (D+0 and D+1). Fire emissions are set to zero for the remainder of the forecast horizon. Hourly injection heights are calculated based on the hourly data of 'Mean altitude of maximum injection' and 'Altitude of plume top'.

### 3.2.6 Solver, advection and mixing

The horizontal advection is solved numerically using the higher order Accurate Space Derivatives scheme, documented to be very accurate (Dabdub and Seinfeld, 1994), especially when implemented in combination with a Forester filter (Forester, 1977). The vertical advection as well as the dispersion sub-models is solved using a finite elements scheme (Pepper et al., 1979)for the spatial discretization. For the temporal integration of the dispersion, the q-method (Lambert, 1991) is applied and the temporal integration of the 3-dimensional advection is carried out using a Taylor series expansion to third order. Time integration of the advection is controlled by the Courant-Friedrich-Lewy (CFL) stability criterion. A wind adjustment is included in order to ensure mass conservation.

The vertical diffusion is configured by Kz profiles (Hertel et al., 1995), based on Monin-Obukhov similarity theory for the surface layer. This Kz profile is extended to the whole boundary layer by using a simple extrapolation, which ensures that Kz

is decreasing in the upper part of the boundary layer. The planetary boundary layer (PBL) height is obtained directly from the IFS meteorology.

### 3.2.7 Deposition

Gaseous and aerosol dry-deposition velocities are calculated based on the resistance method for 16 different land-use types and are configured similar to the EMEP model (Emberson et al., 2000b; Simpson et al., 2003), except for the dry deposition of species on water surfaces, where the deposition depends on the solubility of the chemical species and the wind speed (Hertel et al., 1995).

Wet deposition includes in-cloud and below-cloud scavenging and is calculated as the product of scavenging coefficients and the concentration of gases and particles in air (Simpson et al., 2003). The in-cloud scavenging coefficients are dependent on Henry's law constants and the rate at which precipitation is formed.

### 3.2.8 Chemistry and aerosols

The basic chemical scheme in DEHM now includes 74 different species and 158 reactions. It is based on the original scheme by (Strand and Hov, 1994). The original Strand and Hov scheme has been modified in order to improve the description of, amongst other things, the transformations of nitrogen containing compounds. The chemical scheme has been extended with a detailed description of the ammonia chemistry through the inclusion of ammonia ($NH_3$) and related species: ammonium-nitrate ($NH_4NO_3$), ammonium bisulphate ($NH_4HSO_4$), ammonium sulphate ($(NH_4)_2SO_4$) and particulate nitrate ($NO_3$) formed from nitric acid ($HNO_3$) using an aerosol equilibrium approach with reaction rates dependent on the equilibrium (Frohn, 2004). Furthermore, reactions concerning the wet-phase production of particulate sulphate have been included. The photolysis rates are calculated by using a 2-stream version of the Phodis model (Kylling et al., 1995). The original rates for inorganic and organic chemistry have been updated with rates from the chemical scheme applied in the EMEP model (Simpson et al., 2003). SOA formation is included via a VBS-based approach (Bergström et al., 2012b; Zare et al., 2014). In total, DEHM includes nine classes of particulate matter ($PM_{2.5}$, $PM_{10}$, TSP, seasalt< 2.5 mm, sea-salt >2.5 mm, smoke from wood stoves, fresh black carbon, aged black carbon, and organic carbon).

### 3.2.9 Assimilation system

Since the system upgrade in November 2020, the assimilation in DEHM has been based on an updated version of the comprehensive 3D-var data assimilation scheme previously described in (Silver et al., 2016). The NMC method (Kahnert, 2008; Parrish and Derber, 1992) is used to estimate the background error covariance matrix. Two 1-year runs of DEHM using analysed and forecasted ECMWF weather data are performed and their differences are used to estimate the background errors

in spectral space for $O_3$, $NO_2$, $SO_2$, CO, $PM_{2.5}$, and $PM_{10}$. For the analysis and reanalysis runs, surface in-situ observations of the six species are assimilated at an hourly basis in DEHM.

## 3.3 EMEP

### 3.3.1 Model Overview

The EMEP MSC-W (European Monitoring and Evaluation Programme Meteorological Synthesizing Centre-West) model is a chemical transport model developed at the Norwegian Meteorological Institute under the EMEP programme of the United Nations Geneva Convention on Long-range Transboundary Air Pollution. The EMEP MSC-W model system allows several options with regard to the chemical schemes used and the possibility of including aerosol dynamics. (Simpson et al., 2012) described an early version of the EMEP MSC-W model in detail, while updates to the model since 2012 have been documented and evaluated in the annual status reports of EMEP (see (Emep, 2023) and references therein). The forecast version of the EMEP MSC-W model (EMEP-CWF) has been in operation since June 2006. The scheduled model updates in CAMS ensure that the model version stays as close as possible to the official EMEP Open Source version[3]. Nevertheless, the EMEP-CWF results and performances in CAMS might differ from those presented in the annual EMEP Status Reports, because of different input data (emissions and meteorological driver) and model configurations (Forecast in EMEP-CWF versus Hindcast in EMEP Status Reports).

### 3.3.2 Model geometry

The EMEP-CWF covers the European domain [30°N-76°N] x [30°W-45°E] on a geographic projection with a horizontal resolution of 0.1° x 0.1° (longitude-latitude). Vertically the model uses 20 levels defined as ~~sigma~~ hybrid coordinates. The 10 lowest model levels are within the PBL, and the top of the model domain is at 100 hPa. The lowermost layer has a thickness of approximately 50 meters. Vertical downscaling is used to derive surface concentrations at 3 meters altitude, as described in (Simpson et al., 2012).

### 3.3.3 Forcing Meteorology

The forcing meteorology is retrieved from the IFS model vertical layers covering the EMEP vertical extent on a 0.1°x0.1° horizontal grid resolution with a temporal resolution of 3 hours. The forecast released at 12:00UTC of the previous days is used. The meteorological parameters included to force the EMEP forecast are: 3D fields of the horizontal wind components (U,V), potential temperature, specific humidity, and cloud fraction. The 2D fields are land-sea mask, surface pressure, friction velocity (u*), large scale and convective precipitation, soil water, snow depth, fraction of snow cover, fraction of ice cover, sensible heat flux, latent heat flux, sea surface temperature, 2m temperature and 2m relative humidity. The IFS forecasts do not include 3D precipitation, which is needed by the EMEP-CWF model. Therefore, a 3D precipitation estimate is derived from large-scale precipitation and convective precipitation (surface variables).

[3] https://github.com/metno/emep-ctm (last accessed 30/10/2024)

### 3.3.4 Chemical initial and boundary conditions

Boundary conditions are taken from chemical species available in the CAMS-G~~the g~~lobal ~~IFS~~ forecast model of the previous day at 3hr temporal resolution (Table 2). In cases where ~~IFS~~ CAMS-Global chemical boundary conditions are not available, default boundary conditions are specified for $O_3$, CO, NO, $NO_2$, $CH_4$, $HNO_3$, PAN, $SO_2$, isoprene, $C_2H_6$, some VOCs, Sea salt, Saharan dust and $SO_4$, as annual mean concentrations along with a set of parameters for each species describing seasonal, latitudinal and vertical distributions. It should be noted however that unavailability of CAMS-Global is very exceptional (less than once a year), and in general due to data transfer issues. The EMEP forecasts are initialised by the EMEP 3D VAR analysis of the previous day.

### 3.3.5 Emissions

The common annual anthropogenic emissions CAMS-REG are implemented as explained in Section 2.5.1. Temporal disaggregation is based on CAMS-REG-TEMPO v4.1. Chemical disaggregation for PM species follows the tables that come with CAMS-REG while VOC emissions are speciated for each source-sector based on a lumped-species approach as described in (Simpson et al., 2012; Bergström et al., 2022) .

The hourly GFAS wildfire emission for D-2 (i.e. the last full day available when launching the forecast system) are used for the analysis (D-1) and the first two days of the forecast (D+0 and D+1). Fire emissions are set to zero for the remainder of the forecast horizon.

The mineral dust source in the EMEP model is based on (Alfaro and Gomes, 2001; Fécan et al., 1998; Gomes et al., 2003; Marticorena and Bergametti, 1995; Marticorena et al., 1997).

Natural emissions of Biogenic Volatile Organic Compounds (BVOCs) are based on Table 3 of (Simpson et al., 2012).

### 3.3.6 Solver, advection and mixing

The numerical solution of the advection terms of the continuity equation is based on the scheme of (Bott, 1989). The fourth order scheme is utilized in the horizontal directions. In the vertical direction, a second order version applicable to variable grid distances is employed.

The turbulent diffusion coefficients (Kz) are first calculated for the whole 3D model domain on the basis of local Richardson numbers. The planetary boundary layer (PBL) height is then calculated using methods described in (Simpson et al., 2012). For stable conditions, Kz values are retained. For unstable situations, new Kz values are calculated for layers below the mixing height using the O'Brien interpolation.

### 3.3.7 Deposition

Parameterisation of dry deposition is based on a resistance formulation. The deposition module makes use of a stomatal conductance algorithm which was originally developed for ozone fluxes, but which is now applied to all gaseous pollutants when stomatal control is important (Emberson et al., 2000a; Simpson et al., 2003; Tuovinen et al., 2004). Non-stomatal deposition for $NH_3$ is parameterised as a function of temperature, humidity, and the molar ratio $SO_2/NH_3$.

Both gaseous and particulate nitrogen species are scavenged in the EMEP model according to their wet scavenging ratios and collection efficiencies listed in Table S20 of (Simpson et al., 2012). In-cloud and sub-cloud scavenging ratios are considered for gases and in-cloud scavenging ratios and sub-cloud scavenging efficiencies for particles.

### 3.3.8 Chemistry and aerosols

The EmChem19 chemical scheme couples the sulphur and nitrogen chemistry to the photochemistry and organic aerosol formation using about 200 reactions between ca. 130~~0~~ species (Bergström et al., 2022; Simpson et al., 2020b; Andersson-Sköld and Simpson, 1999). The standard model version distinguishes 2 size fractions for aerosols, fine aerosol ($PM_{2.5}$) and coarse aerosol ($PM_{2.5\text{-}10}$). The aerosol components presently accounted for are $SO_4$, $NO_3$, $NH_4$, anthropogenic primary PM, organic aerosols, and sea salt. Also aerosol water is calculated. Dry deposition parameterisation for aerosols follows standard resistance-formulations, accounting for diffusion, impaction, interception, and sedimentation. Wet scavenging is treated with simple scavenging ratios, taking into account in-cloud and sub-cloud processes. For secondary organic aerosol (SOA) a volatility-basis set approach (Simpson et al., 2012) is used, which is a somewhat simplified version of the mechanisms discussed in detail by(Bergström et al., 2012a). The EmChem19a scheme also has explicit toluene and benzene with different SOA yields to the o-xylene surrogate that was used previously.

### 3.3.9 Assimilation system

The EMEP data assimilation system (EMEP-DAS) is based on the 3D-Var implementation for the MATCH model (Kahnert, 2008). The background error covariance matrix is estimated following the NMC method (Parrish and Derber, 1992). Recent changes involved increased computational efficiency, tuning of model and observation representation uncertainties, and improved impact of the assimilation in the vertical.

The EMEP-DAS delivers analyses of D-1~~yesterday~~ (driven by the operational IFS forecast of 00UTC of yesterday) assimilating $O_3$, $NO_2$, CO, $PM_{2.5}$, and $PM_{10}$ surface observations. ~~For $NO_2$, satellite observations from OMI used to be assimilated up to 2021 too.~~

## 3.4 EURAD-IM

### 3.4.1 Model Overview

The EURAD-IM (European Air pollution Dispersion - Inverse Model) system consists of 5 major parts: the meteorological driver WRF (Weather Research and Forecasting[4]), the pre-processors EEP and PREP for preparation of anthropogenic emission data and observations, the EURAD-IM Emission Model EEM, and the chemistry transport model EURAD (Hass et al., 1995; Memmesheimer et al., 2004). EURAD-IM is a Eulerian meso-scale chemistry transport model involving advection, diffusion, chemical transformation, wet and dry deposition and sedimentation of tropospheric trace gases and aerosols. It includes 3d-var and 4d-var chemical data assimilation (Elbern et al., 2007) and is able to run in nesting mode.

### 3.4.2 Model geometry

To cover the CAMS domain from 25°E to 45°W and 30°N to 72°N, two lambert conformal projections subdomains with respectively 45 km (199x166 grid boxes) and 9 km horizontal resolution (581x481 grid boxes) are used. The model domain with the finer resolution covering the entire European part of the CAMS domain is nested within the halo domain with the coarser resolution.

Variables are horizontally staggered using an Arakawa C grid. Vertically, the atmosphere is divided by 23 terrain-following sigma coordinate layers between the surface and the 100 hPa pressure level. About 15 layers are within the first 2 km of the atmosphere The thickness of the lowest layer is about 35 m. No vertical downscaling is used to derive surface concentrations from the first model level.

### 3.4.3 Forcing Meteorology

The meteorological forcing is obtained from 3-hourly IFS forecasts, but unlike the other models, t~~T~~he Weather Research and Forecast (WRF) model is used to compute ~~for the calculation of~~ meteorological fields on the grid needed to drive the EURAD-IM CTM. This intermediate processing is essentially for historical reasons as in the past the IFS temporal and spatial resolution required interpolation for use in the CTM. A direct use the IFS data to dynamically drive EURAD-IM has been developed and is currently in the testing to enter the operational production in the near future~~Initial and boundary values for the WRF simulations are derived from 3-hourly IFS meteorological fields. The main motivation to use WRF is to improve the spatial and temporal interpolation of IFS fields towards the EURAD-IM geometry~~.

[4] https://www.mmm.ucar.edu/models/wrf, last accessed 30/10/2024

### 3.4.4 Chemical initial and boundary conditions

The CAMS- -Global ~~IFS~~ 00:00 UTC forecast for the previous day is extracted from the MARS archive at ECMWF using 36 model levels with a temporal resolution of 3 hours. The full list of species used from the ~~IFS~~ CAMS-Global model is given in Table 2. Sea salt concentrations from ~~IFS~~ CAMS-Global are divided by the constant 4.3 for the conversion from wet to dry mass.

### 3.4.5 Emissions

The common annual anthropogenic emissions CAMS-REG are implemented as explained in Section 2.5.1. The VOC and PM split, the vertical distribution of area sources, and the emission strength per hour are calculated within the EURAD-IM CTM with the distribution profiles provided with the CAMS-REG-AP_v6.1/2019 inventory (Kuenen et al., 2022). The VOC and PM split depends on source category and country, the vertical distribution only depends on the source category. The CAMS-TEMPO v4.1 (Guevara et al., 2021) profiles are used for the annual, monthly, weekly and daily distribution of emissions.

Biogenic emissions and $NO_x$ emissions from soil are calculated within the EURAD-IM CTM with ~~the Model of Emissions of Gases and Aerosols from Nature (~~MEGAN~~)~~ (Guenther et al., 2012). Fire emissions are taken into account using hourly data from ~~the Global Fire Assimilation System Version 1.2 (~~GFASv1.2~~)~~ product (Kaiser et al., 2012). Zero fire emissions are assumed for D+2 and D+3 forecasts.

### 3.4.6 Solver, advection and mixing

The positive definite advection scheme of (Bott, 1989), implemented in a one-dimensional realisation, is used to solve the advective transport. An operator splitting technique is employed (Mcrae et al., 1982) to handle the varying numerical specificities of processes to be solved.

An Eddy diffusion approach is used to parameterize the vertical sub-grid-scale turbulent transport. The calculation of vertical Eddy diffusion coefficients is based on the specific turbulent structure in the individual regimes of the planetary boundary layer (PBL) according to the PBL height and the Monin-Obukhov length (Holtslag and Nieuwstadt, 1986). A semi-implicit (Crank-Nicholson) scheme is used to solve the diffusion equation.

The sub-grid cloud scheme in EURAD-IM was derived from the cloud model in the EPA Models-3 Community Multiscale Air Quality (CMAQ) modelling system (Roselle and Binkowski, 1999). Convective cloud effects on both gas phase species and aerosols are considered.

### 3.4.7 Deposition

The gas phase dry deposition modelling follows the method proposed by (Zhang et al., 2003). Dry deposition of aerosol species is treated size dependent, using the resistance model of (Petroff and Zhang, 2010) with consideration of the canopy. Dry deposition is applied as lower boundary condition of the diffusion equation.

Wet deposition of gases and aerosols is derived from the cloud model in the CMAQ modelling system (Roselle and Binkowski, 1999). The wet deposition of pollen is treated according to (Baklanov and Sørensen, 2001).

Size dependent sedimentation velocities are calculated for aerosol and pollen species. The sedimentation process is parameterized with the vertical advective transport equation and solved using the fourth order positive definite advection scheme of (Bott, 1989).

### 3.4.8 Chemistry and aerosols

In the EURAD-IM CTM, the gas phase chemistry is represented by an extension of the Regional Atmospheric Chemistry Mechanism (RACM) (Stockwell et al., 1997) based on the Mainz Isoprene Mechanism (MIM) (Geiger et al., 2003). A 2-step Rosenbrock method is used to solve the set of stiff ordinary differentials equations (Sandu and Sander, 2006). Photolysis frequencies are derived using the FTUV model (fast TUV) according to (Tie et al., 2003). The radiative transfer model therein is based on the Tropospheric Ultraviolet-Visible Model (TUV) developed by (Madronich and Weller, 1990).

The modal aerosol dynamics model MADE (Ackermann et al., 1998) is used to provide information on the aerosol size distribution and chemical composition. To solve for the concentrations of the secondary inorganic aerosol components, a FEOM (fully equivalent operational model) version, using the HDMR (high dimensional model representation) technique (Nieradzik, 2005; Rabitz and Aliş, 1999), of an accurate mole fraction based thermodynamic model (Friese and Ebel, 2010) is used. The updated SORGAM module (Li et al., 2013) simulates secondary organic aerosol formation.

### 3.4.9 Assimilation system

The EURAD-IM assimilation system (Elbern et al., 2007) includes (i) the EURAD-IM CTM and its adjoint, (ii) the formulation of both background error covariance matrices for the initial states and the emission, and their treatment to precondition the minimisation problem, (iii) the observational basis and its related error covariance matrix, and (iv) the minimisation including the transformation for preconditioning. The quasi-Newton limited memory L-BFGS algorithm described in (Liu and Nocedal, 1989; Nocedal, 1980) is applied for the minimisation.

Currently assimilated in the EURAD-IM analysis and interim re-analysis are surface in-situ observations of $O_3$, $NO_2$, $SO_2$, CO, $PM_{2.5}$, $PM_{10}$.

651

652

## 3.5 GEM-AQ

### 3.5.1 Model Overview

GEM-AQ is a numerical weather prediction model where air quality processes (gas phase and aerosols) are implemented on-line in the host meteorological model, the Global Environmental Multiscale (GEM) model, developed at Environment and Climate Change Canada (Côté et al., 1998a). The model is used for operational air quality forecasting in Poland. Also, it is used in a research project to investigate air quality in different environmental conditions (Struzewska and Kaminski, 2008, 2012; Struzewska et al., 2015; Struzewska et al., 2016). ~~Application of the GEM-AQ to modelling of satellite retrieved NO2 column was carried out by (Szymankiewicz et al., 2014) and (Kawka et al., 2021).~~

### 3.5.2 Model geometry

The GEM-AQ model can be configured to simulate atmospheric processes over a broad range of scales, from the global scale down to the meso-gamma scale. An arbitrarily rotated latitude-longitude mesh focuses resolution on any part of the globe. In the CAMS regional production, the model is run in the limited area mode with a resolution of 0.1° x 0.1° on a spherical coordinate system. The coordinates are the following: lower-left (17.4°N / 22.1°W), upper-right (58.6°N/ 86.6°E)~~, and are generated internally based on lower-left corner, grid extent and the numerical equator location~~. In the vertical, GEM-AQ uses the generalised sigma vertical coordinate system. It has terrain-following sigma surfaces near the ground that transform to pressure surfaces higher in the atmosphere. The model top is set at 10 hPa.

### 3.5.3 Forcing Meteorology

The operational IFS model provides meteorological fields for the initial and boundary conditions used by the meteorological part of the GEM-AQ model. The GEM-AQ model is started using the 12-hour forecast (valid at 00:00 UT of the following day) as the initial conditions. The IFS data are used as boundary conditions with a nesting interval of 3 hours. The IFS meteorological fields are computed from spectral coefficients for the target GEM-AQ grid. Meteorological fields, in the GEM-AQ model domain, are constrained within the nesting zone (absorber), which is defined over 10 grid points on each lateral boundary of the limited area domain.

~~The operational IFS model provides meteorological fields for initial and boundary conditions used by the meteorological part of the GEM-AQ model. The GEM-AQ model is started using the 12-hour forecast (valid at 00:00 UT of the following day) as initial conditions. The IFS data are used as boundary conditions with a nesting interval of 3 hours. The IFS meteorological fields are computed from spectral coefficients for the target GEM-AQ grid. Meteorological fields, within the GEM-AQ model domain, are constrained and relaxed to the IFS global model every 3 hours. Thus, the meteorological fields are 'dynamically interpolated' by the GEM meteorological model to the required transport and chemistry time steps.~~

### 3.5.4 Chemical initial and boundary conditions

Chemical species of the CAMS -~~-~~Global ~~IFS~~ forecast for the previous day are used with a temporal resolution of 3 hours (Table 2). For dust aerosols, the three available size bins from the ~~IFS~~ CAMS-Global model are distributed uniformly over the 10 corresponding bins in GEM-AQ. For organic matter aerosol, black carbon and sulphates, the same log-normal based profile was applied. For organic aerosol and black carbon, hydrophobic and hydrophilic components were summed as "total organic aerosol" and "total black carbon aerosol" before applying size-bin distribution profiles.

### 3.5.5 Emissions

The common annual anthropogenic emissions CAMS-REG are implemented as explained in Section 2.5.1. ~~In those emissions, the following fields are available: $SO_2$, NOx, CO, NMVOC, $NH_3$, $PM_{10}$ and $PM_{2.5}$.~~ Based on this information, emission fluxes for 15 gaseous species (9 hydrocarbons and 6 inorganics) and 4 aerosol components (primary organic aerosol, black carbon, sulphates, nitrates) are derived using factors provided by TNO. Total emission fluxes for each aerosol component are distributed into 12 bins in the GEM-AQ aerosol module.

Anthropogenic emissions are distributed within the 7 lowest model layers (up to 1350 m) with injection height profiles for each of the GNFR sectors re-mapped for the GEM-AQ levels (Bieser et al., 2011). Temporal profiles modulating annual and diurnal variation of emission fluxes for each GNFR are used.

For biogenic emissions, a temperature-dependent, ~~a~~ monthly averaged MEGAN-MACC (Sindelarova et al., 2014) ~~(Guenther et al., 2012)~~ dataset for the year 2010 was used specifically to avoid the short-term variability of reactive biogenic VOCs that would otherwise be generated in an online approach. In contrast to the online method, this approach provides an anticipated variability range, particularly by reducing the influence of online factors such as meteorological errors and extreme values.~~dataset valid for 2010 was used in order to avoid short-term variability of reactive biogenic VOC generated on-line in the model.~~

### 3.5.6 Solver, advection and mixing

The set of non-hydrostatic Eulerian equations (with a switch to revert to the hydrostatic primitive equations) maintains the model's dynamical validity right down to the meso-gamma scales. The time discretization of the model dynamics is fully implicit, 2 time-level (Côté et al., 1998b; Côté et al., 1998a). The spatial discretization for the adjustment step employs a staggered Arakawa C grid that is spatially offset by half a mesh length in the meridional direction. It is second-order accurate, whereas the interpolations for the semi-Lagrangian advection are of fourth-order accuracy.

Deep convective processes are handled by Kain-Fritch convection parameterisation (Kain and Fritsch, 1990). The vertical diffusion of momentum, heat and tracers is a fully implicit scheme based on turbulent kinetic energy (TKE) theory.

### 3.5.7 Deposition

The effects of dry deposition are included as a flux boundary condition in the vertical diffusion equation. Dry deposition velocities are calculated from a `big leaf' multiple resistance model (Wesely, 1989; Aamaas et al., 2013) with aerodynamic, quasi-laminar layer, and surface resistances acting in series. The process assumes 15 land-use types and takes snow cover into account. Wet deposition takes into account cloud scavenging for soluble gas species and aerosols.

### 3.5.8 Chemistry and aerosols

The gas-phase chemistry mechanism currently used in the GEM-AQ model is based on a modification of version 2 of the Acid Deposition and Oxidants Model (ADOM) (Venkatram et al., 1988), derived from the condensed mechanism of (Lurmann et al., 1986). The ADOM-II mechanism comprises 47 species, 98 chemical reactions and 16 photolysis reactions. In order to account for background tropospheric chemistry, 4 species ($CH_3OOH$, $CH_3OH$, $CH_3O_2$, and $CH_3CO_3H$) and 22 reactions were added. All species are solved using a mass-conserving implicit time stepping discretization, with the solution obtained using Newton's method. Heterogeneous hydrolysis of $N_2O_5$ is calculated using the on-line distribution of aerosol. Although the model meteorology is calculated up to 10 hPa, the focus of the chemistry is in the troposphere where all species are transported throughout the domain. ~~To avoid the overhead of stratospheric chemistry in this version (a combined stratospheric/tropospheric chemical scheme is currently being developed), both the ozone and NOy fields are replaced with a climatology above 100 hPa after each transport time step. Ozone fields are taken from the HALOE (Halogen Occultation Experiment) climatology (Hervig et al., 1993), while NOy fields are taken from the CMAM (Canadian Middle Atmosphere Model).~~ To avoid the overhead of stratospheric chemistry, the ozone and NOy fields are replaced above 100 hPa with those from the CAMS-Global model. Additionally, stratospheric columns for absorbing species used in photolysis calculations (cf., ozone) are taken from the CAMS-Global model. Photolysis rates (J values) are calculated on-line every chemical time step using the method described in ~~of~~ (Landgraf and Crutzen, 1998). In this method, radiative transfer calculations are done using a delta-two stream approximation for 8 spectral intervals in the UV and visible applying pre-calculated effective absorption cross sections. This method also allows for scattering by cloud droplets and for clouds to be presented over a fraction of a grid cell. The host meteorological model provides both cloud cover and water content. The J value package used was developed for MESSy (Jöckel et al., 2006) and is implemented in GEM-AQ.

The current version of GEM-AQ has 5 size-resolved aerosol types, viz. sea salt, sulphate, black carbon, organic carbon and dust as well as nitrates. The microphysical processes that describe the formation and transformation of aerosols are calculated by a sectional aerosol module (Gong et al., 2003). The particle mass is distributed into 12 logarithmically spaced bins from

0.005 to 10.24-micron radius. This size distribution leads to an additional 60 advected tracers. The following aerosol processes are accounted for in the aerosol module: nucleation, condensation, coagulation, sedimentation and dry deposition, in-cloud oxidation of $SO_2$, in-cloud scavenging, and below-cloud scavenging by rain and snow.

### 3.5.9 Assimilation system

Data assimilation in the GEM-AQ modelling system is done with Optimal Interpolation method (Robichaud and Ménard, 2014) and is applied to the forecast. Error statistics are computed with the Hollingsworth - Lönnberg (HL) method (Hollingsworth and Lönnberg, 1986). It estimates the correlation length and the ratio of observation to model error variances by a least-square fit of a correlation model against the sample of the spatial autocorrelation of observation-minus-model residuals.

Currently, data assimilation is done at each forecast hour for $O_3$, $NO_2$, $SO_2$, CO, $PM_{10}$ and $PM_{2.5}$, using surface observations.

## 3.6 LOTOS-EUROS

### 3.6.1 Model Overview

The LOTOS-EUROS model is a 3D chemistry transport model aimed to simulate air pollution in the lower troposphere. The model has been used in a large number of studies for the assessment of particulate air pollution and trace gases (e.g. $O_3$, $NO_2$) (Hendriks et al., 2016; Schaap et al., 2013; Thürkow et al., 2021; Timmermans et al., 2022). A detailed description of the model is given in (Manders et al., 2017). At present the version used in the production is v2.2.009.

### 3.6.2 Model geometry

The domain of LOTOS-EUROS is the CAMS regional domain from 25°W to 45°E and 30°N to 72°N. The projection is regular longitude-latitude, at 0.1°x0.1° grid spacing. In the vertical and for the forecasts there are currently 12 model layers and 2 more reservoir layers at the top, defined by coarsening in a mass conservative way the first 77 model levels of the IFS. ~~For the analyses there are 4 dynamic layers up to 5km agl and a surface layer with a fixed depth of 25 m. The lowest dynamic layer is the mixing layer, followed by 3 reservoir layers. The heights of the reservoir layers are determined by the difference between the mixing layer height and 5 km.~~ For output purposes, the concentrations at measuring height (usually 2.5 m) are diagnosed by assuming that the flux is constant with height and equal to the deposition velocity times the concentration at height *z* (taken as average over the grid cell). This applies for several of the gaseous species, namely $O_3$, NO, $NO_2$, $HNO_3$, $N_2O_5$, $H_2O_2$, CO, $SO_2$ and $NH_3$. For aerosols, the same approach is utilized, only sedimentation velocity is used instead of deposition velocity.

### 3.6.3 Forcing Meteorology

The forcing meteorology is retrieved from the 00:00 and 12:00 UTC runs of the IFS model at hourly (surface fields) or 3-hourly temporal resolution (model layer fields). The meteorological data is retrieved on a regular horizontal resolution of about 9~~15~~ km and for all layers covered by the model's vertical extent. The meteorological variables included are 3-hourly 3D fields for wind direction, wind speed, temperature, humidity and density, ~~substantiated~~ augmented by hourly 2D gridded fields of mixing layer height, surface wind and temperature, precipitation rates, heat fluxes, cloud cover and surface variables snow depth, sea ice cover and volumetric soil water.

### 3.6.4 Chemical initial and boundary conditions

The lateral and top boundary conditions for trace gases and aerosols are obtained from the CAMS-G~~g~~lobal daily forecasts (see Table 2). LOTOS-EUROS uses a bulk approach for the aerosol size distribution differentiating between a fine and a coarse fraction, but for dust and sea salt there are 5 distinct size classes: ff: 0.1-1 µm, f:1-2.5 µm, ccc: 2.5-4 µm, cc: 4-7 µm, c:7-10 µm. When the chemical boundary conditions from ~~IFS~~ CAMS-Global are missing (which is very rare, typically less than once a year, and can, e.g., be due to delays in the file transfer or other serious technical issues at ECMWF), the model uses

climatological boundary concentrations derived from ~~IFS~~ CAMS-Global data. The forecasts are initialised with the LOTOS-EUROS forecast of the previous day.

### 3.6.5 Emissions

The common annual anthropogenic emissions CAMS-REG are implemented as explained in Section 2.5.1. Injection height distribution from the EuroDelta study is implemented, which is per SNAP (or more recently, GNFR) category. Time profiles used are defined per country and GNFR emission category type.

Biogenic NMVOC emissions are calculated online using actual meteorological data and a detailed landuse and tree species database including emission factors from (Köble and Seufert, 2001). The isoprene emissions follow the mathematical description of the temperature and light dependence of the isoprene emissions, proposed by (Guenther et al., 1993). Sea salt emissions are parameterised following (Martensson et al., 2003; Monahan, 1986) from the wind speed at 10-meter height.

The fire emissions are taken from the near real-time GFAS fire emissions database. For the forecast, we assume persistence, so that the latest downloaded emission for the specific hour is used. When the hourly emission is more than 3 days old, it is set to zero.

Mineral dust emissions within the modelling domain are calculated online based on the sand blasting approach by (Marticorena and Bergametti, 1995) with soil moisture inhibition as described by (Fécan et al., 1998). Finally, a parameterization using land cover and temperature is used for handling soil NOx emissions, based on (Yienger and Levy, 1995).

### 3.6.6 Solver, advection and mixing

The transport consists of advection in 3 dimensions, horizontal and vertical diffusion, and entrainment/detrainment. The advection is driven by meteorological fields ($u$,$v$), which are input every 3 hours. The vertical wind speed $w$ is calculated by the model as a result of the divergence of the horizontal wind fields. A linear advection scheme is used to ensure tracer mass conservation, which also allows more efficient parallelization and reduced model complexity. This scheme uses piece-wise linear functions to define sub-grid concentrations, which is sometimes referred to as MUSCL (”Monotonic Upwind-centered Scheme for Conservation Laws”) following (Van Leer, 1984).

Vertical diffusion is described using the standard $K_z$ theory. Vertical exchange is calculated employing the new integral scheme by (Yamartino et al., 2007). For the forecasting set-up with 12 layers, atmospheric stability values and functions, including Kz values, are derived based on the surface heat fluxes from ECMWF meteorology and similarity profiles following the IFS approach (Ecmwf, 2021) to adapt for land-use specific conditions. For the 5-layer version in the assimilation, a correction is made for the vertical diffusion to correct for the height difference between surface and mixing layer.

### 3.6.7 Deposition

The dry deposition in LOTOS-EUROS is parameterised following the resistance approach. The laminar layer resistance and the surface resistances for acidifying components are described following the EDACS system (Van Zanten et al., 2010), the deposition velocities for particles are based on (Zhang et al., 2001). Wet deposition is divided between in-cloud and below-cloud scavenging. The in-cloud scavenging module is based on the approach described in (Seinfeld and Pandis, 1998) and (Banzhaf et al., 2012).

### 3.6.8 Chemistry and aerosols

LOTOS-EUROS uses the TNO CBM-IV scheme, which is a modified version of the original CBM-IV (Gery et al., 1989). $N_2O_5$ hydrolysis is described explicitly based on the available (wet) aerosol surface area (using $\gamma = 0.05$) (Schaap et al., 2004). Aqueous phase and heterogeneous formation of sulphate is described by a simple first order reaction constant (Barbu et al., 2009; Schaap et al., 2004). Inorganic aerosol chemistry is represented using ISORROPIA II (Fountoukis and Nenes, 2007) and secondary organic aerosols formation based on a VBS scheme (Bergström et al., 2012a; Zare et al., 2014) will be included in the operational forecast version in the future~~at the end of 2023~~.

### 3.6.9 Assimilation system

The LOTOS-EUROS model is equipped with a data assimilation package with the ensemble Kalman filter technique (Curier et al., 2012). The ensemble is created by specification of uncertainties for emissions (NOx, VOC, $NH_3$ and aerosol), ozone deposition velocity, and ozone top boundary conditions. Currently, data assimilation is performed for $O_3$, $NO_2$, $PM_{10}$ and $PM_{2.5}$ surface observations, OMI $NO_2$ is also assimilated.

## 3.7 MATCH

### 3.7.1 Model Overview

The Multi-scale Atmospheric Transport and Chemistry model (MATCH) (Robertson et al., 1999) is an off-line chemical transport model (CTM) with a flexible design, accommodating different weather data forcing on different resolutions and projections, and a range of alternative schemes for deposition and chemistry.

### 3.7.2 Model geometry

The model's geometry is taken from the input weather data. To reduce computational costs, the vertical resolution is reduced compared to the ECMWF operational model by merging pairs of IFS vertical layers, while retaining the use of hybrid vertical coordinates. The horizontal resolution in the MATCH simulation matches that of the meteorological forcing, which is currently provided on a 0.1° latitude–longitude grid. ~~The vertical resolution is reduced with respect to the ECMWF operational model by combining pairs of IFS layers; hybrid vertical coordinates are used. The horizontal geometry of the MATCH simulation is the same as the meteorological forcing (currently a lat-lon grid with 0.1° resolution).~~ The lowest 78 layers of the ECMWF model are lumped in 39 levels~~The lowest 76 layers of the ECMWF model are lumped in 26 levels~~, which then are used for the air quality simulations. The model top is at about 8000 m height. The model domain covers the area between 28.8° W to 45.8° E and 29.2° N to 72.0° N. The grid is an Arakawa C-grid with staggered wind components. ~~The current operational system uses various tiles of physiography derived from CLC/SEI inventory[5] (Simpson et al., 2012).~~

### 3.7.3 Forcing Meteorology

The forcing meteorology for MATCH forecasts is retrieved from the 12:00 UTC run of the IFS modelling system on a 0.1°×0.1° spatial grid and with a temporal resolution of ~~one~~ three hour. For the analyses, the 00:00 UTC analysis of the IFS is used at 0.2°×0.2° resolution. The reason for applying a coarser resolution in the analysis is twofold: 1) the delivery time is rather short from when the in-situ observations are available, 2) the analysis increments are on a larger scale. The meteorological variables included are 3D fields of the horizontal wind components (U, V), temperature, specific humidity, cloud cover, cloud water content, cloud ice water content, and surface fields of surface pressure, logarithm of surface pressure, surface temperature, sea surface temperature, snow depth, albedo, roughness height, total cloud cover, precipitation, and volumetric soil water at the surface.

~~[5] www.sei.org/projects/sei-european-land-cover-map (last accessed 30/10/2024)~~

### 3.7.4 Chemical initial and boundary conditions

The lateral boundary conditions for trace gases and aerosols are obtained from the ~~IFS~~ CAMS-gGlobal forecasts at 3-hourly resolution for the following species: $O_3$, CO, HCHO, NO, $NO_2$, $SO_2$, $HNO_3$, PAN, $CH_4$, $C_5H_8$, o-xylene, sulphate and $C_2H_6$ (see Table 2). ~~When~~ In the event that the chemical boundary conditions from ~~IFS~~ CAMS-Global would be ~~are~~ missing (which has never happened in practice but could in theory happen due to due to corruption or other technical issues), the model uses seasonal climatological boundary concentrations instead.

### 3.7.5 Emissions

The common annual anthropogenic emissions CAMS-REG are implemented as explained in Section 2.5.1. Temporal disaggregation is based on the GENEMIS tables (Ebel et al., 1997), using a GNFR to SNAP matrix. The vertical distribution of the emissions depends on the sector. Near-surface emission sources (SNAP 2,6,7,8,10) are distributed in the lowest 90 m; for other sectors the emissions are allocated over varying model levels up to a maximum of about 1100 m height. According to the sector, the anthropogenic VOC emissions are split into the MATCH chemical mechanism surrogate species: $C_2H_6$, $NC_4H_{10}$, $C_2H_4$, $C_3H_6$, OXYLENE, BENZENE, TOLUENE, $CH_3OH$, $C_2H_5OH$, HCHO, $CH_3CHO$, $CH_3COC_2H_5$; the particulate matter components elemental carbon, organic matter, anthropogenic dust (other than soil and road dust) are allocated to two bins ($PM_{2.5}$ and PM-coarse), as well as the road dust estimated according to (Schaap et al., 2009) and (Omstedt et al., 2005), and the teluric dust calculated according to (Zender et al., 2003).

Biogenic emissions of isoprene, monoterpenes and sesquiterpenes are calculated following (Simpson et al., 2012; Simpson et al., 1995; Bergström et al., 2012a), taking into account temperature at 2 m, radiation fluxes and the vegetation cover. ~~Exception is made for the isoprene oxidation for which the chain of reactions is following the Carter-1 chemical mechanism, which has proven to give the comparable results with fewer reactions (Carter, 1996; Langner et al., 1998).~~

The dimethyl sulphide - DMS – emissions from the Ocean and Baltic Sea are also considered; whereas the particulate matters from sea salt are calculated according to the parameterisation proposed by (Sofiev et al., 2011).

The GFAS biomass burning emissions are taken into the model mapping the following species into the MATCH chemical mechanism: NOx, $SO_2$, CO, $CH_4$, $C_2H_4$, $C_2H_6$, $C_3H_6$, $C_4H_{10}$, $C_8H_{10}$, benzene, toluene, $CH_3OH$, $C_2H_5OH$, formaldehyde, acetaldehyde, OC, BC, $PM_{2.5}$, and $PM_{10}$. ~~Half of these grid emissions are vertically distributed between the surface and the top of the plume (GFAS parameter) according to a parabolic curve, and the other half is uniformly distributed among the same levels.~~ The vertical injection is made by a parabolic curve with central height taken from the GFAS INJH parameter. In case the injection height is missing for a GFAS emission cell this is assigned from some neighbour height present. The diurnal

emission profile is based on the D-1 GFAS hourly data filled up with GFAS data for D-2 for the not yet available hours in D-1. This diurnal hourly profile is repeated throughout the forecast.

### 3.7.6 Solver, advection and mixing

Mass conservative transport schemes are used for advection and turbulent transport. The advection is formulated as a Bott-like scheme (Robertson et al., 1999). A second order transport scheme is used in the horizontal as well as the vertical. The vertical diffusion is described by an implicit mass conservative first order scheme, where the exchange coefficients for neutral and stable conditions are parameterized following (Holtslag and Nieuwstadt, 1986). In the convective case the turbulent Courant number is directly determined from the turnover time in the boundary layer.

Part of the dynamical core is the initialisation and adjustment of the horizontal wind components. This is a very important step to ensure mass conservative transport. The initialisation is based on a procedure proposed by (Heimann and Keeling, 1989), where the horizontal winds are adjusted by means of the difference between the input surface pressure tendency, and the calculated pressure tendency assumed to be an error in the divergent part of the wind field.

Boundary layer parameterisation is based on surface heat and water vapour fluxes as described by (Van Ulden and Holtslag, 1985) for land surfaces, and (Burridge, 1977) for sea surfaces. The boundary layer height is calculated from formulations proposed by (Zilitinkevich and Mironov, 1996) for the neutral and stable case, and from (Holtslag et al., 1995) for the convective case. These parameterisations drive the formulations for dry deposition and vertical diffusion.

### 3.7.7 Deposition

Dry deposition of gases and aerosols is modelled using a resistance approach (based on the scheme in (Simpson et al., 2012)), which includes stomatal and non-stomatal pathways for vegetated surfaces. In t~~T~~he current operational system, the model applies this scheme across ~~uses~~ various physiographic tiles ~~of physiography~~ derived from the CLC/SEI inventory[6] (Simpson et al., 2012). MATCH uses 3D-precipitation (estimated in the model, based on the surface precipitation and 3D cloud water information from the IFS forecast) and separates wet scavenging into in-cloud and sub-cloud scavenging. For most gaseous components the scavenging is assumed to be proportional to the precipitation intensity (with higher scavenging ratios in-cloud than sub-cloud). For the particulate components in-cloud scavenging is also treated using simple scavenging ratios while the sub-cloud scavenging is treated using a scheme based on (Berge, 1993) with size dependent collection efficiencies (as in (Simpson et al., 2012)).

[6] www.sei.org/projects/sei-european-land-cover-map (last accessed 30/10/2024)

### 3.7.8 Chemistry and aerosols

The photochemistry scheme is based on the EMEP MSC-W chemistry scheme (Simpson et al., 2012), with a modified scheme for isoprene, based on the so-called Carter-1 mechanism (Carter, 1996; Langner et al., 1998). The standard MATCH setup used in CAMS treats particles as bulk aerosol in two size classes, fine ($PM_{2.5}$) and coarse ($PM_{2.5-10}$) particles. Particle formation from gases include secondary inorganic aerosol (ammonium sulphate and nitrate) and secondary organic aerosol. Ammonium nitrate equilibrium is calculated according to (Mozurkewich, 1993). Coarse nitrate formation from gas-phase $HNO_3$ is also included (Strand and Hov, 1994). Secondary organic aerosol formation from oxidation of volatile organic compounds is treated using a volatility basis set scheme based on ~~The SOA description is based on~~ (Hodzic et al., 2016). Exception is made for the isoprene oxidation for which the chain of reactions is following the Carter-1 chemical mechanism, which has proven to give the comparable results with fewer reactions (Carter, 1996; Langner et al., 1998).

### 3.7.9 Assimilation system

The model for data assimilation is an integrated part of the MATCH modelling system. The data assimilation scheme as such is a variational spectral scheme (Kahnert, 2008), implying that the background covariance matrices are modelled in spectral space. The limitation is that covariance structures are described as isotropic and homogeneous. The advantage is that the background error matrix becomes block diagonal, and there are no scale separations as the covariance between spectral components are explicitly handled. The block diagonal elements are the covariance between wave components at model layers and chemical compounds.

Modelling the background error covariance matrices is the central part in data assimilation. This is conducted by means of the so-called NMC approach (Parrish and Derber, 1992). The CTM (MATCH) is run for a 3-month period for photochemistry and aerosols with analysed and forecasted ECMWF weather data. The differences are assumed to mimic the background errors, and the statistics in spectral space are generated for different combinations of the model compounds: $O_3$, $NO_2$, NO, $SO_2$, CO, $PM_{2.5}$, $PM_{10}$.

The scheme is fully intermittent in hour-by-hour steps and the above-listed components are assimilated from in-situ measurements. The analysed components are propagated by chemistry and transport into unobserved components as NMVOCs, PAN and $NH_3$.

## 3.8 MINNI

### 3.8.1 Model Overview

MINNI (Italian Integrated Assessment Modelling System for supporting the International Negotiation Process on Air Pollution and assessing Air Quality Policies at national/local level; (D'elia et al., 2021; Mircea et al., 2014) has been developed to support the Italian Ministry for Environment and Territory and Sea. The core of the modelling system is the 3-dimensional offline Eulerian CTM FARM (Flexible Air quality Regional Model, (Silibello et al., 2008) that accounts for the transport, chemistry and removal of atmospheric pollutants.

### 3.8.2 Model geometry

For the CAMS regional forecast, the model is configured with a regular latitude-longitude grid of 0.15° ×~~*~~ 0.10° resolution. The domain spans from -25° to 45.05° degree East and from 30° to 72° degree North. The model uses z-level terrain following mesh with the first central grid point at 20 m AGL (above ground level) and the last one at 6290 m AGL. No vertical downscaling is applied to extrapolate concentrations from 20 meters above the ground to the surface.

### 3.8.3 Forcing Meteorology

The forcing meteorology is retrieved from the 12:00 UTC run of the IFS modelling system on a 0.1°x0.1° spatial grid and with a temporal resolution of one hour. The meteorological variables included are 3D fields such as temperature, relative humidity, pressure and wind velocity and 2D fields such as boundary layer height, roughness length, albedo, sea surface temperature, total cloud cover and precipitation.

### 3.8.4 Chemical initial and boundary conditions

The lateral and top boundary conditions for trace gases and aerosols are obtained from the CAMS-G~~g~~lobal daily forecasts with a 3-hr temporal resolution (see Table 2). The initial condition is taken from the previous forecast of the MINNI model.

### 3.8.5 Emissions

The common annual anthropogenic emissions CAMS-REG are implemented as explained in Section 2.5.1. Point emissions are summed up to ~~diffuse~~ gridded emissions for each GNFR sector, since no information was available about the characterization of the point sources in terms of injection height. Conservative mass horizontal interpolation has been applied to map the emissions on the actual model domain. Vertical splitting has been applied for each GNFR sector adapting the vertical injection profiles provided by TNO to the actual model levels. Temporal emission profiles for each GNFR sector, as they were provided by TNO, have been applied considering local hour (i.e. the time zones shift has been taken into account).

$PM_{2.5}$ has been speciated following the TNO table as a function of country and sector and AERO3 (Binkowski and Shankar, 1995; Binkowski, 1999) species size fractions below 2.5µm. The coarse component ($PM_{10}$-$PM_{2.5}$) was associated to non-speciated coarse mode since MINNI dispersion model considers all the secondary aerosol fraction as $PM_{2.5}$. This method leaves the detailed chemical speciation out but ensures mass conservation.

The NMVOC speciation originated from the TNO table as a function of country and sector obtaining the v01-v25 species. The mapping among the v01-v25 species to SAPRC99 species has been done in agreement with the choices made and tested in the frame of EURODELTA III intercomparison exercise (Colette et al., 2017).

Biogenic emissions are computed with the MEGAN model v.2.04 (Guenther et al., 2006), and NOx emissions from soil following (Williams et al., 1992) approach.

Erosion and resuspension of the dust are calculated by means of method proposed by (Vautard et al., 2005). Road dust emissions are parameterized following (Zender et al., 2003).

Fire emissions are taken into account using hourly data from the GFAS database considering emissions from D-1 for AN (D-1) and FC (D+0 and D+1, zero for the remaining days).

#### 3.8.6 Solver, advection and mixing

FARM is a 3-dimensional Eulerian model with first order turbulence closure. Physical and chemical processes influencing the concentration fields within the modelling domain are described by a system of partial differential equations (PDE). The numerical integration of the above system of PDEs is performed by a method that splits the multi-dimensional problem into time dependent one-dimensional problems, which are then solved sequentially over the time step.

Partial differential equations involved in horizontal and vertical advection-diffusion operators are solved in FARM using the schemes employed in CALGRID model (Yamartino et al., 1992). In particular, horizontal advection-diffusion operators are solved using a finite elements method based on Blackman cubic polynomials. The coefficients of a cell-centered cubic polynomial are constrained to maintain high-accuracy and low-diffusion characteristics and to avoid undesirable negative concentrations. In addition, a filter is used for filling undesired short wavelength minima. The numerical integration of the vertical diffusion equation is performed in a hybrid way employing a hybrid semi-implicit Crank-Nicholson / fully implicit scheme (Yamartino et al., 1992).

The calculation of horizontal diffusion coefficients is based on Stress tensor formulation of (Smagorinsky, 1963) also including a dependence on the local stability class and wind speed. For the calculation of vertical diffusion coefficients, the (Lange, 1989) approach to boundary layer scaling regimes is used. Mixing due to deep convection is not explicitly taken into account.

Two different schemes to compute the PBL scaling parameters are used. In the daytime, the (Maul et al., 1980) version of (Carson, 1973)encroachment method is used. During night-time, the minimum value between (Nieuwstadt, 1981) and (Venkatram, 1980) is used.

### 3.8.7 Deposition

The dry deposition velocities are modelled following a resistance analogy approach, as an inverse sum of a series of 3 resistances: the aerodynamic resistance, the quasi-laminar layer resistance and the surface resistance. Aerodynamic resistance is dependent on surface characteristics and atmospheric stability conditions (described through friction velocity and Monin-Obukhov length). Quasi-laminar layer resistance is parameterised using (Hicks et al., 1987). Surface resistance is approximated as a set of parallel resistance associated with leaf stomata, leaf cuticles, lower canopy and surface soil, litter and water (Wesely, 1989). Deposition to water surfaces is based on (Slinn et al., 1978) ~~work~~.

The deposition velocity of particulate species also depends on particle size distribution and density because of gravitational settling. Sedimentation velocity acts in parallel to the other resistances. Hygroscopic growth is considered over water for particles less than 2 µm. For particles ranging from 0.1 to 1 µm deposition velocity is computed as the inverse of the resistance computed from canopy height, friction velocity and Monin-Obukhov length.

The parameterization of wet deposition follows the (Simpson et al., 2012) approach, including in-cloud and below-cloud scavenging of gas and particles.

### 3.8.8 Chemistry and aerosols

The gas-phase chemical mechanism used for CAMS forecast is SAPRC-99 with the inclusion of Polycyclic aromatic hydrocarbons (PAHs) and Mercury chemistry; moreover, a simplified aqueous phase mechanism is included for $SO_2$ oxidation and chemical processes involving Mercury in both gas and aqueous phases.

A simple approach is used to estimate photolysis rates based on look-up tables to calculate the rate constants for photolysis reactions (Nenes et al., 1998). Photolysis rates are computed and adjusted according to local solar zenith angle using an empirical formula based on (Peterson, 1976) data.

The aerosols module is AERO3 (Binkowski and Shankar, 1995; Binkowski, 1999). In AERO3 the representation of the particle size is three-modal (Aitken, accumulation and coarse), following lognormal distributions. The aerosol species included are sulphate, nitrate, ammonium, anthropogenic primary and secondary organic aerosol, biogenic secondary organic aerosol, elemental carbon, sea-salt and dust. The aerosol dynamics takes into account nucleation, condensation and coagulation processes. The gas/particle mass transfer is implemented by means of ISORROPIA v1.7 (Nenes et al., 1998) and SORGAM (Schell et al., 2001a) for secondary inorganic and organic aerosol, respectively.

### 3.8.9 Assimilation system

The assimilation scheme used ~~in CAMS~~ is optimal interpolation: the correlation function is factorized in vertical and horizontal components. The horizontal component has pollutant dependent fixed correlation length with a terrain-following exponential decay. The vertical component is modelled with a Cressman function dependent on the boundary layer height. The system assimilates $NO_2$, $O_3$, $SO_2$, CO, $PM_{10}$ and $PM_{2.5}$. In case of aerosol components, the correction applied to each of them is proportional to their content in PM. At present, only data from surface stations are assimilated. More details are available in (Adani and Uboldi, 2023).

## 3.9 MOCAGE

### 3.9.1 Model Overview

The MOCAGE 3D multi-scale Chemistry and Transport Model has been designed for both research and operational applications in the field of environmental modelling. Since 2000, MOCAGE has been allowing to cover a wide range of topical issues ranging from chemical weather forecasting, tracking and backtracking of accidental point source releases, trans-boundary pollution assessment, assimilation of remote sensing measurements of atmospheric composition, to studies of the impact of anthropogenic emissions of pollutants on climate change (Guth et al., 2018; Cussac et al., 2020).

### 3.9.2 Model geometry

For the CAMS Regional Service, MOCAGE operates on a regular latitude-longitude grid at 0.1 resolution covering the 28° to 72° North and 26°W to 46°E domain, for both forecast and assimilation. The products delivered for the CAMS service are issued from the regional domain only. In the vertical, 47 hybrid levels go from the surface up to 5 hPa, with approximately 8 levels in the Planetary Boundary Layer (i.e. below 2km), 16 in the free troposphere and 24 in the stratosphere. The thickness of the lowest layer is about 40 m. There is no downscaling applied to surface concentration.

### 3.9.3 Forcing Meteorology

The forcing meteorology is retrieved from the IFS model vertical layers covering the MOCAGE vertical extent on a 0.1°x0.1° horizontal grid resolution with a temporal resolution of one hour for the 3 first forecast days and 3 hours for the last forecast day. The forecast released at 12UTC of the previous days is used. The meteorological parameters used for the dynamics calculation in MOCAGE are: horizontal and vertical winds, temperature, humidity, cloud fraction, ~~and~~ surface pressure, albedo, precipitations and incoming radiative flux. The variables relevant for the deposition module are soil humidity and temperature, wind speed and direction, specific humidity, pressure at ground level, and sensible heat flux.

### 3.9.4 Chemical initial and boundary conditions

Chemical initial values in the regional domain are provided by MOCAGE 24h forecast from the day before. The boundary conditions are taken from global CAMS operational suite for the species (chemical and aerosols) that are distributed (see Table 2). For aerosols, the 2 or 3 bins from ~~IFS~~ CAMS-Global are summed to get total concentration and then distributed onto the 6 MOCAGE bins considering Mean ~~IFS~~ CAMS-Global bin size as emission modes. A factor 4.3 is applied to convert Sea Salt from wet to dry fractions. Aerm03 (of diameter larger than 10µm) is only marginally distributed within MOCAGE $PM_{10}$ sea salt because of the matching between bins and log-normal modes. For the species not included in Table 2, the concentrations from the MOCAGE global domain are used, which helps to introduce smoothly, on the horizontal as well as on the vertical, these chemical boundary conditions into the CAMS regional domain.

### 3.9.5 Emissions

The common annual anthropogenic emissions CAMS-REG are implemented as explained in Section 3.2. Temporal disaggregation is based on the GENEMIS tables (Ebel et al., 1997), using a GNFR to SNAP matrix. Chemical disaggregation for PM species and VOCs is based on sector and country-dependent split factors proposed by TNO.

Isoprene biogenic emissions are computed online using MEGAN model (Guenther et al., 2012), while other biogenic emissions are computed from CAMS global biogenic emission inventory (version 3.1). NOx soil emissions are taken from the CAMS-GLOB-SOILv2.2 emission inventory.

Concerning biomass burning sources, GFAS emissions are emitted according to an 'umbrella' profile, with a maximum injecting height climatologically determined. GFAS "near real time" observation-based fire emissions are made available with a 8-hr delay. So that when the forecast system is initiated, most GFAS emission cover Day-2 of the forecast to be produced. As a consequence, the 2-day persistence is interpreted in a way that fire emissions are only applied for D+0.

### 3.9.6 Solver, advection and mixing

The chemical solver used is a semi-implicit solver as presented in (Cariolle and Teyssedre, 2007).

Concerning physical and chemical parameterisations, an operator splitting approach is used. Parameterisations are called alternatively in forward and reverse order, with the objective to reduce systematic errors.

Meteorological forcings are read every 3 hours from IFS input data, and are linearly interpolated to yield hourly values, which is the time-step for advection; smaller time-steps are used for physical processes and chemistry, but the meteorological variables are kept constant over each hour. MOCAGE is based upon a semi-lagrangian advection scheme (Williamson and Rasch, 1989), using a cubic polynomial interpolation in all 3 directions.

For sub-gridscale transport processes, vertical diffusion is treated following (Louis, 1979) and transport by convection is from (Bechtold et al., 2001). Scavenging within convective clouds is following (Mari et al., 2000), allowing to compute wet removal processes directly within the convective transport parameterisation. ~~Wet deposition in stratiform clouds and below clouds follows (Giorgi and Chameides, 1986).~~

### 3.9.7 Deposition

Wet deposition in stratiform clouds and below clouds follows (Giorgi and Chameides, 1986). A description of MOCAGE surface exchanges module is presented in (Michou et al., 2005). The dry deposition parameterisation relies on a fairly classical surface resistance approach (Wesely, 1989), but with a refined treatment of the stomatal resistance, similar to the one used in

Meteo-France numerical weather prediction models (Noilhan and Planton, 1989). Sedimentation of aerosol follows (Nho-Kim et al., 2004).

### 3.9.8 Chemistry and aerosols

The MOCAGE configuration for CAMS comprises 118 species and over 300 reactions and photolysis. It is a merge of reactions of the RACM scheme (Stockwell et al., 1997) with the reactions relevant to the stratospheric chemistry of REPROBUS (Lefevre et al., 1994). Aqueous chemistry for the formation of sulphate is represented, following (Ménégoz et al., 2009). Detailed heterogeneous chemistry on Polar Stratospheric Clouds (types I, II) is accounted for, as described in (Lefevre et al., 1994). Other heterogeneous chemistry processes are currently not included.

Photolysis is taken into account using a multi-entry look-up table computed off-line with the TUV software version 4.6 (Madronich, 1987). Photolysis depends on month (including monthly aerosol climatologies), solar zenith angle, ozone column above each cell (as the model extends to the mid-stratosphere, it is actually the ozone profile computed by MOCAGE which is used at every time step), altitude and surface albedo in the UV. They are computed for clear-sky conditions and the impact of cloudiness on photolysis rates is applied afterwards.

The aerosol module of MOCAGE includes the primary species dusts, black carbon, sea salts, organic carbon, and the secondary inorganic species sulphate, nitrate and ammonium. The formation and the multi-phasic equilibrium of inorganic secondary aerosols are modelled by the ISORROPIA-II module. Details on MOCAGE aerosol simulation evaluation can be found in (Martet et al., 2009) for dusts, in (Nho-Kim et al., 2005) for black carbon, and in (Sič et al., 2015) for the latest version of MOCAGE primary aerosol module. The implementation and the evaluation of secondary inorganic aerosols in MOCAGE are described by (Guth et al., 2016). Further improvements of the representation of aerosols in MOCAGE are expected in the future with on-going work regarding organic secondary aerosols.

### 3.9.9 Assimilation system

MOCAGE operations for CAMS use the assimilation system based upon MOCAGE and PALM (Lahoz et al., 2007). As a first approximation, background error standard deviations are prescribed as proportional to background amounts. In order to spread assimilation increments spatially, background error correlations are modelled using a generalized diffusion operator (Weaver and Courtier, 2001). Several assimilation strategies are available in PALM but for CAMS MOCAGE uses a 3D-VAR technique, with an assimilation window that is 1h every hour.

For surface analyses (NRT, IRA and VRA), MOCAGE assimilates $O_3$, $NO_2$, CO, $PM_{10}$ and $PM_{2.5}$ in-situ surface observations. The species are assimilated independently every hour without any cross-species covariances, and then the increments per

species are added to the analysis that serves at initial condition for computing the background of the next hour of the assimilation process, in this reanalysis mode.

An hourly assimilation cycle is also used to update the atmospheric state of aerosols, with the assimilation of French lidars (mini-MPL) and some ceilometers from the European network E-profile in the regional domain of MOCAGE. The quantity modified during the assimilation process is the 3D field of total mass of all aerosol types and all sizes all together. The split per aerosol type and particle size is not modified during the assimilation. This hourly assimilation cycle is the backbone and every day at 00 UTC, the +96h forecast is initialised from this assimilation cycle.

## 3.10 MONARCH

### 3.10.1 Model Overview

The MONARCH model is a fully online multiscale chemical weather prediction system for regional and global-scale applications (Badia and Jorba, 2015; Badia et al., 2017; Jorba et al., 2012; Klose et al., 2021; Pérez et al., 2011). The system is based on the meteorological Nonhydrostatic Multiscale Model on the B-grid (NMMB; (Janjic and Gall, 2012)), developed and widely verified at the National Center for Environmental Prediction (NCEP). The model couples online the NMMB with the gas-phase and aerosol continuity equations to solve the atmospheric chemistry processes in detail. The model is designed to account for the feedbacks among gases, aerosol particles and meteorology. Currently, it can consider the direct radiative effect of aerosols while ignoring cloud–aerosol interactions.

### 3.10.2 Model geometry

The hybrid pressure-sigma coordinate is used in the vertical direction and the Arakawa B-grid is applied in the horizontal direction. The regional model is formulated on a rotated longitude–latitude grid, with the Equator of the rotated system running through the middle of the integration domain, resulting in more uniform grid distances. In the operational regional CAMS forecasts, the model is configured for a regional domain covering Europe and part of northern Africa with a regular horizontal grid spacing on the rotated projection of 0.15º (lower-left corner at 16.37ºN 22.14ºW, upper-right corner at 58.56ºN 88.18ºE) and the top of the domain is set at 50hPa using 24 vertical layers. Surface concentrations of gases and aerosols are derived directly from the first model level; no particular vertical downscaling is implemented. The depth of the first vertical layer of the model is around 45 m and about 7 layers are set below 2 km.

### 3.10.3 Forcing Meteorology

The forcing meteorology is retrieved from the IFS model on a 0.125°x0.125° horizontal grid resolution (the native resolution is remapped as close as possible to the MONARCH grid to optimise transfer time) with a temporal resolution of 6 hours and dynamically interpolated to the final chemistry grid and time steps using the meteorological component of MONARCH. The IFS forecast released at 12:00UTC of the previous days is used. The meteorological variables obtained from IFS are: Skin temperature, Soil temperature, Soil moisture, Snow depth, Sea-ice mask, Sea-level pressure, U component of the wind, V component of the wind, Temperature, Geopotential height, Relative humidity or specific humidity, Cloud water content.

### 3.10.4 Chemical initial and boundary conditions

The variables used from chemical species available in the CAMS-Gglobal ~~IFS~~ forecast model are detailed in Table 2. Note that $CH_4$ is not used from ~~IFS~~ CAMS-Global because the MONARCH chemical mechanism considers a constant $CH_4$ concentration of 1.85 ppmv. A remapping has been applied to couple the modal distribution of the ~~IFS~~ CAMS-Global aerosols

with the aerosols distribution of the MONARCH model (see Table 2). The forecasts are initialised by the model results of the previous day.

### 3.10.5 Emissions

The common annual anthropogenic emissions CAMS-REG are implemented as explained in Section 2.5.1. The High-Elective Resolution Modelling Emission System version 3 (HERMESv3; (Guevara et al., 2019)) is used to pre-process the anthropogenic, ocean and biomass burning emissions for the MONARCH model. HERMESv3 is an open source, parallel and stand-alone multiscale atmospheric emission modelling framework that processes gaseous and aerosol emissions for use in atmospheric chemistry models.

CAMS_REG-AP NMVOC and $PM_{2.5}$ emissions are speciated using the sector and country-dependent split factors proposed by TNO. In terms of NOx, a fraction of 90% NO and 10% $NO_2$ is considered for all sectors except for road transport, in which the following fractions are applied: (i) 95% NO, 4.2% $NO_2$ and 0.8 HONO for gasoline road transport and (ii) 70% NO, 28.3% $NO_2$ and 1.7% HONO for diesel road transport (Rappenglück et al., 2013). The vertical distribution of anthropogenic emissions is performed following the sector-dependent profiles proposed by TNO. The temporal distribution follows the gridded CAMS-REG-TEMPO v4.1 profiles (Guevara et al., 2021).

The biogenic emissions for NMVOC and NO are computed on-line within the MONARCH model using the Model of Emissions of Gases and Aerosols from Nature version 2.04 (MEGANv2.04; (Guenther et al., 2006)), while monthly oceanic emissions of DMS are obtained from the CAMS-GLOB-OCEA v3.1 dataset (Granier et al., 2019; Lana et al., 2011).

Mineral dust emissions can be calculated online using one of the schemes described in (Klose et al., 2021). For sea salt aerosol emissions, multiple source functions are available (Spada et al., 2013).

Finally, biomass burning emissions (forest, grassland and agricultural waste fires) of organic carbon, black carbon, $SO_2$, and DMS are taken from the GFASv1.~~3~~4 dataset. This product reports hourly emissions at a horizontal gridded resolution of 0.1° x 0.1°. The vertical allocation of GFAS emissions is done using the maximum fire plume injection height and distributing uniformly all the emissions across the layers below this height. The persistence of the fires in forecast mode is set to 2 days, afterwards biomass burning emissions are set to zero.

### 3.10.6 Solver, advection and mixing

Different chemical processes were implemented following a modular operator splitting approach to solve the advection, diffusion, emission, dry and wet deposition, and chemistry processes. In order to maintain consistency with the meteorological solver, the chemical species are advected and mixed at the corresponding time step of the meteorological tracers following the

principles described in (Janjic and Gall, 2012) and references therein. The advection scheme is Eulerian, positive definite and monotone, maintaining a consistent mass conservation of the chemical species within the domain of study. Lateral diffusion is formulated following the Smagorinsky non-linear approach, while vertical diffusion is based on the Mellor–Yamada–Janjic level 2.5 turbulence closure scheme.

The convective mixing, however, is treated differently for aerosols and gases. The scheme implemented for aerosols is described in detail in (Pérez et al., 2011) and follows a relaxation approach similar to the Betts-Miller-Janjic convective parameterization of the NMMB. On the other hand, the convective mixing of gases is solved following the sub-grid cloud scheme of (Foley et al., 2010) as described in (Badia et al., 2017).

### 3.10.7 Deposition

The deposition processes implemented in the MONARCH model are dry deposition, in-cloud grid-scale, and in-cloud subgrid-scale scavenging for gases and aerosols, and below cloud scavenging for aerosols only.

For gases, the dry deposition scheme follows the classical deposition velocity analogy, enabling the calculation of deposition fluxes from airborne concentrations. The canopy resistance is simulated following (Wesely, 1989). The cloud-chemistry processes are included in the system considering both the sub-grid and grid-scale scheme described in (Foley et al., 2010). The processes included are the scavenging, vertical mixing and wet-deposition. Only in-cloud scavenging is considered in the current implementation (Badia et al., 2017).

Regarding aerosols, the parameterization of the aerosol dry deposition is based on (Zhang et al., 2001) which includes simplified empirical parameterizations for the deposition processes of Brownian diffusion, impaction, interception and gravitational settling. Wet scavenging of aerosols by precipitation is computed separately for convective and grid-scale (stratiform) precipitation. The model includes parameterizations for in-cloud scavenging, and for below cloud scavenging. Detailed description of the schemes can be found in (Pérez et al., 2011).

### 3.10.8 Chemistry and aerosols

A gas-phase module combined with a hybrid sectional-bulk mass-based aerosol module is implemented in the MONARCH model. The gas-phase chemical mechanism used is the Carbon Bond 2005 chemical mechanism (CB05; (Yarwood. G. et al., 2005)) extended with Chlorine chemistry (Sarwar et al., 2012). The rate constants were updated based on evaluations from (Atkinson et al., 2004; Sander et al., 2006). The photolysis scheme used is the Fast-J scheme (Wild et al., 2000). It is coupled with physics of each model layer (e.g., aerosols, clouds, absorbers as ozone) and it considers grid-scale clouds from the atmospheric driver.

The aerosol module in MONARCH model solves the life cycle of sea salt, dust, organic matter (both primary and secondary), black carbon, sulphate, and nitrate aerosols. While a sectional approach is used for dust and sea salt, a bulk description of the other aerosol species is adopted. A simplified gas–aqueous–aerosol mechanism accounts for sulphur chemistry (Spada, 2015). The production of secondary nitrate–ammonium aerosol is solved using the thermodynamic equilibrium model EQSAM (Metzger et al., 2002). The coarse nitrate production is computed with an uptake reaction of $HNO_3$ on dust and sea salt coarse particles. The formation of SOA is considered using a simple non-volatile scheme accounting for the contribution of anthropogenic, biomass burning, and biogenic formation (Pai et al., 2020). Hygroscopic growth is considered for all aerosol components except mineral dust.

### 3.10.9 Assimilation system

The MONARCH assimilation system (MONARCH-DA) is based on a Local Ensemble Transform Kalman Filter (LETKF) scheme (Di Tomaso et al., 2022; Di Tomaso et al., 2017; Escribano et al., 2022; Hunt et al., 2007; Miyoshi and Yamane, 2007; Schutgens et al., 2010) coupled to the model through I/O routines. MONARCH ensemble is created by perturbing anthropogenic, biomass burning, soil and ocean emissions that are pre-processed by HERMESv3 or that are modelled by MONARCH via a physically-based scheme for dust aerosol. For analysis production in CAMS, MONARCH ensemble is run at a horizontal resolution of 0.2° latitude × 0.2° longitude in a rotated grid and initialised by the ensemble forecast of the previous day.

Hourly surface observations from in-situ measurements are currently assimilated operationally for $O_3$, $NO_2$, $SO_2$, CO, $PM_{10}$, $PM_{2.5}$. For near-real time operational analysis production, previous-day observations are combined with a MONARCH 24-hour ensemble forecast initialised at 12 UTC of the previous day.

## 3.11 SILAM

### 3.11.1 Model Overview

The System for Integrated modeLling of Atmospheric coMposition SILAM (silam.fmi.fi) is a global-to-sub-km chemistry transport model developed for a wide range of atmospheric composition and air quality assessment tasks (Sofiev et al., 2015b), emergency decision support applications (Sofiev et al., 2008), and data assimilation and source inversion problems (Vira and Sofiev, 2015; Sofiev et al., 2013). The model incorporates Eulerian and Lagrangian dispersion frameworks (the Eulerian transport routine is used for CAMS) and a set of chemical and physical transformation modules for the troposphere and the stratosphere (Carslaw et al., 1995; Damski et al., 2007; Yarwood. G. et al., 2005; Sofiev, 2000; Sofiev et al., 2010). Apart from the transport and physico-chemical cores described below, SILAM includes a set of supplementary tools including a meteorological pre-processor, input-output converters, reprojection and interpolation routines, etc. In the operational forecasts, these enabled direct forcing of the model by the ECMWF IFS meteorological fields.

SILAM has been extensively evaluated in a variety of regional and global air quality projects (Brasseur et al., 2019; Huijnen et al., 2010; Kouznetsov et al., 2020; Petersen et al., 2019; Sofiev et al., 2015b; Xian et al., 2019) and health impact assessment studies (Korhonen et al., 2008; Kukkonen et al., 2020; Lehtomäki et al., 2018).

### 3.11.2 Model geometry

The centre points of the model grid cover 25.05°W to 44.95°E and 30.05°N to 71.95°N on a regular latitude longitude grid of 0.1°resolution. Following (Sofiev, 2002), SILAM uses a multi-vertical approach with the meteorology-resolving grid corresponding to the tropospheric part of the IFS vertical: hybrid levels from 69 to 137. The chemical transformations and vertical fluxes are computed based on 10 thick staggered layers, with the thickness increasing from 25 m for the lowest layer to 1000-2000 m in the free troposphere. The layer tops are located at 25, 75, 175, 375, 775, 1500, 2700, 4700, 6700 and 8700m above the surface. Within the thick layers, the sub-grid information is used to evaluate the weighted averages of the high-resolution meteorological parameters and effective diffusion coefficients after (Sofiev, 2002).

### 3.11.3 Forcing Meteorology

Meteorological forcing is the ECMWF IFS operational forecasts taken from the 12:00UTC forecast of the previous day extracted at a resolution of 0.1° and temporal frequency of one hour for the first 72 hours and three hours for the last day of the forecast. The list of meteorological parameters extracted is: U and V components of 10m wind [m/s], 2m temperature [K], dew point temperature 2m [K] accumulated large scale rain [kg/m$^2$], accumulated convective rain [kg/m$^2$], surface roughness [m], total cloud cover [fract], convective available potential energy [J/kg], U and V -wind components at model levels [m/s],

temperature at model levels [K], cloud water at model levels [kg/kg], cloud ice at model levels [kg/kg], specific humidity at model levels [kg/kg], cloud cover at model levels[fract], logarithm of surface pressure.

### 3.11.4 Chemical initial and boundary conditions

Boundary conditions are taken from the CAMS-Global ~~-IFS~~ (see Table 2). The full fields are imported every 3 hours; in-between, the linear interpolation is applied. The forecasts are initialised with the SILAM forecast of the previous day.

### 3.11.5 Emissions

The common annual anthropogenic emissions CAMS-REG are implemented as explained in Section 3.2. The $PM_{2.5}$ emissions are split into EC, OC and mineral components, and OC is mapped to the volatility bins according to (Shrivastava et al., 2008). Emissions of biogenic VOCs, wind-blown dust, and sea salt are computed online in dedicated SILAM modules (Poupkou et al., 2010; Sofiev et al., 2011; Soares et al., 2016; Sofieva et al., 2022). GFAS hourly emissions from wild-land fires are replicated from D-2 to D+1 for forecast and shut down after; in the analysis mode it is used as is.

Emissions of 6 pollen species are computed online following the heat-sum approach for trees (Sofiev et al., 2015b), climatological season for grasses and mugwort species, and multi-criteria hybrid model for ragweed (Prank et al., 2013).

### 3.11.6 Solver, advection and mixing

The SILAM Eulerian transport core (Sofiev et al., 2015a) is based on the coupled developments: refined advection scheme of (Galperin and Sofiev, 1994) and vertical diffusion and dry deposition algorithm of (Sofiev, 2002)and (Kouznetsov and Sofiev, 2012). The methods are compatible, in a sense that both use the same set of variables to determine the sub-grid distribution of tracer mass. The approach, in particular, allows computing correct vertical exchange using high-resolution input data but low-resolution chemistry and diffusion grids. The later feature is used in the vertical setup with thick layers.

Diffusion is parameterised following the first-order K-theory based closure. Horizontal diffusion is embedded into the advection routine, which itself has zero numerical viscosity, thus allowing full control over the diffusion fluxes. The vertical diffusivity parameterisation follows the approach suggested by (Groisman and Genikhovich, 1997) and (Sofiev et al., 2010). The procedure diagnoses all the similarity theory parameters using the profiles of the basic meteorological quantities: wind, temperature and humidity. Output includes the value of eddy diffusivity for scalars at some reference height (taken to be 1m).

The model uses process-wise splitting and 1-D advection implementation flipping the order of processes every other time step.

### 3.11.7 Deposition

Dry deposition parameterisation for gases generally follows the resistive analogy of (Wesely, 1989). Deposition velocities for aerosols are evaluated using the original (Kouznetsov and Sofiev, 2012) algorithm. Wet deposition parameterisation is based on the scavenging coefficient after (Sofiev, 2000) for gas species and follows the generalised formulations of (Kouznetsov and Sofiev, 2012) for aerosols.

### 3.11.8 Chemistry and aerosols

The main gas-phase chemical mechanism is CB05 with additions for SOx from (Sofiev, 2000) and organics from VBS (Volatility-Basis Set, (Shrivastava et al., 2008)). The heterogeneous scheme is an updated version of the DMAT model scheme (Sofiev, 2000). The formation pathways of secondary inorganic aerosols follow the VBS approach extended with the feedback to the main gas-phase chemical module. The aerosol size distribution is represented via sectional approach, with species-specific bin selections. Each bin is characterised with its lower and upper borders, as well as the mass-mean diameter, which is precomputed / predefined for each bin and species from its size spectrum. Primary anthropogenic aerosols are emitted into bins with mass-mean diameter of 0.5 μm (fine aerosol, dry size) and 6 μm (coarse aerosols, dry size). Secondary inorganic aerosols were put into 0.2 and 0.7 μm bins, plus a separate 3 μm bin for coarse nitrates formed on the sea salt surface. The dust size spectrum is described with 4 bins from 0.3 μm up to 20 μm. Finally, the seasalt spectrum is represented with 5 bins, from 0.05 μm up to 20 μm of mass-mean nominal diameter. Throughout computations, the particles are transported in accordance with their mass-mean diameter corrected with regard to actual humidity and the particle solubility. External mixing is assumed.

### 3.11.9 Assimilation system

The embedded data assimilation is based on the 3d- and 4d-dimensional variational approach, as well as with the EnKF (Vira and Sofiev, 2012, 2015). Tangent-linear (if needed) and adjoint formulations exist for the transport module, the transformation schemes and for the deposition modules. The assimilation procedure has been tested for both initialising the concentration fields and for refinement of the emission (Sofiev, 2019). The observation operators exist for in-situ observations and for the vertically integrated columns observed by the nadir-looking satellites. For the near-real time operational analyses in CAMS, the previous-day observations are used in a 3D-VAR data assimilation suite. That routine assimilates in-situ observations of $NO_2$, $O_3$ and $PM_{2.5}$, $PM_{10}$, $SO_2$ and CO.

# 4 Post-processing

## 4.1 ENSEMBLE model

All eleven individual operational model ~~results~~ deliver their results to the CRPU (Météo-France for NRT/FC and NRT/AN, and INERIS for IRA and VRA, using the product definition introduced in Section 2.2). An ENSEMBLE model is subsequently computed as a median of all available operational models. As explicated in Section 3, there are slight differences in the individual model geometry even if they are as close as possible to the common grid. Five models are operated their forecasts directly on the target grid (CHIMERE, DEHM, EMEP, LOTOS-EUROS, and SILAM), one uses area-weighted interpolation of overlapping polygon (EURAD-IM), and the other models use a bilinear interpolation ~~requirement~~ to deliver model output on the common ~~same~~ grid. The ENSEMBLE is computed across all models at each horizontal and vertical grid point of the common grid. Each of the model deliver the full list of required ~~and for each~~ species.

Relying on 11 different models offers a very comprehensive view on the various possible representations of key atmospheric processes relevant to air quality (see the wide range of modelling design detailed in Section 3) and thus a characterisation of the intrinsic modelling uncertainty. The flipside of this diversity is a relatively higher risk of one model not being able to deliver in a timely basis. A median ENSEMBLE is computed everyday no matter how many models are successfully delivered for that given day. A Key Performance Indicator is documented to track the number of models which have delivered on time to be included in the ENSEMBLE for either the analyses or the forecasts (Figure 2~~1~~). The fact that timeliness of forecast delivery is higher than for analyses might seem counterintuitive as forecast are expected earlier, but this is due to the fact that most analyses are produced later due to the late availability of assimilated observations, and not necessarily used at present as initial conditions of the forecast.

Using the median to compute such an ensemble is a very robust approach to cope with potential missing members, and it has been shown to outperform individual models for average performances (Galmarini et al., 2004). It is however a very conservative approach and developments are ongoing, in particular to improve the skills of the system to capture air quality exceedance detections by making use of machine learning algorithm coupled to the raw CAMS regional forecasts. Firstly, optimised forecasts at observation sites are produced operationally for 4 pollutants (PM10, PM2.5, NO2 and O3) at thousands of AQ e-reporting stations throughout Europe on a daily basis and for the 96hr forecast period. This product is referred to as CAMS-MOS (Model Output Statistics)[7]. The underlying algorithm is a random forest using as predictor air pollutant concentration in the ENSEMBLE CTM as well as meteorological variables (temperature at 2m, relative humidity, wind speed and boundary layer height) (Bertrand et al., 2022). It is trained on a daily basis using the past 3 days of observations. As such,

[7]https://confluence.ecmwf.int/display/CKB/CAMS+Regional%3A+European+Air+Quality+Forecast+Optimised+at+Observation+Sites+data+documentation (accessed 24 April 2025)

CAMS-MOS is a statistical model of the meteorological dependant ENSEMBLE error, which proved very effective in improving the forecast skills in detecting exceedances of air quality information thresholds. Second, an weighted ensemble forecast at the same resolution as the CTMs (10x10km2) has been developed. It consists of an optimum weighting of the 11 models calibrated on the past 7 days, but in this case the weights are constant and uniform and not dependent on meteorological predictors. CAMS-MOS is already available in the ADS as an operational product. But the weighted ensemble is still experimental. With the rapid development of machine learning and artificial intelligence, such experimental products will be further developed in the future.

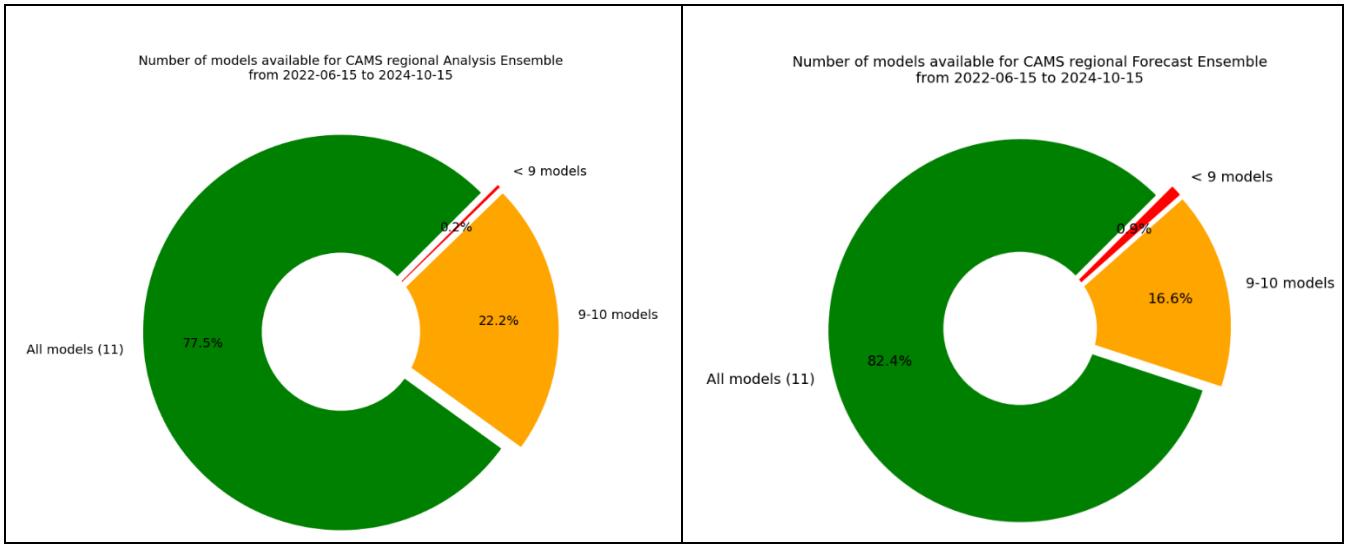


*Figure 2: Distribution of the number of operational models having delivered on time to be included in the ENSEMBLE computation for the period 15/06/2022-15/10/2024: left NRT/AN (analysis) and right: NRT/FC (forecasts).*

### 4.2 Evaluation and Quality Control (EQC)

Evaluation and quality control is an essential part of CAMS in order to ensure the reliability and transparency of the products. For all the chemical species where a dense enough monitoring network allows a recurrent and statistically significant evaluation, synthetic performance reports are produced and made available on the CAMS website[8]. These evaluations focus primarily on the surface in-situ air quality regulatory monitoring networks for $O_3$, $NO_2$, $PM_{10}$, and $PM_{2.5}$. For the assimilated products, the evaluation is performed on about one third of the stations, deliberately left out of the assimilation workflow (Section 2.3). The forecasts are evaluated using all available surface stations whose spatial representativity ranges from rural to urban background air quality. The skill scores are updated on a daily frequency and available publicly through an interactive interface on the CAMS EQC pages for the ENSEMBLE and individual models. Quarterly summaries are produced in publicly

[8] https://atmosphere.copernicus.eu/regional-services, last accessed 30/10/2024

available reports. They also include an evaluation of the models in the troposphere against above-surface measurements (aircraft and space borne remote sensing and profiling). For the Interim and Validated reanalyses, the evaluation reports are produced on an annual basis.

The present article is essentially a description of the system rather than a detailed analysis of its performance. Nevertheless, we present here several ~~a couple of~~ evaluation diagnostics for illustration purposes. Therefore, the performances of individual models contributing to the ENSEMBLE are anonymised as it would be too complex to enter here in the details of the performances of each model, which relate to intrinsic parametrisations. Such analysis is left for a dedicated future publication, but the interested user can also consult the interactive viewers and reference public reports on the Evaluation and Quality Control website to analyse the performances of individual models.

In Figure 3 we show the root mean square error for surface ozone and $PM_{10}$ taken as the median over each quarter since the beginning of the CAMS production at the end of 2014 and over hundreds of European air quality monitoring stations. The figure is divided in two parts as urban background stations were only included in the evaluation as of fall 2018 (note also that the vertical scales differ). It appears clearly that while the spread of the models was still substantial in the first part of the period, the system has reached a level of maturity since 2017 with more homogeneous performances between the various models and very few outliers. The ENSEMBLE model appears to give better scores overall. It can be surpassed in terms of RMSE in some occasions but not always by the same model, therefore still illustrating the added value of the multi-model ensemble approach. The range of performances is today about 12-18µg/m$^3$ for the RMSE (root mean square error) of daily maxima ozone, so that the Key Performance Indicator of 18µg/m$^3$ is not always met depending on the models and the season. For $PM_{10}$, the RMSE is between 5 to 8µg/m$^3$ so that the same KPI of 18µg/m$^3$ is usually met. Without entering in a more detailed analysis, it is visible that the scores are still gradually improving over the 2018-2023 period. Over the recent years, the median ENSEMBLE seems to produce more systematically better performances and becomes more difficult to beat.

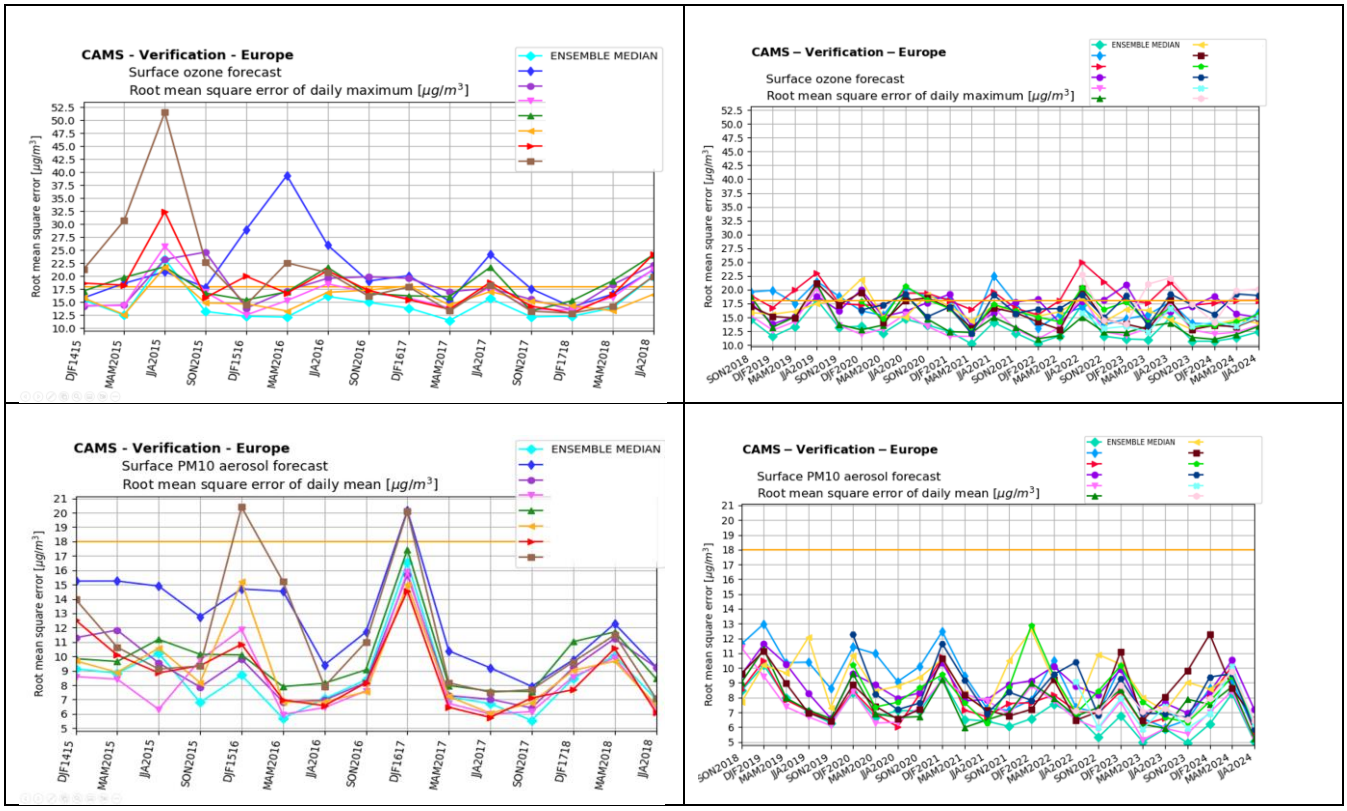


*Figure 3: Evolution of the skill scores of the CAMS Regional Air Quality Forecasts (individual models and ENSEMBLE median) between 2014 and 2024 (divided in two parts: before and after 2018 as urban background stations were not included in the evaluation over the first period, and fewer models were available) Each point is the quarterly median of the RMSE (µg/m$^3$) computed at regulatory air quality monitoring stations for top: daily maximum ozone and bottom: daily mean $PM_{10}$. The straight yellow line corresponds to the Key Performance Indicator for RMSE of 18µg/m$^3$.*

In the European Air Quality regulation, detrimental air quality situations are identified in terms of various exceedance levels depending on the air pollutants. For $PM_{10}$, the daily mean concentrations should not exceed 50µg/m$^3$ more than 35 days (EC, 2008). The performance of the CAMS Regional reanalyses in capturing that threshold can be assessed through the performance diagram presented in Figure 4. On the x-axis the success ratio is the number of hits divided by the number of hits and false alarms. On the y-axis, the probability of detection is the number of hits divided by the number of hits and misses. The dashed lines provide the frequency bias defined as the ratio of the total number of predicted exceedances to the total number of observed exceedances. For this example, for the year 2021, the ENSEMBLE median has the best success ratio, but some individual models outperform in terms of probability of detection. It is not possible to point one single model which would outperform systematically the ENSEMBLE (the best performing model will vary depending on the targeted pollutant, threshold, geographic area, etc.). Therefore the reference product remains the median ENSEMBLE which provides the best

scores for conservative annual average metrics, but interested users can refer to the annual evaluation report to select alternative depending on their specific needs.

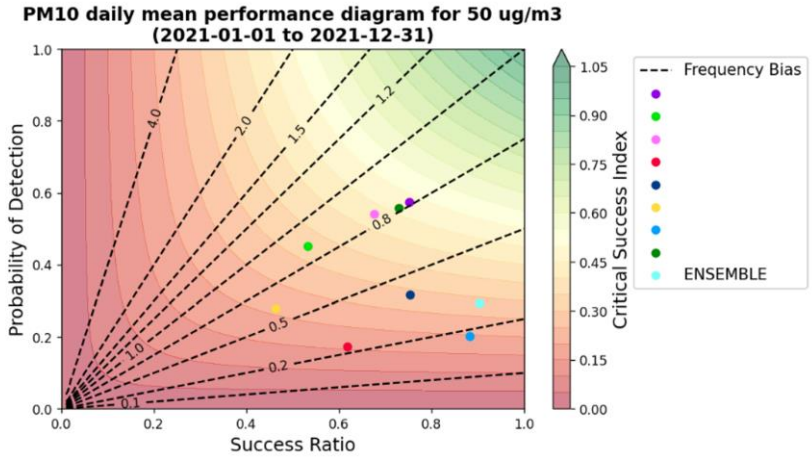


*Figure 4: Performance of the CAMS Regional ENSEMBLE and individual models reanalyses in capturing air quality threshold detection for daily mean $PM_{10}$ above 50µg/m$^3$ in 2021.*

An illustration of the evaluation above the surface is provided in Figure 5. The ~~total~~ tropospheric column of $NO_2$ in the CAMS regional ENSEMBLE forecast is compared to the observations from the TROPOMI instrument on board the Sentinel 5p~~P~~ satellite. The higher spatial resolution (approximately 5km) available since the launch of the instrument allows reaching out to urban level $NO_2$ concentrations therefore providing an excellent opportunity for the evaluation of spatial patterns of air pollution. Beyond surface and total columns, it is also essential to assess the performances of the vertical structure as illustrated for the comparison with ozone soundings in Belgium (Uccle). Here both the regional forecast and analyses are compared to assess the impact of surface assimilation of air quality measurement on the vertical profiles. The CAMS global model forecast is also included along with the CAMS regional ensemble range for the forecast and the analysis. A more detailed analysis of the comparison with satellite data can be found in (Douros et al., 2022).

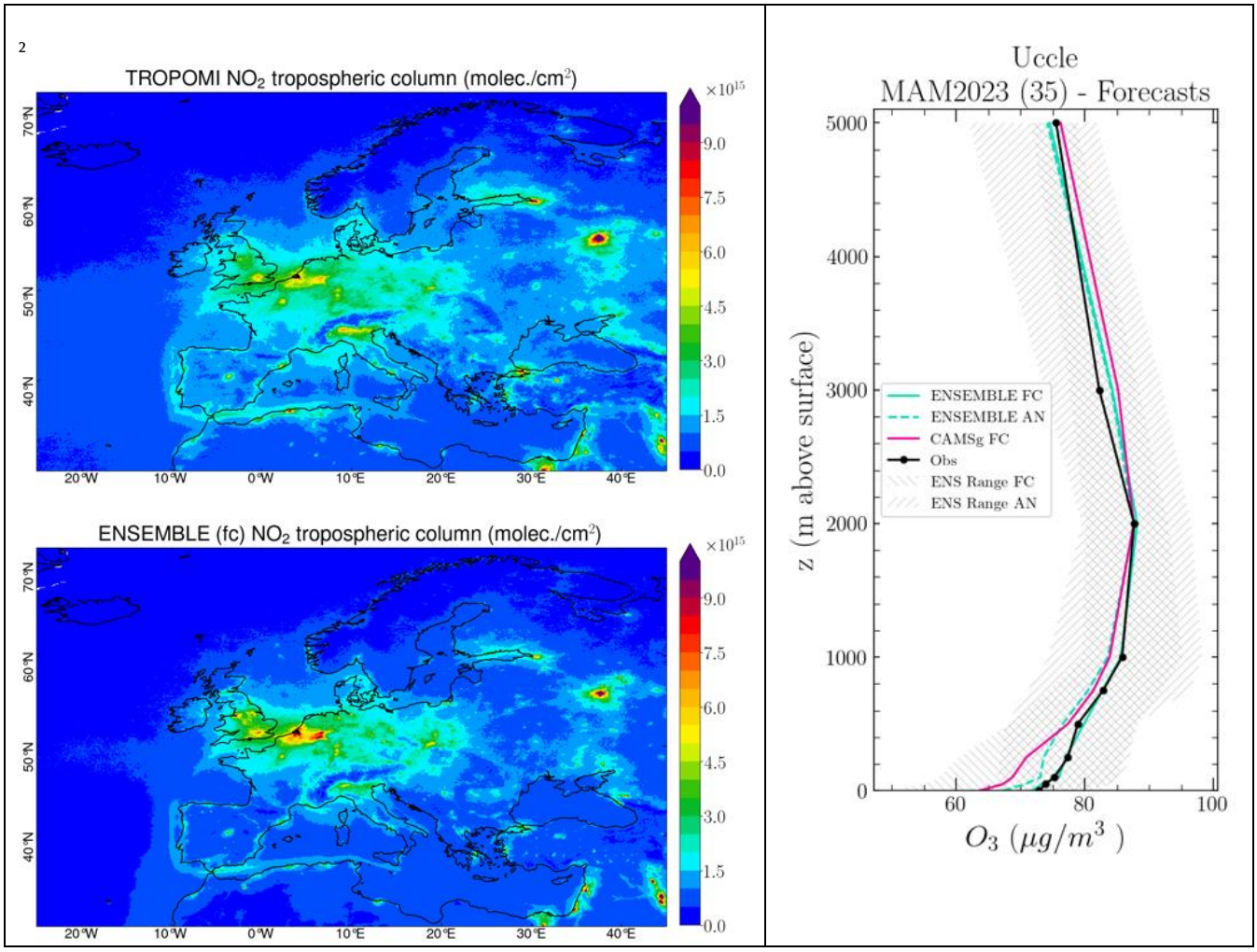


*Figure 5: Left: Evaluation over MAM-2023 of the CAMS Regional ensemble forecasts against TROPOMI satellite $NO_2$ tropospheric columns ($10^{15}$ molecules/$cm^2$). The CAMS $NO_2$ profiles have been multiplied with the TROPOMI kernels to remove the dependency on the retrieval a-priori profile shape. Right: Regional and global CAMS forecast and regional analyses of ozone compared to vertical profiles measured with ozone sondes over Uccle, Brussels, Belgium for MAM-2023 (μg/$m^3$). source: CAMS2_83 Evaluation and Quality Control Service, https://atmosphere.copernicus.eu/regional-services*

### 4.3 Dissemination and further use of the CAMS Regional Products

The results of the CAMS regional production system are made available publicly on the website https://atmosphere.copernicus.eu/european-air-quality-forecast-plots where maps and time series of the various air pollutant and pollen species can be displayed. The results of the median ENSEMBLE as well as each individual model are available for both forecast and analysis products with a three years retention time. Daily means, daily maxima, and hourly fields are available. The list of vertical levels available for interactive plotting on the website is: surface, 100m, 1000m, 3000m and

5000m (note that more vertical levels are available on the ADS). The model spread can also be assessed by selecting any grid point in the map to display the time series of the 4 day forecast including modelled dispersion which provides an information on the uncertainty in the ensemble forecast (Figure 6).

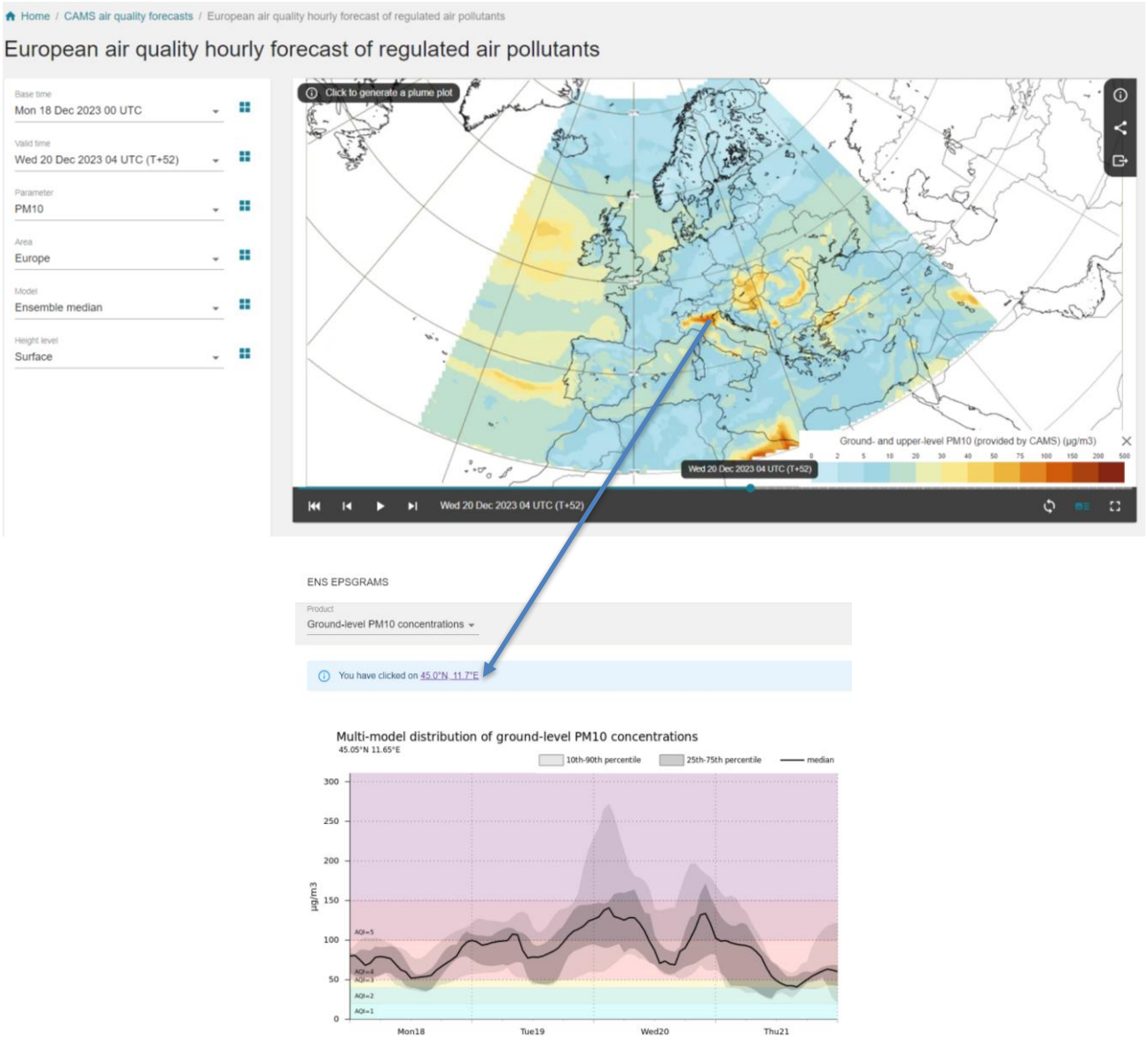


*Figure 6: Screenshot of the CAMS Regional Production website displaying air quality forecasts over Europe (atmosphere.copernicus.eu6)*

The Copernicus Atmosphere Data Store (ADS) constitutes an important dissemination pathway for the CAMS Regional production system. All the numerical data can be freely retrieved through the website ads.atmosphere.copernicus.eu where automated requests can be built to download entire fields or custom extractions in either grib or netcdf formats.

The typical use of CAMS Regional forecast product is for national and local air quality management agencies to understand the day-to-day air quality situation and anticipate major air pollution events. This can be done either by a qualitative analysis of quicklooks available on the CAMS website or external companies that have developed alternative visualisation tools.

The numerical data obtained on the ADS can also be used as background information for national or local scale air quality modelling applications. Such uses range from the nesting of a Chemistry Transport Model as three-dimensional and hourly concentrations of several chemical species are available in the CAMS Regional Forecast. They can also be used to feed gaussian city-scale surface air quality models. There are also reported uses of the CAMS Regional Forecast to inform machine-learning air quality statistical prediction tools (Bertrand et al., 2022; Petetin et al., 2022).

The use of CAMS Regional reanalyses is rather to inform longer term air quality applications. They can be used as background information for land-use regression models used in air quality policy products or exposure assessment for health impact studies (Horálek et al., 2022). They are also the primary source of information for the Interim Assessment Report produced annually by the CAMS Policy Service and serves as background information for European Member States in the Regulatory Air Quality reporting obligations (Hamer et al., 2023).

## 5 Conclusion & Perspectives

The regional production of the Copernicus Atmosphere Monitoring Service is today a well-established reference for air quality forecast and analysis in Europe~~an~~ and beyond. It is constituted of a unique ensemble of eleven European Chemistry-Transport models operated in ten countries under the management of a Centralised Regional Production Unit. The system follows strict requirements in order to produce consistent air quality products through the ensemble of individual CTM. Those requirements include in particular forcing fields such as meteorology, chemical hemispheric boundary conditions, and surface fluxes of anthropogenic and wildfire emissions. But the added value of the use of an ensemble of models also lies in the diversity of the modelling strategy. As of today, the ensemble offers a very wide array of choices in terms of model design and structure, as well as regarding the formulation of underlying physical and chemical processes or forcing and coupling at the interfaces (land, sea, biosphere, …).

In the present paper, we provide a comprehensive scientific documentation of the technical characteristics for the common forcing requirements as well as the diversity in modelling design brought about by the individual contributing modelling

groups. We also explained how the billions of data produced on a daily basis are aggregated centrally, evaluated and disseminated for a wide range of air quality applications. The CAMS Service has been operational since the end of 2014 and has reached today a high level of performance and stability. Since 2017 the spread of model performances has converged and it continues to improve gradually over the years.

As an operational service, the Regional Production of CAMS follows closely the research developments in the field of air quality modelling. A substantial part of the model development is undertaken independently by the modelling teams through various research projects and PhD work at national level. The international benchmarking activities (such as the AQMEII or Eurodelta initiatives, (Galmarini et al., 2017; Colette et al., 2017)) are also an important source of information to identify model development priorities. More recently, the European Union has launched a series of research projects devoted to the Evolution of Copernicus in the Horizon Europe Programme[9].

In order to ensure a continuous improvement, the system follows a regular development cycle. The individual models are improved in time so that they remain in the state of the art of chemistry transport modelling. When the progress becomes mature enough, system upgrades are scheduled on a bi-annual basis to allow individual modelling groups to bring their development into the operational model version. These bi-annual upgrades are also the opportunity to carry coordinated changes, such as the regular update of anthropogenic emission fluxes. Through these upgrades, the portfolio of products is also continuously expanding. For instance, in addition to the 19 chemical species already being delivered, the current plan at the time of submission of the present article (i.e. for the year 2024) is to include new PM species such as ammonium nitrate and a tracer of shipping emissions.

A large part of the research effort in relation to the Regional Production is related to Chemistry-Transport deterministic modelling. But there are also interesting prospects in the coupling between machine learning and physical and chemical modelling. The Regional Service already produces operationally optimised ~~is about to launch operational~~ forecasts at station level on the basis of Model Output Statistics which relies on ~~or any other~~ Machine Learning ~~Postprocessing which promises~~ to offer ~~open~~ unprecedented performance in particular for air quality threshold detection (Bertrand et al., 2022). Novel methodologies to compute the ENSEMBLE model from the eleven individual production and move away from the conservative median approach are also under consideration.

Besides the modelling developments, the uptake of innovative observations is also instrumental in the long-term perspective of CAMS. The production of deposition fluxes is a good illustration of the need to make the best of available observations. While CTMs are producing by nature deposition fluxes, they are not systematically quality checked and therefore the output

[9] https://atmosphere.copernicus.eu/copernicus-research-whats-horizon

products are limited at present to ambient air concentrations. A mid-term development is therefore ongoing to benchmark wet and dry deposition fluxes to ensure their robustness. To achieve this, CAMS relies on the network of deposition data collected in the EMEP network of rural supersites in Europe. But there are also promising prospects in the uptake of near-real-time advanced observations of atmospheric composition at the supersites of the ACTRIS European Research Infrastructure, in particular with regards to particulate matter chemical composition and source apportionment. Lastly, in the outlook of the future perspectives there are also high expectations regarding the uptake of geostationary satellite retrievals with the perspective of the launch of the Sentinel 4 satellite which will bring unprecedented high-frequency atmospheric composition information over Europe.

## 6 Data Availability

Copernicus is funded under the Copernicus Regulation and operated by ECMWF under the ECMWF Agreement. Access to all Copernicus (previously known as GMES or Global Monitoring for Environment and Security) Information and Data is regulated under Regulation (EU) No 1159/2013 of the European Parliament and of the Council of 12 July 2013 on the European Earth monitoring programme, under the ECMWF Agreement and under the European Commission's Terms and Conditions. Access to all Copernicus information is regulated under Regulation (EU) No 1159/2013 and under the ECMWF Agreement.

The Copernicus Licence is free of charge, worldwide, non-exclusive, royalty free and perpetual. Access to Copernicus Products is given for any purpose in so far as it is lawful, whereas use may include, but is not limited to: reproduction; distribution; communication to the public; adaptation, modification and combination with other data and information; or any combination of the foregoing.

The full terms of the Copernicus Licence are available at: https://ads.atmosphere.copernicus.eu/api/v2/terms/static/licence-to-use-copernicus-products.pdf

## 7 Code Availability

Following the Copernicus Programme Data Policy, the Regional Production data and information are available on a full, open, and free-of-charge basis, subject to limitations concerning registration, dissemination formats, and access restrictions. The Copernicus Atmosphere Data Store is located at: https://ads.atmosphere.copernicus.eu/.

The CHIMERE ~~v2020~~ model is available to registered users through the ~~on its~~ dedicated website at https://www.lmd.polytechnique.fr/chimere/, the actual version used in CAMS is ~~,~~ available at https://zenodo.org/records/14724119~~and for download at https://doi.org/10.14768/8afd9058-909c-4827-94b8-69f05f7bb46d~~.

The DEHM model used in CAMS is available at https://zenodo.org/records/14628278~~for collaborative requests to J. H. Christensen; jc@envs.au.dk~~.

The EMEP model is available at https://github.com/metno/emep-ctm under the GPLv3 licence. The model version for CAMS is updated once or twice a year in the frame of the regular updates in the CAMS regional service. The current version is ~~close to the one archived on~~ https://zenodo.org/records/14507729~~https://doi.org/10.5281/zenodo.4230110~~.

The EURAD-IM version 5.11.1 source code used in CAMS is https://doi.org/10.5281/zenodo.15198902. ~~is not publicly available for download, but code and data are available on request by e-mail.~~

The GEM model is a free software that can be redistributed and/or modified under the terms of the GNU Lesser General Public License published by the Free Software Foundation. It is available on a repository administered by Environment and Climate Change Canada at https://github.com/ECCC-ASTD-MRD/gem/. GEM-AQ includes an additional source code tree accessed via an interface routine in GEM. The GEM-AQ code used in CAMS is available at https://zenodo.org/records/14720848.

~~The air quality part of the GEM-AQ model code is available upon request from the Institute of Environmental Protection. The meteorological part of the GEM-AQ model is available from Environment and Climate Change Canada (https://github.com/ECCC-ASTD-MRD).~~

The LOTOS-EUROS model is available to registered users ~~upon user request~~ from the website https://airqualitymodeling.tno.nl/lotos-euros/open-source-version/ the version used in CAMS is available at https://zenodo.org/records/14711996.

The MATCH model as used in CAMS is available at https://zenodo.org/records/14719885~~Access for implementation is only granted to the extent it is needed for the Parties concerned to carry out their tasks in the CAMS2_40 project and provided that SMHI can grant Access Rights to the MATCH CTM (Chemistry Transport Model), including version control, build environment, scripting system for production, and the legal restrictions or limits. This includes limitations imposed on licenses of software and data. Access Rights are subject to written request. The Access Rights are granted for the purpose of the CAMS Project only and may be restricted if this results in the infringement of third party rights. All commercial and third party software are excluded and no Access Rights are granted~~.

The FARM code embedded in the MINNI System as used in CAMS is available at https://zenodo.org/records/14650298 ~~https://hpc-forge.cineca.it/projects/open/20~~

The MOCAGE source code used in CAMS is ~~not publicly~~ available at https://doi.org/10.5281/zenodo.14625973~~for download, but code and data are available on request by e-mail~~.

The MONARCH model is available at https://earth.bsc.es/gitlab/es/monarch under the GPLv3 licence. The version used in CAMS is https://zenodo.org/records/5215467.

The SILAM code is available at https://github.com/fmidev/silam-model under the GPLv3 licence. The model is updated several times a year, including two CAMS-related updates. The version used in CAMS is https://zenodo.org/records/14608973~~The GitHub release follows the most recent operational release~~.

## 8 Author Contribution

AC designed and drafted the overall manuscript and coordinated all contributions.

GC, FB, EB, VG, FM, AR, VP, CM, OF, AJ, VHP and LR contributed to drafting the centralised production specifics and general review of the draft.

MA, JA, AB, RB, DB, JB, GB, AC, JHC, FC, IDE, MDI, GD, EDT, JD, JE, HF, YF, JF, EF, LF, MG, CG, GG, MG, AG, JG, RH, MK, JWK, RKo, RKr, ACL, JL, VL, FM, AM, MM, AN, MO, CPGP, JP, AP, BR, LR, AS, MS, PS, DS, MS, AS, JS, CT, RT, TT, ST, ST, AUn, AUp, AV, PvV, LV, ZY contributed to draft the specificities of individual model description.

HE contributed to draft the text on model evaluation

JK, HdvG: contributed to draft the text on emissions.

MR, OF, VP, AR, EB, provided plots and figures

## 9 Competing Interest

The authors declare that they have no conflict of interest.

## 10 Acknowledgements

The activities described in this paper have been funded by the Copernicus Atmosphere Monitoring Service. ECMWF implements the Copernicus Atmosphere Monitoring Service and the Copernicus Climate Change Service with funding from the European Union on behalf of the European Commission.

INERIS acknowledged the support of the French Ministry in Charge of Ecology for continuous support in developing the CHIMERE model and related air quality forecasting activities.

FMI acknowledges the support of Academy of Finland projects PS4A (grant 318194) and ALL-Impress (grant 329215) for the pollen module developments.

The computing resources and the related technical support for MINNI forecast are provided by CRESCO/ENEAGRID High Performance Computing infrastructure and its staff. CRESCO/ENEAGRID High Performance Computing infrastructure is funded by ENEA, the Italian National Agency for New Technologies, Energy and Sustainable Economic Development and by Italian and European research programmes (see http://www.cresco.enea.it/english).

*Table 1: Overview of the main characteristics and configurations of the eleven chemistry-transport models as used in the CAMS Regional Production*

| | | CHIMERE | DEHM | EMEP | EURAD-IM | GEM-AQ | LOTOS-EUROS | MATCH | MINNI | MOCAGE | MONARCH | SILAM |
|---|---|---|---|---|---|---|---|---|---|---|---|---|
| **Discretisation** | **Horizontal resolution** | 0.1° x 0.1° regular lat-lon | 0.1° x 0.1° regular lat-lon | 0.1° x 0.1° regular lat-lon | 9x9 km Lambert conformal | 0.1° x 0.1° lat-lon spherical grid | 0.1° x 0.1° regular lat-lon | 0.1° x 0.1° regular lat-lon | 0.15° x 0.1° regular lat-lon | 0.1° x 0.1° regular lat-lon | 0.15° x 0.15° rotated regular lat-lon | 0.1° x 0.1° regular lat-lon |
| | **number of vertical levels** | 9 | 29 | 20 | 23 | 28 | 12 | 26 | 14 | 47 | 24 | 10 |
| | **top altitude** | 500hPa | 100hPa | 100hPa | 100hPa | 10hPa | 200hPa | 8000m | 7040m | 5hPa | 50hPa | 8700m |
| | **depth of lowermost layer** | 20m | 20m | 50m | 35m | 20m | 20m | 45m | 40m | 40m | 40m | 25m |
| | **number of lower layers** | 7 below 2km | 12 below 1km | 10 in PBL | 15 below 2km | 14 below 5km | 7 below 1km | 10 below 850hPa | 8 below 1km | 8 below 2km | 7 below 2km | 5 below 1km |
| **Initial & boundary conditions & meteorology** | **Meteorological driver** | D-1 00:00 UTC IFS, 3hrly | D-1 12:00 UTC IFS, 3hrly | D-1 12:00 UTC IFS, 3hrly | D-1 12:00 UTC IFS for FC, IFS analysis for AN, 3hrly for FC, 6hrly for AN, downscaled with WRF | D-1 12:00 UTC IFS, 3hrly | D-1 00:00/12:00 UTC IFS, 3hrly | D-1 12:00 UTC IFS, 3hrly | D-1 12:00 UTC IFS, 1hrly | D-1 12:00 UTC IFS for FC, 1hrly (from +00h to +72h), 3hrly (from +72h to +96h) ; D00:00 UTC IFS for AN, 1hrly | D-1 12:00 UTC IFS, 6hrly, downscaled with NMMB | D-1 12:00 UTC IFS, 1hrly (from +00h to +72h), 3hrly (from +72h to +96h) |

| | | CHIMERE | DEHM | EMEP | EURAD-IM | GEM-AQ | LOTOS-EUROS | MATCH | MINNI | MOCAGE | MONARCH | SILAM |
|---|---|---|---|---|---|---|---|---|---|---|---|---|
| | **Boundary values** | CAMS-Global ~~IFS~~ | CAMS-Global ~~IFS~~ | CAMS-Global ~~IFS~~ | CAMS-Global ~~IFS~~ | CAMS-Global ~~IFS~~ | CAMS-Global ~~IFS~~ | CAMS-Global ~~IFS~~ | CAMS-Global ~~IFS~~ | CAMS-Global ~~IFS~~+ MOCAGE global for additional species | CAMS-Global ~~IFS~~ | CAMS-Global ~~IFS~~ & SILAM |
| | **Initial values** | Previous forecast | Previous forecast | Previous analysis | Previous forecast | Previous forecast | Previous forecast | Previous forecast | Previous forecast | Previous forecast | Previous forecast | Previous forecast |
| **Emissions anthropogenic** | **Inventory** | CAMS-REG v6.1 REF2 2022 | CAMS-REG v6.1 REF2 2022 | CAMS-REG v6.1 REF2 2022 | CAMS-REG v6.1 REF2 2022 | CAMS-REG v6.1 REF2 2022 | CAMS-REG v6.1 REF2 2022 | CAMS-REG v6.1 REF2 2022 | CAMS-REG v6.1 REF2 2022 | CAMS-REG v6.1 REF2 2022 | CAMS-REG v6.1 REF2 2022 | CAMS-REG v6.1 REF2 2022 |
| | **Temporal disaggregation** | TNO | CAMS-REG-TEMPO_v4.1 | CAMS-REG-TEMPO_v4.1 | CAMS-REG-TEMPO_v4.1 | CAMS-REG-TEMPO_v4.1 | CAMS-REG-TEMPO_v4.1 | GENEMIS | CAMS-REG-TEMPO_v3.2 | GENEMIS | CAMS-REG-TEMPO_v4.1 | TNO |
| **Emissions: natural & biogenic** | **in-domain soil and road dust emissions** | (Marticorena and Bergametti, 1995) | none | (Marticorena and Bergametti, 1995; Marticorena et al., 1997; Dabdub and Seinfeld, 1994; Gomes et al., 2003; Fécan et al., 1998) Road dust emissions currently switched off. | Based on DREAM model | (Marticorena and Bergametti, 1995) | (Marticorena and Bergametti, 1995) and soil moisture inhibition as in (Fécan et al., 1998) | Road dust from (Schaap et al., 2009) and (Omstedt et al., 2005) and mineral dust based on the DEAD model of (Zender et al., 2003) (mainly attributed to the Mediterranean area). | Erosion and resuspension from (Vautard et al., 2005), soil suitable for mobilization parameterized following (Zender et al., 2003) | (Ginoux et al., 2001) and ECOCLIMAP database | Mineral dust scheme based on (Klose et al., 2021) and (Pérez et al., 2011) | SILAM dust source, SILAM sea salt source, Silam BIO-VOC source |

| | | CHIMERE | DEHM | EMEP | EURAD-IM | GEM-AQ | LOTOS-EUROS | MATCH | MINNI | MOCAGE | MONARCH | SILAM |
|---|---|---|---|---|---|---|---|---|---|---|---|---|
| | **in-domain sea-salt emissions** | (Martensson et al., 2003) (Monahan, 1986) | (Martensson et al., 2003) (Monahan, 1986) | (Martensson et al., 2003) (Monahan, 1986; Tsyro et al., 2011) | (Sofiev et al., 2011) | (Gong et al., 2003) | (Martensson et al., 2003) {Monahan, 1986 #822 | (Sofiev et al., 2011) | (Zhang et al., 2005) | (Sič et al., 2015) | (Jaeglé et al., 2011) | (Sofiev et al., 2011) |
| | **Birch, Grass, Olive, Ragweed,** | yes | yes | yes | yes | yes | yes | yes | yes | yes | yes | yes |
| | **Biogenic emissions** | MEGAN V2.10 (Guenther et al., 2012) | MEGAN v2.04 (Guenther et al., 2006) | (Simpson et al., 2012) | MEGAN V2.10 (Guenther et al., 2012) | MEGAN-MACC climatology | (Guenther et al., 1993) with detailed tree types for Europe | (Simpson et al., 2012) | MEGAN v2.04 (Guenther et al., 2006) | CAMS-GLOB-BIOv3.1 (Sinderalova et al, 2022) isoprene from MEGAN v2.04 (Guenther et al., 2006) | MEGAN v2.04 (Guenther et al., 2006) | Dynamic biogenic, (Poupkou et al., 2010) |
| | **Soil NOx** | MEGAN V2.10 (Guenther et al., 2012) | GEIA (Yienger and Levy, 1995) | CAMS-GLOB-SOIL v2.4 (Simpson et al., 2023) | MEGAN V2.10 (Guenther et al., 2012) | none | (Yienger and Levy, 1995) | none | (Williams et al., 1992) | CAMS-GLOB-SOILv2.2 (Simpson et al, 2021) | MEGAN v2.04 (Guenther et al., 2006) | none |
| | **Wildfires emissions** | Hourly emissions from D-2 cycled for AN (D-1) and FC (D+0 and D+1, zero for the remaining days) | last available 24h cycle over D-2 and D-1 cycled for AN (D-1) and FC (D+0 and D+1, zero for the remaining days) | Hourly emissions from D-2 cycled for AN (D-1) and FC (D+0 and D+1, zero for the remaining days) | last available 24h cycle over D-2 and D-1 cycled for AN (D-1) and FC (D+0 and D+1, zero for the remaining days) | last available 24h cycle over D-2 and D-1 cycled for AN (D-1) and FC (D+0 and D+1, zero for the remaining days) | Hourly emissions from D-2 cycled for AN (D-1) and FC (D+0 and D+1, zero for the remaining days) | Hourly emissions from D-1 for AN (D-1) and last available 24h from D-2 and D-1 cycled for FC (D+0 to D+4) | Hourly emissions from D-1 for AN (D-1) and FC (D+0 and D+1, zero for the remaining days) | Hourly emissions from D-2 cycled for AN (D-1) and FC (D+0 and D+1, zero for the remaining days) | Hourly emissions from D-2 cycled for AN (D-1) and FC (D+0 and D+1, zero for the remaining days) | Hourly emissions from D-2 cycled for AN (D-1) and FC (D+0 and D+1, zero for the remaining days) |

| | | CHIMERE | DEHM | EMEP | EURAD-IM | GEM-AQ | LOTOS-EUROS | MATCH | MINNI | MOCAGE | MONARCH | SILAM |
|---|---|---|---|---|---|---|---|---|---|---|---|---|
| Chemistry/Physics | Gas phase chemistry | MELCHIOR2 (Derognat et al., 2003), 44 gaseous species and 120 reactions | Modified (Strand and Hov, 1994), 74 species and 158 reactions | EmChem 19a, (Bergström et al., 2022) 127 species and 198 reactions (Simpson et al., 2020a) | RACM-MM (Geiger et al., 2003) | Modified ADOM IIB mechanism, 51 species and 120 reactions | Modified CBM-IV (Schaap et al., 2004) | EmChem 09 (Simpson et al., 2012) and (Langner et al., 1998) | SAPRC 99 (Carter, 2000) | RACM (tropospheric) and REPROBUS (stratospheric) | CB05 (Yarwood. G. et al., 2005) | CBM-IV |
| | Heterogeneous chemistry | Conversion of NO2 into HNO3 and N2O5 and Conversion of HO2 into H2O2 | Oxidation of NO2 by O3 on aerosols | Aerosol-uptake of HNO3, HO2 and to NO3 and O3 and hydrolysis of N2O5(Stadtler et al., 2018) | Hydrolysis of N2O5 | Hydrolysis of N2O5 | Hydrolysis of N2O5 | Hydrolysis of N2O5, aerosol uptake of HNO3 and CH3O2H | none | only relevant for polar stratospheric clouds | Hydrolysis of N2O5 and aerosol uptake of HNO3 on dust and sea salt | Sofiev (2000) |
| | Aerosol size distribution | 10 bins from 10 nm to 40 µm | 2 size fractions: PM2.5 and coarse fraction of PM10 | 2 size fractions: PM2.5 and coarse fraction of PM10 | 3 log-normal modes: 2 fine + 1 coarse | 12 bins from 10nm to 20.5µm | 5 size bins for dust and sea-salt, 2 size bins for other aerosols | 2 size fractions: PM2.5 and coarse fraction of PM10 | 3 log3 log-normal model: Aitken, accumulation and coarse | 6 bins | 8 bins for dust and sea salt. Fine mode for BC, OM, SO4 and NH4. Coarse and fine mode for NO3 | 2 bins, except for dust (4 bins from 10nm to 30µm) and sea salt (5 bins from 10nm to 30µm) |

| | | CHIMERE | DEHM | EMEP | EURAD-IM | GEM-AQ | LOTOS-EUROS | MATCH | MINNI | MOCAGE | MONARCH | SILAM |
|---|---|---|---|---|---|---|---|---|---|---|---|---|
| | **Inorganic aerosols** | (Couvidat et al., 2018): Thermodynamic equilibrium for particles under 1 µm and a dynamic approach for particles above 1 µm. Thermodynamic for the H+-NH4+-SO42--NO3--Na+-Cl--H2O system is based on ISORROPIA 2.1. | (Frohn, 2004) | MARS (Binkowski and Shankar, 1995), thermodynamic equilibrium for the SO4-HNO3-NO3-NH3-NH4-H2O system | thermodynamic equilibrium for the H+-NH4+-SO42--NO3--H2O system (Friese and Ebel, 2010) | (Gong et al., 2003) | ISORROPIA-2 (Fountoukis and Nenes, 2007) | (Mozurkewich, 1993) | ISORROPIA v1.7 (Nenes et al., 1998) | ISORROPIA-2 (Guth et al., 2016) | EQSAM (Metzger et al., 2002) | (Sofiev, 2000) |
| | **Secondary organic aerosols** | (Bessagnet et al., 2009) | VBS approach (NPAS scheme of (Bergström et al., 2012a)) | VBS approach (NPAS scheme, (Bergström et al., 2012a; Simpson et al., 2012)) | updated SORGAM module (Li et al., 2013) | (Jiang, 2003) | not included | VBS schemes for ASOA and BSOA (Bergström et al., 2012a)) (Hodzic et al., 2016) | SORGAM (Schell et al., 2001b) | (Castro et al., 1999) | non-volatile scheme for anthropogenic, biogenic and pyrogenic precursors (Pai et al., 2020) | VBS |
| | **Aqueous phase chemistry** | SO2 oxidation by O3 and H2O2 | SO2 oxidation by O3 and H2O2 (Jonson et., 2000) | SO2 oxidation by ozone and H2O2 and metal ion-catalyzed O2(Jonson et al., 2000) | 10 gas/aqueous phase equilibria, 5 irreversible S(IV) -> S(VI) transformations | SO2 oxidation | SO2 oxidation | SO2 oxidation | SO2 oxidation (Seinfeld and Pandis, 1998) | SO2 oxidation | SO2 oxidation by ozone and H2O2 | SO2 oxidation, nitrate formation (Sofiev, 2000), heterogeneous nitrate formation on sea salt particles |

| | | CHIMERE | DEHM | EMEP | EURAD-IM | GEM-AQ | LOTOS-EUROS | MATCH | MINNI | MOCAGE | MONARCH | SILAM |
|---|---|---|---|---|---|---|---|---|---|---|---|---|
| | **Dry deposition: gases** | resistance approach (Wesely, 1989) | resistance approach (Simpson et al., 2003; Emberson et al., 2000a) | resistance approach, including non-stomatal deposition of NH3 (Simpson et al., 2012) | resistance approach (Zhang et al., 2003) | resistance approach | resistance approach (Erisman et al., 1994) | resistance approach (Simpson et al., 2012) | resistance approach (Wesely, 1989) | resistance approach (Michou et al., 2005) | resistance approach (Wesely, 1989) | resistance approach (Wesely, 1989) |
| | **Dry deposition: aerosols** | gravitational settling | gravitational settling (Simpson et al., 2003; Emberson et al., 2000a) | (Simpson et al., 2012; Venkatram and Pleim, 1999) | resistance approach (Petroff and Zhang, 2010) | gravitational settling | (Zhang et al., 2001) | resistance approach (Simpson et al., 2012) | gravitational settling (Binkowski and Shankar, 1995) | (Sič et al., 2015) | (Zhang et al., 2001; Pérez et al., 2011) | (Kouznetsov and Sofiev, 2012) |
| | **Wet deposition** | In-cloud scavenging for all gas/aerosols is taken into account. Below cloud by rain and snow falls is taken into account for soluble gas (HNO3, H2O2) and particles | (Simpson et al., 2003) | In-cloud and sub-cloud scavenging ratios for gases; in-cloud scavenging ratios and sub-cloud scavenging efficiencies for aerosols. (Berge, 1993; Simpson et al., 2012) | CMAQ (Salameh et al., 2007) | Below cloud scavenging for soluble gas species and aerosols | (Banzhaf et al., 2012) | gases: species dependent in-cloud and sub-cloud scavenging ratios; particles: in-cloud scavenging ratio, sub-cloud scavenging (Berge, 1993) and (Simpson et al., 2012) | (Simpson et al., 2003) | Convective: (Mari et al., 2000) Stratiform: (Giorgi and Chameides, 1986),(Slinn et al., 1978; Slinn, 1983) | (Foley et al., 2010; Pérez et al., 2011) | SILAM |
| **Assimilation** | **Assimilation method** | Kriging-based analysis | 3D-Var | Intermittent 3d-var | Intermittent 3d-var | Optimal Interpolation | ENKF | Intermittent 3d-var | Optimal Interpolation | 3D VAR | LETKF (Di Tomaso et al., 2017) | Intermittent 3d-var |

| | | CHIMERE | DEHM | EMEP | EURAD-IM | GEM-AQ | LOTOS-EUROS | MATCH | MINNI | MOCAGE | MONARCH | SILAM |
|---|---|---|---|---|---|---|---|---|---|---|---|---|
| | **Assimilated surface pollutants** | NO2, O3, PM2.5, PM10, CO, SO2 | NO2, O3, CO, SO2, PM2.5, PM10 | NO2, O3, SO2, CO, PM2.5, PM10 | NO2, O3, CO, SO2, PM2.5, PM10 | NO2, O3, PM2.5, PM10, CO, SO2 | NO2, O3, PM2.5, PM10 | NO2, O3, CO, SO2, PM2.5, PM10 | NO2, O3, CO, SO2, PM2.5, PM10 | NO2, O3, PM2.5, PM10 | NO2, O3, CO, SO2, PM2.5, PM10 | NO2, O3, CO, SO2, PM2.5, PM10 |
| | **assimilated satellite** | none | none | NO2 (OMI) until 2021, currently disabled | currently none | none | NO2 (OMI) until 2021 | none | none | ground-based lidars from French network, ceilometers from e-profile, SO2 Tropomi | none | none |
| | **Assimilation of concentrations** | Yes | Yes | Yes | Yes | Yes | None | Yes | Yes | Yes | Yes | Yes |
| | **Assimilation of emissions** | None | None | None | None | None | Yes | None | None | None | None | None |
| | **Assimilation of deposition** | None | None | None | None | None | Yes | None | None | None | None | None |
| | **Assimilation of other processes** | None | None | None | None | None | Ozone top boundary | None | None | None | None | None |

| | | CHIMERE | DEHM | EMEP | EURAD-IM | GEM-AQ | LOTOS-EUROS | MATCH | MINNI | MOCAGE | MONARCH | SILAM |
|---|---|---|---|---|---|---|---|---|---|---|---|---|
| | **Frequency of assimilation** | Hourly | Hourly | Hourly | Hourly | Hourly | Hourly | Hourly | Hourly | Hourly | Hourly | Hourly |

1561

*Table 2: Overview of the matching between chemical species used as boundary conditions from the CAMS-Global ~~IFS~~ model and the eleven regional models of the CAMS Regional production*

| ~~IFS~~ CAMS-Global | CHIMERE | DEHM | EMEP | EURAD | GEM-AQ | LOTOS EUROS | MATCH | MINNI | MOCAGE | MONARCH | SILAM |
|---|---|---|---|---|---|---|---|---|---|---|---|
| aermr01 (wet) (sea salt 0.03-0.5 µm radius) | sea salt bins 3 to 5 | SS_25= aermr01/ 4.3+ 0.5*aermr02/4.3 | SS_25= aermr01/ 4.3+ 0.5*aermr02/4.3 | not used | not used | SS bins 1=aermr01/4.3 (where SS_25 = SS bin 1 and 2) | SS_25=aermr01/4.3+0.4*aermr02/4.3 | SS bin [1-2.5µm] = aermr01/ 4.3+0.40 *aermr02 /4.3 | SS bins 1-6 = aermr01/ 4.3 | SS bin 1=0.34*aermr01/4.3 SS bin 2=0.30*aermr01/4.3 + 0.02*aermr02/4.3 | SS bin 0.5µm = aermr01/ 4.3 |
| aermr02 (wet) (sea salt 0.5-5 µm radius) | sea salt bins 6 to 8 | SS_co= 0.5*aermr02/4.3 | SS_co=0.5*aermr02/4.3 | not used | not used | SS bins 2=0.1*aermr02/4.3 SS bins 3=0.2*aermr02/4.3 SS bins 4=0.4*aermr02/4.3 SS bins 5=0.3*aermr02/4.3 | SS_co=0.6*aermr02/4.3 | SS bin [2.5-10µm] = 0.60*aermr02/4.3 | SS bins 1-6 = aermr02/ 4.3 | SS bin 3=0.13*aermr02/4.3 SS bin 4=0.18*aermr02/4.3 SS bin 5=0.35*aermr02/4.3 SS bin 6=0.32*aermr02/4.3+ 0.06*aermr03/4.3 | SS bin 3µm = aermr02/ 4.3 |
| aermr03 (wet) (sea salt 5-20 µm radius) | sea salt bin 9 | not used | not used | not used | not used | not used | not used | not used | SS bins 1-6 = aermr03/ 4.3 | SS bin 7=0.40*aermr03/4.3 SS bin 8=0.54*aermr03/4.3 | SS bin 9µm = 0.5*aermr02/4.3 SS bin 20µm = 0.5*aermr02/4.3 |
| aermr04 (dust 0.03-0.55 µm radius) | dust bins 4 to 6 | DUST_25=aermr04+ aermr05 | DUST_25= aermr04+ aermr05 | DUST_acc=0.05 total ~~IFS~~ CAMS-Global dust, DUST_coa=0.95 total CAMS-Global~~IFS~~ dust | dust bins 3-7 | dust bin 1 = 0.2*aermr04+ 0.2*aermr05 dust bin 2 = 0.8*aermr04+ 0.8*aermr05 | dust_25= aermr04+ aermr05+ 0.11*aermr06 | dust bin [1-2.5µm] = aermr04+ aermr05+ aermr06* 0,11 | Dust bins 1-6 | DUST bin 1 = 0.03 * aermr04 DUST bin 2 = 0.14 * aermr04 | Dust 0.3µm = 0.4*aermr04 Dust 1.5µm = 0.6*aermr04 |

| | | | | | | | | | | | |
|---|---|---|---|---|---|---|---|---|---|---|---|
| aermr05 (dust 0.55-0.9 µm radius) | dust bin 7 | not used | DUST_25= aermr04+ aermr05 | DUST_acc=0.05 total ~~IFS~~ CAMS-Global dust, DUST_coa=0.95 total CAMS-Global~~IFS~~ dust | dust bins 8 | | dust_25= aermr04+ aermr05+ 0.11*aermr06 | used above in dust bin [1-2.5um] | Dust bins 1-6 | DUST bin 3 = 0.82 * aermr04 + 0.11 * aermr05 | Dust 6µm = aermr05 |
| aermr06 (dust 0.9-20 µm radius) | dust bins 7 to 10 | DUST_co = 0,4*aermr06 | DUST_co =0,4*aermr06 | DUST_acc=0.05 total ~~IFS~~ CAMS-Global dust, DUST_coa=0.95 total CAMS-Global~~IFS~~ dust | dust bins 9-12 | dust bin 3 = 0.08*aermr06 dust bin 4 = 0.16*aermr06 dust bin 5 = 0.16*aermr06 | dust_co= 0.44*aermr06 | dust bin [2.5-10µm] = aermr06* 0,44 | Dust bins 1-6 | DUST bin 4 = 0.89 * aermr05 + 0.01 * aermr06 DUST bin 5 = 0.11 * aermr06 DUST bin 6 = 0.23 * aermr06 DUST bin 7 = 0.50 * aermr06 DUST bin 8 = 0.14 * aermr06 | Dust 6µm = 0.4*aermr06 Dust 20µm = 0.6*aermr06 |
| aermr07 hydrophilic OM | PPM bins 3 to 6 | not used | not used | 80% accumulation mode, 20% Aitken mode | OC bins 1-12 | POM_25 | EC_25=0.7*aermr07; EC_co=0.15*aermr07 | AORPA bin 0-1µm = 0,00050* aermr07+ 0,00050* aermr08 AORPA bin 1-2.5µm = 0,44955* aermr07+ 0,44955* aermr08 AORA bin 0-1µm = 0,00050* aermr07 + 0,00050* aermr08 AORA | OC bins 1-6 | hydrophilic POM | Non-volatile bin of organic aerosol |

| | | | | | | | | | | | |
|---|---|---|---|---|---|---|---|---|---|---|---|
| | | | | | | | | bin 1-2.5µm = 0,49950* aermr07 + 0,49950* aermr08 | | | |
| aermr08 hydrophobic OM | PPM bins 3 to 6 | not used | not used | 80% accumulation mode, 20% Aitken mode | OC bins 1-12 | POM_25 | EC_25=0.7*aermr08; EC_co=0.15*aermr08 | AORB bin 0-1µm = 0,00010* aermr07 + 0,00010* aermr08 AORB bin 1-2.5µm = 0,09990* aermr07 + 0,09990* aermr08 | OC bins 1-6 | hydrophobic POM | Non-volatile bin of organic aerosol |
| aermr09 hydrophilic BC | PPM bins 3 to 6 | BCfresh | not used | 70% accumulation mode, 30% Aitken mode | BC bins 1-12 | EC_25 | OC_25=0.7*aermr09 OC_co=0.15*aermr09 | AEC bin 0-1µm = 0,0011*aermr09+0,001*aermr10 | BC bins 1-6 | hydrophilic BC | EC |
| aermr10 hydrophobic BC | PPM bins 3 to 6 | BCaged | not used | 70% accumulation mode, 30% Aitken mode | BC bins 1-12 | EC_25 | OC_25=0.7*aermr10 OC_co=0.15*aermr10 | AEC bin 1-2.5µm = 0,999*aermr09+0,999*aermr10 | BC bins 1-6 | hydrophobic BC | EC |
| aermr11 Sulphate Aerosol | SO4 bins 3 to 6 | SO4 | SO4 | 90% accumulation mode, 10% Aitken mode | SO4 bins 1-12 | SO4_25 | SO4 | SO4 bin 0-1µm = 0,001*aermr11 SO4 bin 1-2,5µm = 0,999*aermr11 | MOCAGE-global | SO4 | SO4 split equaly on 2 modes |
| aermr16 Nitrate fine mode | not used | not used | NO3_F (0-2.5 µm) | 90% accumulation mode, 10% | not used | NO3_25 | NO3_f | NO3 bin 0-1µm = 0,001*aermr16 NO3 bin | MOCAGE-global | not used | not used |

| | | | | | | | | | | | |
|---|---|---|---|---|---|---|---|---|---|---|---|
| | | | | Aitken mode | | | | 1-2,5µm = 0,999*aermr16 + 0,55*aermr17 | | | |
| aermr17 Nitrate coarse mode | not used | not used | NO3_C (2.5-10 µm) | not used | not used | NO3_co | NITRATE(coarse) | Coarse unspecified =0.45*aermr17 | MOCAGE-global | not used | not used |
| aermr18 Ammonium | not used | not used | NH4_F (0-2.5 µm) | 90% accumulation mode, 10% Aitken mode | not used | NH4_25 | NH4_f | NH4 bin 0-1µm = 0,001*aermr18 NH4 bin 1-2,5µm = 0,999*aermr18 | MOCAGE-global | not used | not used |
| aerm19 Biogenic SOA | OM | OM | not used | not used | BSOA | not used | SOA | BSOA | BSOA | not used | BSOA |
| aerm20 Anthropogenic SOA | OM | OM | not used | not used | ASOA | not used | SOA | ASOA | ASOA | not used | ASOA |
| CHOCHO (Glyoxal) | CHOCHO | not used | CHOCHO | CHOCHO | CHOCHO | not used | CHOCHO | CHOCHO | CHOCHO | not used | CHOCHO |
| C2H6 (ethane) | C2H6 | C2H6 | C2H6 | C2H6 | C2H6 | not used | C2H6 | ALK1 | MOCAGE-global | C2H6 | 2xPAR5 |
| C5H8 (isoprene) | C5H8 | C5H8 | C5H8 | C5H8 | C5H8 | C5H8 | C5H8 | C5H8 | MOCAGE-global | C5H8 | C5H8 |
| CH4_c (methane) | CH4 | not used | CH4 | not used | CH4 | CH4 | CH4 | CH4 | MOCAGE-global | not used | not used |

| | | | | | | | | | | | |
|---|---|---|---|---|---|---|---|---|---|---|---|
| CO (carbon monoxide) | CO | CO | CO | CO | CO | CO | CO | CO | CO | CO | CO |
| GO3 (ozone) | O3 | O3 | O3 | O3 | O3 | O3 | O3 | O3 | O3 | O3 | O3 |
| H2O2 (hydrpogen peroxyde) | not used | not used | not used | H2O2 | H2O2 | not used | seasonal climatological conc used | not used | MOCAGE-global | H2O2 | not used |
| HCHO (formaldehyde) | HCHO | HCHO | HCHO | HCHO | HCHO | HCHO | HCHO | HCHO | MOCAGE-global | HCHO | HCHO |
| HNO3 (nitric acid) | HNO3 | HNO3 | HNO3 | HNO3 | HNO3 | HNO3 | HNO3 | HNO3 | MOCAGE-global | HNO3 | HNO3 |
| NO (nitrogen monoxide) | not used | NO | NO | NO | NO | NO | NO | NO | MOCAGE-global | NO | NO |
| NO2 (nitrogen dioxide) | NO2 | NO2 | NO2 | NO2 | NO2 | NO2 | NO2 | NO2 | MOCAGE-global | NO2 | NO2 |
| PAN (Peroxyacetyl nitrate) | PAN | PAN | PAN | PAN | PAN | PAN | PAN | PAN | MOCAGE-global | PAN | PAN |
| SO2 (Sulphur dioxide) | SO2 | SO2 | SO2 | SO2 | SO2 | SO2 | SO2 | SO2 | SO2 | SO2 | SO2 |

1564

1565

## References


Aamaas, B., Peters, G. P., and Fuglestvedt, J. S.: Simple emission metrics for climate impacts, Earth Syst. Dynam., 4, 145-170, 2013.

Ackermann, I. J., Hass, H., Memmesheimer, M., Ebel, A., Binkowski, F. S., and Shankar, U.: Modal aerosol dynamics model for Europe: development and first applications, Atmospheric Environment, 32, 2981-2999, http://dx.doi.org/10.1016/S1352-2310(98)00006-5, 1998.

Adani, M. and Uboldi, F.: Data assimilation experiments over Europe with the Chemical Transport Model FARM, Atmospheric Environment, 306, 119806, 2023.

Alfaro, S. C. and Gomes, L.: Modeling mineral aerosol production by wind erosion: Emission intensities and aerosol size distributions in source areas, Journal of Geophysical Research: Atmospheres, 106, 18075-18084, 2001.

Andersson-Sköld, Y. and Simpson, D.: Comparison of the chemical schemes of the EMEP MSC-W and IVL photochemical trajectory models, Atmospheric Environment, 33, 1111-1129, 1999.

Atkinson, R., Baulch, D. L., Cox, R. A., Crowley, J. N., Hampson, R. F., Hynes, R. G., Jenkin, M. E., Rossi, M. J., and Troe, J.: Evaluated kinetic and photochemical data for atmospheric chemistry: Volume I - gas phase reactions of Ox, HOx, NOx and SOx species, Atmos. Chem. Phys., 4, 1461-1738, 10.5194/acp-4-1461-2004, 2004.

Badia, A. and Jorba, O.: Gas-phase evaluation of the online NMMB/BSC-CTM model over Europe for 2010 in the framework of the AQMEII-Phase2 project, Atmospheric Environment, 115, 657-669, 2015.

Badia, A., Jorba, O., Voulgarakis, A., Dabdub, D., Pérez García-Pando, C., Hilboll, A., Gonçalves, M., and Janjic, Z.: Description and evaluation of the Multiscale Online Nonhydrostatic AtmospheRe CHemistry model (NMMB-MONARCH) version 1.0: gas-phase chemistry at global scale, Geoscientific Model Development, 10, 609-638, 2017.

Baklanov, A. and Sørensen, J.: Parameterisation of radionuclide deposition in atmospheric long-range transport modelling, Physics and Chemistry of the Earth, Part B: Hydrology, Oceans and Atmosphere, 26, 787-799, 2001.

Banzhaf, S., Schaap, M., Kerschbaumer, A., Reimer, E., Stern, R., van der Swaluw, E., and Builtjes, P. J. H.: Implementation and evaluation of pH-dependent cloud chemistry and wet deposition in the chemical transport model REM-Calgrid, Atmos. Environ., 49, 2012.

Barbu, A., Segers, A., Schaap, M., Heemink, A., and Builtjes, P.: A multi-component data assimilation experiment directed to sulphur dioxide and sulphate over Europe, Atmospheric Environment, 43, 1622-1631, 2009.

Bechtold, P., Bazile, E., Guichard, F., Mascart, P., and Richard, E.: A mass-flux convection scheme for regional and global models, Quarterly Journal of the Royal Meteorological Society, 127, 869-886, 2001.

Berge, E.: Coupling of wet scavenging of sulphur to clouds in a numerical weather prediction model, Tellus B: Chemical and Physical Meteorology, 45, 1-22, 1993.

Bergström, R., Hayman, G. D., Jenkin, M. E., and Simpson, D.: Update and comparison of atmospheric chemistry mechanisms for the EMEP MSC-W model system — EmChem19a, EmChem19X, CRIv2R5Em, CB6r2Em, and MCMv3.3Em, The Norwegian Meteorological Institute, Oslo, Norway, 2022.

Bergström, R., Denier Van Der Gon, H., Prévôt, A. S., Yttri, K. E., and Simpson, D.: Modelling of organic aerosols over Europe (2002–2007) using a volatility basis set (VBS) framework: application of different assumptions regarding the formation of secondary organic aerosol, Atmospheric Chemistry and Physics, 12, 8499-8527, 2012a.

Bergström, R., Denier van der Gon, H. A. C., Prévôt, A. S. H., Yttri, K. E., and Simpson, D.: Modelling of organic aerosols over Europe (2002–2007) using a volatility basis set (VBS) framework: application of different assumptions regarding the formation of secondary organic aerosol, Atmos. Chem. Phys., 12, 8499-8527, doi:10.5194/acp-12-8499-2012, 2012b.

Bertrand, J. M., Meleux, F., Ung, A., Descombes, G., and Colette, A.: Technical note: Improving the European air quality forecast of Copernicus Atmosphere Monitoring Service using machine learning techniques, Atmos. Chem. Phys. Discuss., 2022, 1-28, 10.5194/acp-2022-767, 2022.

Bessagnet, B., Brignon, J.-M., Le Gall, A.-C., Meleux, F., Schucht, S., and Rouïl, L.: Politiques combinées de gestion de la qualité de l'air et du changement climatique (partie 1): enjeux, synergies et antagonismes, INERIS, Verneuil en Halatte, 2009.

Bessagnet, B., Hodzic, A., Vautard, R., Beekmann, M., Cheinet, S., Honore, C., Liousse, C., and Rouil, L.: Aerosol modeling with CHIMERE - preliminary evaluation at the continental scale, Atmospheric Environment, 38, 2803-2817, 10.1016/j.atmosenv.2004.02.034, 2004.

Bessagnet, B., Menut, L., Colette, A., Couvidat, F., Dan, M., Mailler, S., Létinois, L., Pont, V., and Rouïl, L.: An Evaluation of the CHIMERE Chemistry Transport Model to Simulate Dust Outbreaks across the Northern Hemisphere in March 2014, Atmosphere, 8, 251, 2017.

Bessagnet, B., Menut, L., Curci, G., Hodzic, A., Guillaume, B., Liousse, C., Moukhtar, S., Pun, B., Seigneur, C., and Schulz, M.: Regional modeling of carbonaceous aerosols over Europe—focus on secondary organic aerosols, Journal of Atmospheric Chemistry, 61, 175-202, 2008.

Bieser, J., Aulinger, A., Matthias, V., Quante, M., and Van Der Gon, H. D.: Vertical emission profiles for Europe based on plume rise calculations, Environmental Pollution, 159, 2935-2946, 2011.

Binkowski, F. and Shankar, U.: The Regional Particulate Matter Model .1. Model description and preliminary results, J. Geophys. Res., 100, 26191–26209, 1995.

Binkowski, F. S.: The aerosol portion of Models-3 CMAQ. In Science Algorithms of the EPA Models-3 Community Multiscale Air Quality (CMAQ) Modeling System. Part II: Chapters 9-18, National Exposure Research Laboratory, U.S. Environmental Protection Agency, Research Triangle Park, NC, 1999.

Bott, A.: A Positive Definite Advection Scheme Obtained by Nonlinear Renormalization of the Advective Fluxes, Mon. Wea. Rev., 117, 1006-1015, 1989.

Brandt, J., Silver, J. D., Frohn, L. M., Geels, C., Gross, A., Hansen, A. B., Hansen, K. M., Hedegaard, G. B., Skjoth, C. A., Villadsen, H., Zare, A., and Christensen, J. H.: An integrated model study for Europe and North America using the Danish Eulerian Hemispheric Model with focus on intercontinental transport of air pollution, Atmospheric Environment, 53, 156-176, 2012.

Brasseur, G. P., Xie, Y., Petersen, A. K., Bouarar, I., Flemming, J., Gauss, M., Jiang, F., Kouznetsov, R., Kranenburg, R., and Mijling, B.: Ensemble forecasts of air quality in eastern China–Part 1: Model description and implementation of the MarcoPolo–Panda prediction system, version 1, Geoscientific Model Development, 12, 33-67, 2019.

Burridge, D.: THE METEOROLOGICAL OFFICE OPERATIONAL 10-LEVEL NUMERICAL WEATHER PREDICTION MODEL (DECEMBER 1975), 1977.

Cariolle, D. and Teyssedre, H.: A revised linear ozone photochemistry parameterization for use in transport and general circulation models: multi-annual simulations, Atmospheric chemistry and physics, 7, 2183-2196, 2007.

Carslaw, K. S., Luo, B., and Peter, T.: An analytic expression for the composition of aqueous HNO3-H2SO4 stratospheric aerosols including gas phase removal of HNO3, Geophysical Research Letters, 22, 1877-1880, 1995.

Carson, D.: The development of a dry inversion-capped convectively unstable boundary layer, Quarterly Journal of the Royal Meteorological Society, 99, 450-467, 1973.

Carter, W. P. L.: Condensed atmospheric photooxidation mechanisms for isoprene, Atmospheric Environment, 30, 4275-4290, http://dx.doi.org/10.1016/1352-2310(96)00088-X, 1996.

Carter, W. P. L.: Documentation of the SAPRC-99 Chemical Mechanism for VOC Reactivity Assessment, 2000.

Castro, L., Pio, C., Harrison, R. M., and Smith, D.: Carbonaceous aerosol in urban and rural European atmospheres: estimation of secondary organic carbon concentrations, Atmospheric Environment, 33, 2771-2781, 1999.

Chang, T.: Rain and snow scavenging of HNO3 vapor in the atmosphere, Atmospheric Environment (1967), 18, 191-197, 1984.

Christensen, J., Brandt, J., Frohn, L., and Skov, H.: Modelling of mercury in the Arctic with the Danish Eulerian Hemispheric Model, Atmospheric Chemistry and Physics, 4, 2251-2257, 2004.

Christensen, J. H.: The Danish Eulerian hemispheric model—A three-dimensional air pollution model used for the Arctic, Atmospheric Environment, 31, 4169-4191, 1997.

Colella, P. and Woodward, P. R.: The piecewise parabolic method (PPM) for gas-dynamical simulations, Journal of computational physics, 54, 174-201, 1984.

Colette, A., Bessagnet, B., Meleux, F., Terrenoire, E., and Rouïl, L.: Frontiers in air quality modelling, Geosci. Model Dev., 7, 203-210, 2014.

Colette, A., Bessagnet, B., Vautard, R., Szopa, S., Rao, S., Schucht, S., Klimont, Z., Menut, L., Clain, G., Meleux, F., Curci, G., and Rouïl, L.: European atmosphere in 2050, a regional air quality and climate perspective under CMIP5 scenarios, Atmos. Chem. Phys., 13, 7451-7471, 2013.

Colette, A., Andersson, C., Baklanov, A., Bessagnet, B., Brandt, J., Christensen, J. H., Doherty, R., Engardt, M., Geels, C., Giannakopoulos, C., Hedegaard, G. H., Katragkou, E., Langner, J., Lei, H., Manders, A., Melas, D., Meleux, F., Rouïl, L., Sofiev, M., Soares, J., Stevenson, D. S., Tombrou-Tzella, M., Varotsos, K. V., and Young, P.: Is the ozone climate penalty robust in Europe?, Environmental Research Letters, 10, 084015, 2015.

Colette, A., Andersson, C., Manders, A., Mar, K., Mircea, M., Pay, M. T., Raffort, V., Tsyro, S., Cuvelier, C., Adani, M., Bessagnet, B., Bergström, R., Briganti, G., Butler, T., Cappelletti, A., Couvidat, F., D'Isidoro, M., Doumbia, T., Fagerli, H., Granier, C., Heyes, C., Klimont, Z., Ojha, N., Otero, N., Schaap, M., Sindelarova, K., Stegehuis, A. I., Roustan, Y., Vautard, R., van Meijgaard, E., Vivanco, M. G., and Wind, P.: EURODELTA-Trends, a multi-model experiment of air quality hindcast in Europe over 1990–2010, Geosci. Model Dev., 10, 3255-3276, 10.5194/gmd-10-3255-2017, 2017.

Côté, J., Gravel, S., Méthot, A., Patoine, A., Roch, M., and Staniforth, A.: The operational CMC–MRB global environmental multiscale (GEM) model. Part I: Design considerations and formulation, Monthly Weather Review, 126, 1373-1395, 1998a.

Côté, J., Desmarais, J.-G., Gravel, S., Méthot, A., Patoine, A., Roch, M., and Staniforth, A.: The operational CMC–MRB global environmental multiscale (GEM) model. Part II: Results, Monthly Weather Review, 126, 1397-1418, 1998b.

Couvidat, F., Bessagnet, B., Garcia-Vivanco, M., Real, E., Menut, L., and Colette, A.: Development of an inorganic and organic aerosol model (CHIMERE 2017β v1.0): seasonal and spatial evaluation over Europe, Geosci. Model Dev., 11, 165-194, 10.5194/gmd-11-165-2018, 2018.

Curier, R., Timmermans, R., Calabretta-Jongen, S., Eskes, H., Segers, A., Swart, D., and Schaap, M.: Improving ozone forecasts over Europe by synergistic use of the LOTOS-EUROS chemical transport model and in-situ measurements, Atmospheric environment, 60, 217-226, 2012.

Cussac, M., Marécal, V., Thouret, V., Josse, B., and Sauvage, B.: The impact of biomass burning on upper tropospheric carbon monoxide: a study using MOCAGE global model and IAGOS airborne data, Atmospheric Chemistry and Physics, 20, 9393-9417, 2020.

D'Elia, I., Briganti, G., Vitali, L., Piersanti, A., Righini, G., D'Isidoro, M., Cappelletti, A., Mircea, M., Adani, M., and Zanini, G.: Measured and modelled air quality trends in Italy over the period 2003–2010, Atmospheric Chemistry and Physics, 21, 10825-10849, 2021.

Dabdub, D. and Seinfeld, J. H.: Numerical advective schemes used in air quality models—sequential and parallel implementation, Atmospheric Environment, 28, 3369-3385, 1994.

Damski, J., Thölix, L., Backman, L., Taalas, P., and Kulmala, M.: FinRose--middle atmospheric chemistry transport model, Boreal environment research, 12, 2007.

Denier van der Gon, H. A. C., Bergström, R., Fountoukis, C., Johansson, C., Pandis, S. N., Simpson, D., and Visschedijk, A. J. H.: Particulate emissions from residential wood combustion in Europe – revised estimates and an evaluation, Atmos. Chem. Phys., 15, 6503-6519, 10.5194/acp-15-6503-2015, 2015.

Derognat, C., Beekmann, M., Baeumle, M., Martin, D., and Schmidt, H.: Effect of biogenic volatile organic compound emissions on tropospheric chemistry during the Atmospheric Pollution Over the Paris Area (ESQUIF) campaign in the Ile-de-France region, Journal of Geophysical Research: Atmospheres, 108, 2003.

Di Tomaso, E., Schutgens, N. A. J., Jorba, O., and Pérez García-Pando, C.: Assimilation of MODIS Dark Target and Deep Blue observations in the dust aerosol component of NMMB-MONARCH version 1.0, Geoscientific Model Development, 10, 1107-1129, 2017.

Di Tomaso, E., Escribano, J., Basart, S., Ginoux, P., Macchia, F., Barnaba, F., Benincasa, F., Bretonnière, P. A., Buñuel, A., Castrillo, M., Cuevas, E., Formenti, P., Gonçalves, M., Jorba, O., Klose, M., Mona, L., Montané Pinto, G., Mytilinaios, M., Obiso, V., Olid, M., Schutgens, N., Votsis, A., Werner, E., and Pérez García-Pando, C.: The MONARCH high-resolution reanalysis of desert dust aerosol over Northern Africa, the Middle East and Europe (2007–2016), Earth Syst. Sci. Data, 14, 2785-2816, 10.5194/essd-14-2785-2022, 2022.

Douros, J., Eskes, H., van Geffen, J., Boersma, K. F., Compernolle, S., Pinardi, G., Blechschmidt, A. M., Peuch, V. H., Colette, A., and Veefkind, P.: Comparing Sentinel-5P TROPOMI NO2 column observations with the CAMS-regional air quality ensemble, EGUsphere, 2022, 1-40, 10.5194/egusphere-2022-365, 2022.

Ebel, A., Friedrich, R., and Rodhe, H.: GENEMIS: Assessment, improvement, and temporal and spatial disaggregation of European emission data, in: Tropospheric modelling and emission estimation, Springer, 181-214, 1997.

EC: Directive 2008/50/EC of the European Parliament and of the Council of 21 May 2008 on ambient air quality and cleaner air for Europe, European Commission, Brussels, 2008.

ECMWF: IFS Documentation CY47R3 - Part IV Physical processes, Reading, doi: 10.21957/eyrpir4vj, 2021.

Elbern, H., Strunk, A., Schmidt, H., and Talagrand, O.: Emission rate and chemical state estimation by 4-dimensional variational inversion, Atmospheric Chemistry and Physics, 7, 3749-3769, 2007.

Emberson, L., Ashmore, M., Cambridge, H., Simpson, D., and Tuovinen, J.-P.: Modelling stomatal ozone flux across Europe, Environmental Pollution, 109, 403-413, 2000a.

Emberson, L. D., Ashmore, M. R., Simpson, D., Tuovinen, J.-P., and Cambridge, H. M.: Towards a model of ozone deposition and stomatal uptake over Europe, Norwegian Meteorological Institute, Oslo, Norway, 57, 2000b.

EMEP: Transboundary particulate matter, photo-oxydants, acidifying and eutrophying components, EMEP, Oslo, Norway, 2023.

Erisman, J. W., Van Pul, A., and Wyers, P.: Parametrization of surface resistance for the quantification of atmospheric deposition of acidifying pollutants and ozone, Atmospheric Environment, 28, 2595-2607, http://dx.doi.org/10.1016/1352-2310(94)90433-2, 1994.

Escribano, J., Di Tomaso, E., Jorba, O., Klose, M., Gonçalves Ageitos, M., Macchia, F., Amiridis, V., Baars, H., Marinou, E., Proestakis, E., Urbanneck, C., Althausen, D., Bühl, J., Mamouri, R. E., and Pérez García-Pando, C.: Assimilating spaceborne lidar dust extinction can improve dust forecasts, Atmos. Chem. Phys., 22, 535-560, 10.5194/acp-22-535-2022, 2022.

Fécan, F., Marticorena, B., and Bergametti, G.: Parametrization of the increase of the aeolian erosion threshold wind friction velocity due to soil moisture for arid and semi-arid areas, Annales Geophysicae, 149-157,

Flemming, J., Huijnen, V., Arteta, J., Bechtold, P., Beljaars, A., Blechschmidt, A. M., Diamantakis, M., Engelen, R. J., Gaudel, A., Inness, A., Jones, L., Josse, B., Katragkou, E., Marecal, V., Peuch, V. H., Richter, A., Schultz, M. G., Stein, O.,

and Tsikerdekis, A.: Tropospheric chemistry in the Integrated Forecasting System of ECMWF, Geosci. Model Dev., 8, 975-1003, 10.5194/gmd-8-975-2015, 2015.

Foley, K., Roselle, S., Appel, K., Bhave, P., Pleim, J., Otte, T., Mathur, R., Sarwar, G., Young, J., and Gilliam, R.: Incremental testing of the Community Multiscale Air Quality (CMAQ) modeling system version 4.7, Geoscientific Model Development, 3, 205-226, 2010.

Forester, C.: Higher order monotonic convective difference schemes, Journal of Computational Physics, 23, 1-22, 1977.

Fountoukis, C. and Nenes, A.: ISORROPIA II: a computationally efficient thermodynamic equilibrium model for K+–Ca2+–Mg2+–NH4+–Na+–SO42−–NO3−–Cl−–H2O aerosols, Atmos. Chem. Phys., 7, 4639-4659, doi:10.5194/acp-7-4639-2007, 2007.

Friese, E. and Ebel, A.: Temperature dependent thermodynamic model of the system H+− NH4+− Na+− SO42−− NO3−− Cl−− H2O, The Journal of Physical Chemistry A, 114, 11595-11631, 2010.

Frohn, L.: A study of long-term high-resolution air pollution modelling, Ministry of the Environment, National Environmental Research Institute, Roskilde, Denmark, 2004.

Galmarini, S., Kioutsioukis, I., and Solazzo, E.: E pluribus unum*: ensemble air quality predictions, Atmos. Chem. Phys., 13, 7153-7182, 10.5194/acp-13-7153-2013, 2013.

Galmarini, S., Bianconi, R., Addis, R., Andronopoulos, S., Astrup, P., Bartzis, J., Bellasio, R., Buckley, R., Champion, H., and Chino, M.: Ensemble dispersion forecasting—Part II: Application and evaluation, Atmospheric Environment, 38, 4619-4632, 2004.

Galmarini, S., Koffi, B., Solazzo, E., Keating, T., Hogrefe, C., Schulz, M., Benedictow, A., Griesfeller, J. J., Janssens-Maenhout, G., Carmichael, G., Fu, J., and Dentener, F.: Technical note: Coordination and harmonization of the multi-scale, multi-model activities HTAP2, AQMEII3, and MICS-Asia3: simulations, emission inventories, boundary conditions, and model output formats, Atmos. Chem. Phys., 17, 1543-1555, 10.5194/acp-17-1543-2017, 2017.

Galperin, M. and Sofiev, M.: Errors in the validation of models for long-range transport and critical loads stipulated by stochastic properties of pollution fields., EMEP Chemical Coordinating Centre, Lillestrom, Passau, 162–179, 1994.

Geels, C., Winther, M., Andersson, C., Jalkanen, J.-P., Brandt, J., Frohn, L. M., Im, U., Leung, W., and Christensen, J. H.: Projections of shipping emissions and the related impact on air pollution and human health in the Nordic region, Atmospheric Chemistry and Physics, 21, 12495-12519, 2021.

Geiger, H., Barnes, I., Bejan, I., Benter, T., and Spittler, M.: The tropospheric degradation of isoprene: an updated module for the regional atmospheric chemistry mechanism, Atmospheric Environment, 37, 1503-1519, 2003.

Gery, M. W., Whitten, G. Z., Killus, J. P., and Dodge, M. C.: A photochemical kinetics mechanism for urban and regional scale computer modeling, Journal of Geophysical Research: Atmospheres, 94, 12925-12956, 1989.

Ginoux, P., Chin, M., Tegen, I., Prospero, J. M., Holben, B., Dubovik, O., and Lin, S. J.: Sources and distributions of dust aerosols simulated with the GOCART model, Journal of Geophysical Research: Atmospheres, 106, 20255-20273, 2001.

Giorgi, F. and Chameides, W. L.: Rainout lifetimes of highly soluble aerosols and gases as inferred from simulations with a general circulation model, Journal of Geophysical Research: Atmospheres, 91, 14367-14376, 1986.

Gomes, L., Rajot, J., Alfaro, S., and Gaudichet, A.: Validation of a dust production model from measurements performed in semi-arid agricultural areas of Spain and Niger, Catena, 52, 257-271, 2003.

Gong, S., Barrie, L., Blanchet, J. P., Von Salzen, K., Lohmann, U., Lesins, G., Spacek, L., Zhang, L., Girard, E., and Lin, H.: Canadian Aerosol Module: A size-segregated simulation of atmospheric aerosol processes for climate and air quality models 1. Module development, Journal of Geophysical Research: Atmospheres, 108, AAC 3-1-AAC 3-16, 2003.

Granier, C., Darras, S., van der Gon, H. D., Doubalova, J., Elguindi, N., Galle, B., Gauss, M., Guevara, M., Jalkanen, J. P., and Kuenen, J.: The Copernicus Atmosphere Monitoring Service global and regional emissions (April 2019 version), Copernicus Atmosphere Monitoring Service, 10.24380/d0bn-kx16, 2019.

Groisman, P. Y. and Genikhovich, E. L.: Assessing surface–atmosphere interactions using former Soviet Union standard meteorological network data. Part I: Method, Journal of climate, 10, 2154-2183, 1997.

Guenther, A., Zimmerman, P., Harley, P., Monson, R., and Fall, R.: Isoprene and monoterpene rate variability: model evaluations and sensitivity analyses, J. Geophys. Res., 98, 12609–12617, 1993.

Guenther, A., Karl, T., Harley, P., Wiedinmyer, C., Palmer, P. I., and Geron, C.: Estimates of global terrestrial isoprene emissions using MEGAN (Model of Emissions of Gases and Aerosols from Nature), Atmos. Chem. Phys., 6, 3181-3210, 2006.

Guenther, A., Jiang, X., Heald, C. L., Sakulyanontvittaya, T., Duhl, T. a., Emmons, L., and Wang, X.: The Model of Emissions of Gases and Aerosols from Nature version 2.1 (MEGAN2. 1): an extended and updated framework for modeling biogenic emissions, Geoscientific Model Development, 5, 1471-1492, 2012.

Guevara, M., Tena, C., Porquet, M., Jorba, O., and Pérez García-Pando, C.: HERMESv3, a stand-alone multi-scale atmospheric emission modelling framework–Part 1: global and regional module, Geoscientific Model Development, 12, 1885-1907, 2019.

Guevara, M., Jorba, O., Tena, C., Denier van der Gon, H., Kuenen, J., Elguindi, N., Darras, S., Granier, C., and Pérez García-Pando, C.: Copernicus Atmosphere Monitoring Service TEMPOral profiles (CAMS-TEMPO): global and European emission temporal profile maps for atmospheric chemistry modelling, Earth Syst. Sci. Data, 13, 367-404, 10.5194/essd-13-367-2021, 2021.

Guth, J., Josse, B., Marécal, V., Joly, M., and Hamer, P.: First implementation of secondary inorganic aerosols in the MOCAGE version 2.15.0 chemistry transport model, Geosci. Model Dev., 9, 137-160, 10.5194/gmd-9-137-2016, 2016.

Guth, J., Marécal, V., Josse, B., Arteta, J., and Hamer, P.: Primary aerosol and secondary inorganic aerosol budget over the Mediterranean Basin during 2012 and 2013, Atmospheric Chemistry and Physics, 18, 4911-4934, 2018.

Hamer, P., Fjaeraa, A.-M., Soarez, J., Meleux, F., Colette, A., Ung, A., Raux, B., and Tarrason, L.: Copernicus Atmosphere Monitoring Service Interim Annual Assessment Report on European Air Quality in 2022, ECMWF, Bonn, https://policy.atmosphere.copernicus.eu/reports/CAMS271_2021SCx_D1.1.1._202306_2022_Interim_Assessment_Report_v1.pdf, 2023.

Hansen, K. M., Christensen, J. H., Brandt, J., Frohn, L. M., Geels, C., Skjøth, C. A., and Li, Y. F.: Modeling short-term variability of α-hexachlorocyclohexane in Northern Hemispheric air, Journal of Geophysical Research: Atmospheres, 113, 2008.

Hass, H., Jakobs, H., and Memmesheimer, M.: Analysis of a regional model (EURAD) near surface gas concentration predictions using observations from networks, Meteorology and Atmospheric Physics, 57, 173-200, 1995.

Heidam, N. Z., Christensen, J., Wåhlin, P., and Skov, H.: Arctic atmospheric contaminants in NE Greenland: levels, variations, origins, transport, transformations and trends 1990–2001, Science of the Total Environment, 331, 5-28, 2004.

Heimann, M. and Keeling, C. D.: A three-dimensional model of atmospheric CO2 transport based on observed winds: 2. Model description and simulated tracer experiments, Max-Planck-Institut für Meteorologie1989.

Hendriks, C., Forsell, N., Kiesewetter, G., Schaap, M., and Schöpp, W.: Ozone concentrations and damage for realistic future European climate and air quality scenarios, Atmospheric Environment, 144, 208-219, 2016.

Hertel, O., Christensen, J., Runge, E. H., Asman, W. A., Berkowicz, R., Hovmand, M. F., and Hov, Ø.: Development and testing of a new variable scale air pollution model—ACDEP, Atmospheric Environment, 29, 1267-1290, 1995.

Hervig, M. E., Russell III, J. M., Gordley, L. L., Park, J. H., and Drayson, S. R.: Observations of aerosol by the HALOE experiment onboard UARS: A preliminary validation, Geophysical research letters, 20, 1291-1294, 1993.

Hicks, B., Baldocchi, D., Meyers, T., Hosker, R., and Matt, D.: A preliminary multiple resistance routine for deriving dry deposition velocities from measured quantities, Water, Air, and Soil Pollution, 36, 311-330, 1987.

Hodzic, A., Kasibhatla, P. S., Jo, D. S., Cappa, C. D., Jimenez, J. L., Madronich, S., and Park, R. J.: Rethinking the global secondary organic aerosol (SOA) budget: stronger production, faster removal, shorter lifetime, Atmospheric Chemistry and Physics, 16, 7917-7941, 2016.

Hollingsworth, A.: Toward a monitoring and forecasting system for atmospheric composition: The GEMS Project, Bull. Amer. Meteor. Soc., 89, 1147-1164, https://doi.org/10.1175/2008BAMS2355.1, 2008.

Hollingsworth, A. and Lönnberg, P.: The statistical structure of short-range forecast errors as determined from radiosonde data. Part I: The wind field, Tellus A, 38, 111-136, 1986.

Holtslag, A., Van Meijgaard, E., and De Rooy, W.: A comparison of boundary layer diffusion schemes in unstable conditions over land, Boundary-Layer Meteorology, 76, 69-95, 1995.

Holtslag, A. A. and Nieuwstadt, F. T.: Scaling the atmospheric boundary layer, Boundary-Layer Meteorology, 36, 201-209, 1986.

Horálek, J., Schreiberová, M., Vlasáková, L., Hamer, P., Schneider, P., and Marková, J.: Interim European air quality maps for 2020. PM10, NO2 and ozone spatial estimates based on non-validated UTD data., NILU, Oslo, https://www.eionet.europa.eu/etcs/etc-atni/products/etc-atni-report-19-2021-interim-european-air-quality-maps-for-2020-pm10-no2-and-ozone-spatial-estimates-based-on-non-validated-utd-data, 2022.

1835 Huang, G., Brook, R., Crippa, M., Janssens-Maenhout, G., Schieberle, C., Dore, C., Guizzardi, D., Muntean, M., Schaaf, E.,
1836 and Friedrich, R.: Speciation of anthropogenic emissions of non-methane volatile organic compounds: a global gridded data
1837 set for 1970–2012, Atmospheric Chemistry and Physics, 17, 7683-7701, 2017.

1838 Huijnen, V., Eskes, H., Poupkou, A., Elbern, H., Boersma, K., Foret, G., Sofiev, M., Valdebenito, A., Flemming, J., and
1839 Stein, O.: Comparison of OMI NO 2 tropospheric columns with an ensemble of global and European regional air quality
1840 models, Atmospheric Chemistry and Physics, 10, 3273-3296, 2010.

1841 Hunt, B. R., Kostelich, E. J., and Szunyogh, I.: Efficient data assimilation for spatiotemporal chaos: A local ensemble
1842 transform Kalman filter, Physica D: Nonlinear Phenomena, 230, 112-126, https://doi.org/10.1016/j.physd.2006.11.008,
1843 2007.

1844 Jaeglé, L., Quinn, P. K., Bates, T. S., Alexander, B., and Lin, J.-T.: Global distribution of sea salt aerosols: new constraints
1845 from in situ and remote sensing observations, Atmospheric Chemistry and Physics, 11, 3137, 2011.

1846 Janjic, Z. and Gall, L.: Scientific documentation of the NCEP nonhydrostatic multiscale model on the B grid (NMMB). Part
1847 1 Dynamics, NCAR/TN-489+STR, 2012.

1848 Jöckel, P., Tost, H., Pozzer, A., Brühl, C., Buchholz, J., Ganzeveld, L., Hoor, P., Kerkweg, A., Lawrence, M., and Sander,
1849 R.: The atmospheric chemistry general circulation model ECHAM5/MESSy1: consistent simulation of ozone from the
1850 surface to the mesosphere, Atmospheric Chemistry and Physics, 6, 5067-5104, 2006.

1851 Joly, M. and Peuch, V.-H.: Objective classification of air quality monitoring sites over Europe, Atmospheric Environment,
1852 47, 111-123, 2012.

1853 Jonson, J., Kylling, A., Berntsen, T., Isaksen, I., Zerefos, C., and Kourtidis, K.: Chemical effects of UV fluctuations inferred
1854 from total ozone and tropospheric aerosol variations, Journal of Geophysical Research: Atmospheres, 105, 14561-14574,
1855 2000.

1856 Jorba, O., Dabdub, D., Blaszczak-Boxe, C., Pérez, C., Janjic, Z., Baldasano, J., Spada, M., Badia, A., and Gonçalves, M.:
1857 Potential significance of photoexcited NO2 on global air quality with the NMMB/BSC chemical transport model, Journal of
1858 Geophysical Research: Atmospheres, 117, 2012.

1859 Kahnert, M.: Variational data analysis of aerosol species in a regional CTM: background error covariance constraint and
1860 aerosol optical observation operators, Tellus B: Chemical and Physical Meteorology, 60, 753-770, 2008.

1861 Kain, J. S. and Fritsch, J. M.: A one-dimensional entraining/detraining plume model and its application in convective
1862 parameterization, Journal of Atmospheric Sciences, 47, 2784-2802, 1990.

1863 Kaiser, J., Heil, A., Andreae, M., Benedetti, A., Chubarova, N., Jones, L., Morcrette, J.-J., Razinger, M., Schultz, M., and
1864 Suttie, M.: Biomass burning emissions estimated with a global fire assimilation system based on observed fire radiative
1865 power, Biogeosciences, 9, 527-554, 2012.

1866 Kawka, M., Struzewska, J., and Kaminski, J. W.: Spatial and Temporal Variation of NO 2 Vertical Column Densities
1867 (VCDs) over Poland: Comparison of the Sentinel-5P TROPOMI Observations and the GEM-AQ Model Simulations,
1868 Atmosphere, 12, 896, 2021.

Klose, M., Jorba, O., Gonçalves Ageitos, M., Escribano, J., Dawson, M. L., Obiso, V., Di Tomaso, E., Basart, S., Montané Pinto, G., and Macchia, F.: Mineral dust cycle in the Multiscale Online Nonhydrostatic AtmospheRe CHemistry model (MONARCH) version 2.0, Geoscientific Model Development, 14, 6403-6444, 2021.

Köble, R. and Seufert, G.: Novel maps for forest tree species in Europe, Proceedings of the 8th European symposium on the physico-chemical behaviour of air pollutants:"a changing atmosphere, 17-20,

Korhonen, H., Carslaw, K. S., Spracklen, D. V., Mann, G. W., and Woodhouse, M. T.: Influence of oceanic dimethyl sulfide emissions on cloud condensation nuclei concentrations and seasonality over the remote Southern Hemisphere oceans: A global model study, Journal of Geophysical Research: Atmospheres, 113, 2008.

Kouznetsov, R. and Sofiev, M.: A methodology for evaluation of vertical dispersion and dry deposition of atmospheric aerosols, Journal of Geophysical Research: Atmospheres, 117, 2012.

Kouznetsov, R., Sofiev, M., Vira, J., and Stiller, G.: Simulating age of air and the distribution of SF 6 in the stratosphere with the SILAM model, Atmospheric Chemistry and Physics, 20, 5837-5859, 2020.

Kuenen, J., Visschedijk, A., Jozwicka, M., and Denier Van Der Gon, H.: TNO-MACC_II emission inventory; a multi-year (2003–2009) consistent high-resolution European emission inventory for air quality modelling, Atmospheric Chemistry and Physics, 14, 10963-10976, 2014.

Kuenen, J., Dellaert, S., Visschedijk, A., Jalkanen, J.-P., Super, I., and Denier van der Gon, H.: CAMS-REG-v4: a state-of-the-art high-resolution European emission inventory for air quality modelling, Earth System Science Data, 14, 491-515, 2022.

Kukkonen, J., Savolahti, M., Palamarchuk, Y., Lanki, T., Nurmi, V., Paunu, V.-V., Kangas, L., Sofiev, M., Karppinen, A., and Maragkidou, A.: Modelling of the public health costs of fine particulate matter and results for Finland in 2015, Atmospheric Chemistry and Physics, 20, 9371-9391, 2020.

Kylling, A., Stamnes, K., and Tsay, S.-C.: A reliable and efficient two-stream algorithm for spherical radiative transfer: Documentation of accuracy in realistic layered media, Journal of Atmospheric Chemistry, 21, 115-150, 1995.

Lahoz, W., Geer, A., Bekki, S., Bormann, N., Ceccherini, S., Elbern, H., Errera, Q., Eskes, H., Fonteyn, D., and Jackson, D.: The Assimilation of Envisat data (ASSET) project, Atmospheric Chemistry and Physics, 7, 1773-1796, 2007.

Lambert, J. D.: Numerical methods for ordinary differential systems, Wiley New York1991.

Lana, A., Bell, T., Simó, R., Vallina, S., Ballabrera-Poy, J., Kettle, A., Dachs, J., Bopp, L., Saltzman, E., and Stefels, J.: An updated climatology of surface dimethlysulfide concentrations and emission fluxes in the global ocean, Global Biogeochemical Cycles, 25, 2011.

Landgraf, J. and Crutzen, P.: An efficient method for online calculations of photolysis and heating rates, Journal of the atmospheric sciences, 55, 863-878, 1998.

Lange, R.: Transferability of a three-dimensional air quality model between two different sites in complex terrain, Journal of Applied Meteorology and Climatology, 28, 665-679, 1989.

Langner, J., Bergström, R., and Pleijel, K.: European scale modeling of sulphur, oxidized nitrogen and photochemical oxidants. Model development and evaluation for the 1994 growing season, Swedish Met. and Hydrol. Inst., Norrköping, Sweden, 1998.

Lansø, A. S., Smallman, T. L., Christensen, J. H., Williams, M., Pilegaard, K., Sørensen, L.-L., and Geels, C.: Simulating the atmospheric CO 2 concentration across the heterogeneous landscape of Denmark using a coupled atmosphere–biosphere mesoscale model system, Biogeosciences, 16, 1505-1524, 2019.

Lefevre, F., Brasseur, G., Folkins, I., Smith, A., and Simon, P.: Chemistry of the 1991–1992 stratospheric winter: Three-dimensional model simulations, Journal of Geophysical Research: Atmospheres, 99, 8183-8195, 1994.

Lehtomäki, H., Korhonen, A., Asikainen, A., Karvosenoja, N., Kupiainen, K., Paunu, V.-V., Savolahti, M., Sofiev, M., Palamarchuk, Y., and Karppinen, A.: Health impacts of ambient air pollution in Finland, International journal of environmental research and public health, 15, 736, 2018.

Li, Y., Elbern, H., Lu, K., Friese, E., Kiendler-Scharr, A., Mentel, T. F., Wang, X., Wahner, A., and Zhang, Y.: Updated aerosol module and its application to simulate secondary organic aerosols during IMPACT campaign May 2008, Atmospheric chemistry and physics, 13, 6289-6304, 2013.

Liu, D. C. and Nocedal, J.: On the limited memory BFGS method for large scale optimization, Mathematical programming, 45, 503-528, 1989.

Louis, J.-F.: A parametric model of vertical eddy fluxes in the atmosphere, Boundary-Layer Meteorology, 17, 187-202, 1979.

Lurmann, F. W., Lloyd, A. C., and Atkinson, R.: A chemical mechanism for use in long-range transport/acid deposition computer modeling, Journal of Geophysical Research: Atmospheres, 91, 10905-10936, 1986.

Maas, R. and Grennfelt , P.: Towards Cleaner Air - Scientific Assessment Report 2016, EMEP-Steering body and Working Group on Effects - Convention on Long-Range Transboundary Air Pollution 2016.

Madronich, S.: Photodissociation in the atmosphere: 1. Actinic flux and the effects of ground reflections and clouds, Journal of Geophysical Research: Atmospheres, 92, 9740-9752, 1987.

Madronich, S. and Weller, G.: Numerical integration errors in calculated tropospheric photodissociation rate coefficients, Journal of atmospheric chemistry, 10, 289-300, 1990.

Manders, A. M. M., Builtjes, P. J. H., Curier, L., Denier van der Gon, H. A. C., Hendriks, C., Jonkers, S., Kranenburg, R., Kuenen, J., Segers, A. J., Timmermans, R. M. A., Visschedijk, A., Wichink Kruit, R. J., Van Pul, W. A. J., Sauter, F. J., van der Swaluw, E., Swart, D. P. J., Douros, J., Eskes, H., van Meijgaard, E., van Ulft, B., van Velthoven, P., Banzhaf, S., Mues, A., Stern, R., Fu, G., Lu, S., Heemink, A., van Velzen, N., and Schaap, M.: Curriculum Vitae of the LOTOS-EUROS (v2.0) chemistry transport model, Geosci. Model Dev. Discuss., 2017, 1-53, 10.5194/gmd-2017-88, 2017.

Marécal, V., Peuch, V. H., Andersson, C., Andersson, S., Arteta, J., Beekmann, M., Benedictow, A., Bergstrom, R., Bessagnet, B., Cansado, A., Chéroux, F., Colette, A., Coman, A., Curier, R. L., Denier van der Gon, H. A. C., Drouin, A., Elbern, H., Emili, E., Engelen, R. J., Eskes, H. J., Foret, G., Friese, E., Gauss, M., Giannaros, C., Guth, J., Joly, M., Jaumouilla, E., Josse, B., Kadygrov, N., Kaiser, J. W., Krajsek, K., Kuenen, J., Kumar, U., Liora, N., Lopez, E., Malherbe, L., Martinez, I., Melas, D., Meleux, F., Menut, L., Moinat, P., Morales, T., Parmentier, J., Piacentini, A., Plu, M., Poupkou,

A., Queguiner, S., Robertson, L., Rouil, L., Schaap, M., Segers, A., Sofiev, M., Tarasson, L., Thomas, M., Timmermans, R., Valdebenito, A., van Velthoven, P., van Versendaal, R., Vira, J., and Ung, A.: A regional air quality forecasting system over Europe: the MACC-II daily ensemble production, Geosci. Model Dev., 8, 2777-2813, 2015.

Mari, C., Jacob, D. J., and Bechtold, P.: Transport and scavenging of soluble gases in a deep convective cloud, Journal of Geophysical Research: Atmospheres, 105, 22255-22267, 2000.

Martensson, E., Nilsson, E., de Leeuw, G., Cohen, L., and Hansson, H.-C.: Laboratory simulations and parameterisation of the primary marine aerosol production, J. Geophys. Res., 108, 4297, doi:10.1029/2002JD002263, 2003.

Martet, M., Peuch, V., Laurent, B., Marticorena, B., and Bergametti, G.: Evaluation of long-range transport and deposition of desert dust with the CTM MOCAGE, Tellus B: Chemical and Physical Meteorology, 61, 449-463, 2009.

Marticorena, B. and Bergametti, G.: Modeling the atmospheric dust cycle: 1. Design of a soil-derived dust emission scheme, Journal of geophysical research: atmospheres, 100, 16415-16430, 1995.

Marticorena, B., Bergametti, G., Aumont, B., Callot, Y., N'Doumé, C., and Legrand, M.: Modeling the atmospheric dust cycle: 2. Simulation of Saharan dust sources, Journal of Geophysical Research: Atmospheres, 102, 4387-4404, 1997.

Maul, P., Barber, F., and Martin, A.: Some observations of the meso-scale transport of sulphur compounds in the rural East Midlands, Atmospheric Environment (1967), 14, 339-354, 1980.

McRae, G. J., Goodin, W. R., and Seinfeld, J. H.: Numerical solution of the atmospheric diffusion equation for chemically reacting flows, Journal of Computational Physics, 45, 1-42, 1982.

Meleux, F., Solmon, F., and Giorgi, F.: Increase in summer European ozone amounts due to climate change, Atmospheric Environment, 41, 7577-7587, 2007.

Memmesheimer, M., Friese, E., Ebel, A., Jakobs, H., Feldmann, H., Kessler, C., and Piekorz, G.: Long-term simulations of particulate matter in Europe on different scales using sequential nesting of a regional model, International Journal of Environment and Pollution, 22, 108-132, 2004.

Ménégoz, M., Salas y Melia, D., Legrand, M., Teyssèdre, H., Michou, M., Peuch, V.-H., Martet, M., Josse, B., and Dombrowski-Etchevers, I.: Equilibrium of sinks and sources of sulphate over Europe: comparison between a six-year simulation and EMEP observations, Atmospheric Chemistry and Physics, 9, 4505-4519, 2009.

Menut, L., Bessagnet, B., Briant, R., Cholakian, A., Couvidat, F., Mailler, S., Pennel, R., Siour, G., Tuccella, P., and Turquety, S.: The CHIMERE v2020r1 online chemistry-transport model, Geoscientific Model Development, 14, 6781-6811, 2021.

Metzger, S., Dentener, F., Pandis, S., and Lelieveld, J.: Gas/aerosol partitioning: 1. A computationally efficient model, J. Geophys. Res., 107, 4312, 2002.

Michou, M., Laville, P., Serça, D., Fotiadi, A., Bouchou, P., and Peuch, V.-H.: Measured and modeled dry deposition velocities over the ESCOMPTE area, Atmospheric Research, 74, 89-116, 2005.

Mircea, M., Ciancarella, L., Briganti, G., Calori, G., Cappelletti, A., Cionni, I., Costa, M., Cremona, G., D'Isidoro, M., Finardi, S., Pace, G., Piersanti, A., Righini, G., Silibello, C., Vitali, L., and Zanini, G.: Assessment of the AMS-MINNI

system capabilities to simulate air quality over Italy for the calendar year 2005, Atmospheric Environment, 84, 178-188, https://doi.org/10.1016/j.atmosenv.2013.11.006, 2014.

Miyoshi, T. and Yamane, S.: Local Ensemble Transform Kalman Filtering with an AGCM at a T159/L48 Resolution, Monthly Weather Review, 135, 3841-3861, 10.1175/2007MWR1873.1, 2007.

Monahan, E. C.: The ocean as a source of atmospheric particles, in: The Role of Air-Sea Exchange in Geochemical Cycling, Kluwer Academic Publishers, Dordrecht, Holland, 129–163, 1986.

Morcrette, J. J., Boucher, O., Jones, L., Salmond, D., Bechtold, P., Beljaars, A., Benedetti, A., Bonet, A., Kaiser, J., and Razinger, M.: Aerosol analysis and forecast in the European Centre for medium-range weather forecasts integrated forecast system: Forward modeling, Journal of Geophysical Research: Atmospheres, 114, 2009.

Mozurkewich, M.: The dissociation constant of ammonium nitrate and its dependence on temperature, relative humidity and particle size, Atmospheric Environment. Part A. General Topics, 27, 261-270, http://dx.doi.org/10.1016/0960-1686(93)90356-4, 1993.

Nenes, A., Pandis, S., and Pilinis, C.: ISORROPIA: A New Thermodynamic Equilibrium Model for Multiphase Multicomponent Inorganic Aerosols, Aquatic Geochemistry, 4, 123-152, 1998.

Nho-Kim, E.-Y., Michou, M., and Peuch, V.-H.: Parameterization of size-dependent particle dry deposition velocities for global modeling, Atmospheric Environment, 38, 1933-1942, 2004.

Nho-Kim, E., Peuch, V., and Oh, S.: Estimation of the global distribution of Black Carbon aerosols with MOCAGE, the CTM of Météo-France, J. Korean Meteor. Soc, 41, 587-598, 2005.

Nieradzik, L.: Application of a high dimensional model representation on the atmospheric aerosol module MADE of the EURAD-CTM, Institut fur Geophysik und Meteorologie der Universitat zu Koln, 2005.

Nieuwstadt, F.: The steady-state height and resistance laws of the nocturnal boundary layer: Theory compared with Cabauw observations, Boundary-Layer Meteorology, 20, 3-17, 1981.

Nocedal, J.: Updating quasi-Newton matrices with limited storage, Mathematics of computation, 35, 773-782, 1980.

Noilhan, J. and Planton, S.: A simple parameterization of land surface processes for meteorological models, Monthly weather review, 117, 536-549, 1989.

Omstedt, G., Bringfelt, B., and Johansson, C.: A model for vehicle-induced non-tailpipe emissions of particles along Swedish roads, Atmospheric environment, 39, 6088-6097, 2005.

Pai, S. J., Heald, C. L., Pierce, J. R., Farina, S. C., Marais, E. A., Jimenez, J. L., Campuzano-Jost, P., Nault, B. A., Middlebrook, A. M., Coe, H., Shilling, J. E., Bahreini, R., Dingle, J. H., and Vu, K.: An evaluation of global organic aerosol schemes using airborne observations, Atmos. Chem. Phys., 20, 2637-2665, 10.5194/acp-20-2637-2020, 2020.

Parrish, D. F. and Derber, J. C.: The National Meteorological Center's spectral statistical-interpolation analysis system, Monthly Weather Review, 120, 1747-1763, 1992.

Passant, N.: Speciation of UK emissions of non-methane volatile organic compounds, AEA Technology2002.

Pepper, D., Kern, C., and Long Jr, P.: Modeling the dispersion of atmospheric pollution using cubic splines and chapeau functions, Atmospheric Environment (1967), 13, 223-237, 1979.

Pérez, C., Haustein, K., Jorba, O., Janjic, Z., Huneeus, N., Baldasano, J. M., Black, T., Basart, S., Nickovic, S., Miller, R. L., Perlwitz, J., Schulz, M., and Thomson, M.: Atmospheric dust modeling from meso to global scales with the online NMMB/BSC-Dust model–Part 1: Model description, annual simulations and evaluation, Atmospheric Chemistry and Physics, 11, 13001-13027, 2011.

Petersen, A. K., Brasseur, G. P., Bouarar, I., Flemming, J., Gauss, M., Jiang, F., Kouznetsov, R., Kranenburg, R., Mijling, B., and Peuch, V.-H.: Ensemble forecasts of air quality in eastern China–Part 2: Evaluation of the MarcoPolo–Panda prediction system, version 1, Geoscientific Model Development, 12, 1241-1266, 2019.

Peterson, J. T.: Calculated actinic fluxes (290-700 nm) for air pollution photochemistry applications, US Environmental Protection Agency, Office of Research and Development …1976.

Petroff, A. and Zhang, L.: Development and validation of a size-resolved particle dry deposition scheme for application in aerosol transport models, Geoscientific Model Development, 3, 753-769, 2010.

Peuch, V.-H., Engelen, R., Rixen, M., Dee, D., Flemming, J., Suttie, M., Ades, M., Agustí-Panareda, A., Ananasso, C., Andersson, E., Armstrong, D., Barré, J., Bousserez, N., Dominguez, J. J., Garrigues, S., Inness, A., Jones, L., Kipling, Z., Letertre-Danczak, J., Parrington, M., Razinger, M., Ribas, R., Vermoote, S., Yang, X., Simmons, A., Garcés de Marcilla, J., and Thépaut, J.-N.: The Copernicus Atmosphere Monitoring Service: From Research to Operations, Bulletin of the American Meteorological Society, 103, E2650-E2668, https://doi.org/10.1175/BAMS-D-21-0314.1, 2022.

Peuch, V., Engelen, R., Simmons, A., Lahoz, W., Laj, P., and Galmarini, S.: Monitoring atmospheric composition and climate, research in support of the Copernicus/GMES atmospheric service, Special Issue, Atmos. Chem. Phys., http://www. atmos-chem-phys. net/special_issue310. html, 2014.

Poupkou, A., Giannaros, T., Markakis, K., Kioutsioukis, I., Curci, G., Melas, D., and Zerefos, C.: A model for European Biogenic Volatile Organic Compound emissions: Software development and first validation, Environmental Modelling & Software, 25, 1845-1856, 2010.

Prank, M., Chapman, D. S., Bullock, J. M., Belmonte, J., Berger, U., Dahl, A., Jäger, S., Kovtunenko, I., Magyar, D., and Niemelä, S.: An operational model for forecasting ragweed pollen release and dispersion in Europe, Agricultural and forest meteorology, 182, 43-53, 2013.

Price, C., Penner, J., and Prather, M.: NOx from lightning: 1. Global distribution based on lightning physics, Journal of Geophysical Research: Atmospheres, 102, 5929-5941, 1997.

Rabitz, H. and Aliş, Ö. F.: General foundations of high-dimensional model representations, Journal of Mathematical Chemistry, 25, 197-233, 1999.

Rappenglück, B., Lubertino, G., Alvarez, S., Golovko, J., Czader, B., and Ackermann, L.: Radical precursors and related species from traffic as observed and modeled at an urban highway junction, Journal of the Air & Waste Management Association, 63, 1270-1286, 2013.

Rémy, S., Kipling, Z., Flemming, J., Boucher, O., Nabat, P., Michou, M., Bozzo, A., Ades, M., Huijnen, V., Benedetti, A., Engelen, R., Peuch, V. H., and Morcrette, J. J.: Description and evaluation of the tropospheric aerosol scheme in the

European Centre for Medium-Range Weather Forecasts (ECMWF) Integrated Forecasting System (IFS-AER, cycle 45R1), Geosci. Model Dev., 12, 4627-4659, 10.5194/gmd-12-4627-2019, 2019.

Robertson, L., Langner, J., and Engardt, M.: An Eulerian limited-area atmospheric transport model, Journal of Applied Meteorology and Climatology, 38, 190-210, 1999.

Robichaud, A. and Ménard, R.: Multi-year objective analyses of warm season ground-level ozone and PM 2.5 over North America using real-time observations and Canadian operational air quality models, Atmospheric Chemistry and Physics, 14, 1769-1800, 2014.

Roselle, S. J. and Binkowski, F. S.: Cloud dynamics and chemistry, Science algorithms of the EPA Models-3 Community multiscale air quality (CMAQ) modeling system, 1999.

Rouïl, L., Honore, C., Vautard, R., Beekmann, M., Bessagnet, B., Malherbe, L., Meleux, F., Dufour, A., Elichegaray, C., Flaud, J. M., Menut, L., Martin, D., Peuch, A., Peuch, V. H., and Poisson, N.: PREV'AIR An Operational Forecasting and Mapping System for Air Quality in Europe, Bulletin of the American Meteorological Society, 90, 73-83, 10.1175/2008bams2390.1, 2009.

Salameh, T., Drobinski, P., Menut, L., Bessagnet, B., Flamant, C., Hodzic, A., and Vautard, R.: Aerosol distribution over the western Mediterranean basin during a Tramontane/Mistral event, Annales Geophysicae, 25, 2271-2291, 2007.

Sander, S., Golden, D., Kurylo, M., Moortgat, G., Wine, P., Ravishankara, A., Kolb, C., Molina, M., Finlayson-Pitts, B., and Huie, R.: Chemical kinetics and photochemical data for use in atmospheric studies evaluation number 15, Pasadena, CA: Jet Propulsion Laboratory, National Aeronautics and Space …, 2006.

Sandu, A. and Sander, R.: Simulating chemical systems in Fortran90 and Matlab with the Kinetic PreProcessor KPP-2.1, Atmospheric Chemistry and Physics, 6, 187-195, 2006.

Sarwar, G., Simon, H., Bhave, P., and Yarwood, G.: Examining the impact of heterogeneous nitryl chloride production on air quality across the United States, Atmospheric Chemistry and Physics, 12, 6455-6473, 2012.

Schaap, M., Van Loon, M., Ten Brink, H., Dentener, F., and Builtjes, P.: Secondary inorganic aerosol simulations for Europe with special attention to nitrate, Atmospheric Chemistry and Physics, 4, 857-874, 2004.

Schaap, M., Kranenburg, R., Curier, L., Jozwicka, M., Dammers, E., and Timmermans, R.: Assessing the sensitivity of the OMI-NO2 product to emission changes across Europe, Remote Sensing, 5, 4187-4208, 2013.

Schaap, M., Manders, A. M. M., Hendriks, E. C. J., Cnossen, J. M., Segers, A. J. S., Denier van der Gon, H., Jozwicka, M., Sauter, F. J., Velders, G. J. M., Matthijsen, J., and Builtjes, P. J. H.: Regional Modelling of Particulate Matter for the Netherlands Netherlands Research Program on Particulate Matter, ISSN: 1875-2314, 2009.

Schell, B., Ackermann, I. J., Hass, H., Binkowski, F. S., and Ebel, A.: Modeling the formation of secondary organic aerosol within a comprehensive air quality model system, Journal of Geophysical Research: Atmospheres, 106, 28275-28293, 2001a.

Schell, B., Ackermann, I. J., Hass, H., Binkowski, F. S., and Ebel, A.: Modelling the formation of secondary organic within a comprehensive air quality model system, J. Geophys. Res., 106, 28275-28293, 2001b.

Schutgens, N. A. J., Miyoshi, T., Takemura, T., and Nakajima, T.: Applying an ensemble Kalman filter to the assimilation of AERONET observations in a global aerosol transport model, Atmos. Chem. Phys., 10, 2561-2576, 10.5194/acp-10-2561-2010, 2010.

Seinfeld, J. H. and Pandis, S. N.: Atmospheric Chemistry and Physics, From Air Pollution to Climate Change., New York, USA.1998.

Shaddick, G., Salter, J. M., Peuch, V.-H., Ruggeri, G., Thomas, M. L., Mudu, P., Tarasova, O., Baklanov, A., and Gumy, S.: Global air quality: An inter-disciplinary approach to exposure assessment for burden of disease analyses, Atmosphere, 12, 48, 2020.

Shrivastava, M. K., Lane, T. E., Donahue, N. M., Pandis, S. N., and Robinson, A. L.: Effects of gas particle partitioning and aging of primary emissions on urban and regional organic aerosol concentrations, Journal of Geophysical Research: Atmospheres, 113, 2008.

Sič, B., El Amraoui, L., Marécal, V., Josse, B., Arteta, J., Guth, J., Joly, M., and Hamer, P.: Modelling of primary aerosols in the chemical transport model MOCAGE: Development and evaluation of aerosol physical parameterizations, Geoscientific Model Development, 8, 381-408, 2015.

Silibello, C., Calori, G., Brusasca, G., Giudici, A., Angelino, E., Fossati, G., Peroni, E., and Buganza, E.: Modelling of PM10 concentrations over Milano urban area using two aerosol modules, Environmental Modelling & Software, 23, 333-343, 2008.

Silver, J. D., Christensen, J. H., Kahnert, M., Robertson, L., Rayner, P. J., and Brandt, J.: Multi-species chemical data assimilation with the Danish Eulerian hemispheric model: system description and verification, Journal of Atmospheric Chemistry, 73, 261-302, 2016.

Simpson, D., Benedictow, A., and Darras, S.: The CAMS soil emissions: CAMS-GLOB-SOIL, in: CAMS2_61 – Global and European emission inventories., 59–70, https://doi.org/10.24380/q2si-ti6i, 2023.

Simpson, D., Guenther, A., Hewitt, C., and Steinbrecher, R.: Biogenic emissions in Europe 1. Estimates and uncertainties, J. Geophys. Res., 100, 22875–22890, 1995.

Simpson, D., Fagerli, H., Jonson, J., Tsyro, S., Wind, P., and Tuovinen, J.-P.: The EMEP Unified Eulerian Model. Model Description, The Norwegian Meteorological Institute, EMEP, Oslo, 2003.

Simpson, D., Bergström, R., Briolat, A., Imhof, H., Johansson, J., Priestley, M., and Valdebenito, A.: GenChem v1. 0–a chemical pre-processing and testing system for atmospheric modelling, Geoscientific Model Development, 13, 6447-6465, 2020a.

Simpson, D., Benedictow, A., Berge, H., Bergstrom, R., Emberson, L. D., Fagerli, H., Flechard, C. R., Hayman, G. D., Gauss, M., Jonson, J. E., Jenkin, M. E., Nyiri, A., Richter, C., Semeena, V. S., Tsyro, S., Tuovinen, J. P., Valdebenito, A., and Wind, P.: The EMEP MSC-W chemical transport model - technical description, Atmos. Chem. Phys., 12, 7825-7865, 2012.

Simpson, D., Fagerli, H., Colette, A., Denier van der Gon, H., Dore, C., Hallquist, M., Hansson, H.-C., Maas, R., Rouil, L., Allemand, N., Bergström, B., Bessagnet, B., Couvidat, F., El Haddad, I., Genberg Safont, J., Goile, F., Grieshop, A., Fraboulet, I., Hallquist, A., Hamilton, J., Juhrich, K., Klimont, Z., Kregar, Z., Mawdsely, I., Megaritis, A., Ntziachristos, L.,

Pandis, S., Prévôt, A. S. H., Schindlbacher, S., Seljeskog, M., Sirina-Leboine, N., Sommers, J., and Åström, S.: How should condensables be included in PM emission inventories reported to EMEP/CLRTAP?, EMEP, Oslo, 2020b.

Sindelarova, K., Granier, C., Bouarar, I., Guenther, A., Tilmes, S., Stavrakou, T., Müller, J. F., Kuhn, U., Stefani, P., and Knorr, W.: Global data set of biogenic VOC emissions calculated by the MEGAN model over the last 30 years, Atmos. Chem. Phys., 14, 9317-9341, 10.5194/acp-14-9317-2014, 2014.

Slinn, W., Hasse, L., Hicks, B., Hogan, A., Lal, D., Liss, P., Munnich, K., Sehmel, G., and Vittori, O.: Some aspects of the transfer of atmospheric trace constituents past the air-sea interface, Atmospheric Environment (1967), 12, 2055-2087, 1978.

Slinn, W. G. N.: Precipitation scavenging, US. Department of Energy, Washington, D.C., 1983.

Smagorinsky, J.: General circulation experiments with the primitive equations: I. The basic experiment, Monthly weather review, 91, 99-164, 1963.

Soares, J., Sofiev, M., Geels, C., Christensen, J. H., Andersson, C., Tsyro, S., and Langner, J.: Impact of climate change on the production and transport of sea salt aerosol on European seas, Atmospheric Chemistry and Physics, 16, 13081-13104, 2016.

Sofiev, M.: A model for the evaluation of long-term airborne pollution transport at regional and continental scales, Atmospheric Environment, 34, 2481-2493, 2000.

Sofiev, M.: Extended resistance analogy for construction of the vertical diffusion scheme for dispersion models, Journal of Geophysical Research: Atmospheres, 107, ACH 10-11-ACH 10-18, 2002.

Sofiev, M.: On possibilities of assimilation of near-real-time pollen data by atmospheric composition models, Aerobiologia, 35, 523-531, 2019.

Sofiev, M., Galperin, M., and Genikhovich, E.: Construction and evaluation of Eulerian dynamic core for the air quality and emergency modelling system SILAM

NATO Science for peace and security, Series C: Environmental Security, Air pollution modelling and its application, XIX, Springer, 699-701 pp.2008.

Sofiev, M., Genikhovich, E., Keronen, P., and Vesala, T.: Diagnosing the surface layer parameters for dispersion models within the meteorological-to-dispersion modeling interface, Journal of applied meteorology and climatology, 49, 221-233, 2010.

Sofiev, M., Soares, J., Prank, M., de Leeuw, G., and Kukkonen, J.: A regional-to-global model of emission and transport of sea salt particles in the atmosphere, J. Geophys. Res., 116, doi:10.1029/2010JD014713, 2011.

Sofiev, M., Vira, J., Kouznetsov, R., Prank, M., Soares, J., and Genikhovich, E.: Construction of an Eulerian atmospheric dispersion model based on the advection algorithm of M. Galperin: dynamic cores v. 4 and 5 of SILAM v. 5.5, Geoscientific Model Development Discussions, 8, 2015a.

Sofiev, M., Siljamo, P., Ranta, H., Linkosalo, T., Jaeger, S., Rasmussen, A., Rantio-Lehtimaki, A., Severova, E., and Kukkonen, J.: A numerical model of birch pollen emission and dispersion in the atmosphere. Description of the emission module, International journal of biometeorology, 57, 45-58, 2013.

Sofiev, M., Berger, U., Prank, M., Vira, J., Arteta, J., Belmonte, J., Bergmann, K. C., Chéroux, F., Elbern, H., Friese, E., Galan, C., Gehrig, R., Khvorostyanov, D., Kranenburg, R., Kumar, U., Marécal, V., Meleux, F., Menut, L., Pessi, A. M., Robertson, L., Ritenberga, O., Rodinkova, V., Saarto, A., Segers, A., Severova, E., Sauliene, I., Siljamo, P., Steensen, B. M., Teinemaa, E., Thibaudon, M., and Peuch, V. H.: MACC regional multi-model ensemble simulations of birch pollen dispersion in Europe, Atmos. Chem. Phys., 15, 8115-8130, 10.5194/acp-15-8115-2015, 2015b.

Sofieva, S., Asmi, E., Atanasova, N. S., Heikkinen, A. E., Vidal, E., Duplissy, J., Romantschuk, M., Kouznetsov, R., Kukkonen, J., and Bamford, D. H.: Effects of temperature and salinity on sea-spray-aerosol formation simulated with a bubble-generating chamber, Atmospheric Measurement Techniques Discussions, 2022, 1-40, 2022.

Spada, M.: Development and evaluation of an atmospheric aerosol module implemented within the NMMB/BSC-CTM, 2015.

Spada, M., Jorba, O., Pérez García-Pando, C., Janjic, Z., and Baldasano, J. M.: Modeling and evaluation of the global sea-salt aerosol distribution: sensitivity to size-resolved and sea-surface temperature dependent emission schemes, Atmos. Chem. Phys., 13, 11735-11755, 10.5194/acp-13-11735-2013, 2013.

Stadtler, S., Simpson, D., Schröder, S., Taraborrelli, D., Bott, A., and Schultz, M.: Ozone impacts of gas–aerosol uptake in global chemistry transport models, Atmospheric Chemistry and Physics, 18, 3147-3171, 2018.

Stockwell, W. R., Kirchner, F., Kuhn, M., and Seefeld, S.: A new mechanism for regional atmospheric chemistry modeling, Journal of Geophysical Research: Atmospheres, 102, 25847-25879, 1997.

Strand, A. and Hov, O.: A two-dimensional global study of tropospheric ozone production, J Geophys Res 99, 22877-22895, 1994.

Struzewska, J. and Kaminski, J.: Formation and transport of photooxidants over Europe during the July 2006 heat wave–observations and GEM-AQ model simulations, Atmospheric Chemistry and Physics, 8, 721-736, 2008.

Struzewska, J. and Kaminski, J.: Impact of urban parameterization on high resolution air quality forecast with the GEM–AQ model, Atmospheric Chemistry and Physics, 12, 10387-10404, 2012.

Struzewska, J., Kaminski, J., and Jefimow, M.: Application of model output statistics to the GEM-AQ high resolution air quality forecast, Atmospheric Research, 181, 186-199, 2016.

Struzewska, J., Zdunek, M., Kaminski, J., Łobocki, L., Porebska, M., Jefimow, M., and Gawuc, L.: Evaluation of the GEM-AQ model in the context of the AQMEII Phase 1 project, Atmospheric Chemistry and Physics, 15, 3971-3990, 2015.

Szymankiewicz, K., Kaminski, J. W., and Struzewska, J.: Interannual variability of tropospheric NO 2 column over Central Europe—Observations from SCIAMACHY and GEM-AQ model simulations, Acta Geophysica, 62, 915-929, 2014.

Thürkow, M., Kirchner, I., Kranenburg, R., Timmermans, R., and Schaap, M.: A multi-meteorological comparison for episodes of PM10 concentrations in the Berlin agglomeration area in Germany with the LOTOS-EUROS CTM, Atmospheric Environment, 244, 117946, 2021.

Tie, X., Madronich, S., Walters, S., Zhang, R., Rasch, P., and Collins, W.: Effect of clouds on photolysis and oxidants in the troposphere, Journal of Geophysical Research: Atmospheres, 108, 2003.

Timmermans, R., van Pinxteren, D., Kranenburg, R., Hendriks, C., Fomba, K., Herrmann, H., and Schaap, M.: Evaluation of modelled LOTOS-EUROS with observational based PM10 source attribution, Atmospheric Environment: X, 14, 100173, 2022.

Troen, I. and Mahrt, L.: A simple model of the atmospheric boundary layer: Sensitivity to surface evaporation, Bound.-Layer Meteorol., 37, 129-148, 1986.

Tsyro, S., Aas, W., Soares, J., Sofiev, M., Berge, H., and Spindler, G.: Modelling of sea salt concentrations over Europe: key uncertainties and comparison with observations, Atmos. Chem. Phys., 11, 10367–10388, doi:10.5194/acp-11-10367-2011, 2011.

Tuovinen, J.-P., Ashmore, M., Emberson, L., and Simpson, D.: Testing and improving the EMEP ozone deposition module, Atmos. Environ., 38, 2373–2385, 2004.

van Leer, B.: Multidimensional explicit difference schemes for hyperbolic conservation laws, in: Computing Methods in Applied Sciences and Engineering VI, edited by: Lions, R. G. a. J. L., Elsevier, Amsterdam, 1984.

Van Ulden, A. and Holtslag, A.: Estimation of atmospheric boundary layer parameters for diffusion applications, Journal of Applied Meteorology and Climatology, 24, 1196-1207, 1985.

Van Zanten, M., Sauter, F., RJ, W. K., Van Jaarsveld, J., and Van Pul, W.: Description of the DEPAC module: Dry deposition modelling with DEPAC_GCN2010, RIVM rapport 680180001, 2010.

Vautard, R., Bessagnet, B., Chin, M., and Menut, L.: On the contribution of natural Aeolian sources to particulate matter concentrations in Europe: Testing hypotheses with a modelling approach, Atmospheric Environment, 39, 3291-3303, https://doi.org/10.1016/j.atmosenv.2005.01.051, 2005.

Venkatram, A.: Estimating the Monin-Obukhov length in the stable boundary layer for dispersion calculations, Boundary-Layer Meteorology, 19, 481-485, 1980.

Venkatram, A. and Pleim, J.: The electrical analogy does not apply to modelling dry deposition of particles, Atmos. Environ., 33, 3075-3076, 1999.

Venkatram, A., Karamchandani, P., and Misra, P.: Testing a comprehensive acid deposition model, Atmospheric Environment (1967), 22, 737-747, 1988.

Vira, J. and Sofiev, M.: On variational data assimilation for estimating the model initial conditions and emission fluxes for short-term forecasting of SOx concentrations, Atmospheric environment, 46, 318-328, 2012.

Vira, J. and Sofiev, M.: Assimilation of surface NO 2 and O 3 observations into the SILAM chemistry transport model, Geoscientific Model Development, 8, 191-203, 2015.

Wang, X., Zhang, L., and Moran, M. D.: Development of a new semi-empirical parameterization for below-cloud scavenging of size-resolved aerosol particles by both rain and snow, Geoscientific Model Development, 7, 799-819, 2014.

Weaver, A. and Courtier, P.: Correlation modelling on the sphere using a generalized diffusion equation, Quarterly Journal of the Royal Meteorological Society, 127, 1815-1846, 2001.

Wesely, M. L.: Parameterization of surface resistances to gaseous dry deposition in regional-scale numerical models, Atmospheric Environment (1967), 23, 1293-1304, 1989.

Wild, O., Zhu, X., and Prather, M. J.: Fast-J: Accurate Simulation of In- and Below-Cloud Photolysis in Tropospheric Chemical Models, Journal of Atmospheric Chemistry, 37, 245-282, 10.1023/A:1006415919030, 2000.

Williams, E., Guenther, A., and Fehsenfeldi, F.: An inventory of nitric oxide emissions from soils in the United States, Journal of Geophysical Research: Atmospheres, 97, 7511-7519, 1992.

Williamson, D. L. and Rasch, P. J.: Two-dimensional semi-Lagrangian transport with shape-preserving interpolation, Monthly Weather Review, 117, 102-129, 1989.

Willis, P. T. and Tattelman, P.: Drop-size distributions associated with intense rainfall, Journal of Applied Meteorology and Climatology, 28, 3-15, 1989.

Xian, P., Reid, J. S., Hyer, E. J., Sampson, C. R., Rubin, J. I., Ades, M., Asencio, N., Basart, S., Benedetti, A., and Bhattacharjee, P. S.: Current state of the global operational aerosol multi-model ensemble: An update from the International Cooperative for Aerosol Prediction (ICAP), Quarterly Journal of the Royal Meteorological Society, 145, 176-209, 2019.

Yamartino, R., Scire, J., Carmichael, G., and Chang, Y.: The CALGRID mesoscale photochemical grid model—I. Model formulation, Atmospheric Environment. Part A. General Topics, 26, 1493-1512, 1992.

Yamartino, R. J., Flemming, J., and Stern, R.: Adaptation of analytic diffusivity formulations to Eulerian grid model layers of finite thickness, in: Air Pollution Modeling and Its Application XVII, Springer, 468-477, 2007.

Yarwood. G., Rao, S., Yocke, M., and Whitten, G. Z.: Updates to the Carbon Bond chemical mechanism: CB05, http://www.camx.com/publ/pdfs/CB05_Final_Report_120805.pdf, 2005.

Yienger, J. and Levy, H.: Empirical model of global soil-biogenic NOx emissions, Journal of Geophysical Research: Atmospheres, 100, 11447-11464, 1995.

Yuan, H., Dai, Y., Xiao, Z., Ji, D., and Shangguan, W.: Reprocessing the MODIS Leaf Area Index Products for Land Surface and Climate Modelling, Remote Sensing of Environment, 155, 1171–1187, doi:10.1016/j.rse.2011.01.001, 2011.

Zare, A., Christensen, J., Irannejad, P., and Brandt, J.: Evaluation of two isoprene emission models for use in a long-range air pollution model, Atmospheric Chemistry and Physics, 12, 7399-7412, 2012.

Zare, A., Christensen, J., Gross, A., Irannejad, P., Glasius, M., and Brandt, J.: Quantifying the contributions of natural emissions to ozone and total fine PM concentrations in the Northern Hemisphere, Atmospheric Chemistry and Physics, 14, 2735-2756, 2014.

Zender, C. S., Bian, H., and Newman, D.: Mineral Dust Entrainment and Deposition (DEAD) model: Description and 1990s dust climatology, Journal of Geophysical Research: Atmospheres, 108, 10.1029/2002jd002775, 2003.

Zhang, K. M., Knipping, E. M., Wexler, A. S., Bhave, P. V., and Tonnesen, G. S.: Size distribution of sea-salt emissions as a function of relative humidity, Atmospheric Environment, 39, 3373-3379, https://doi.org/10.1016/j.atmosenv.2005.02.032, 2005.

Zhang, L., Brook, J. R., and Vet, R.: A revised parameterization for gaseous dry deposition in air-quality models, Atmos. Chem. Phys., 3, 2067–2082, 2003.

Zhang, L., Gong, S., Padro, J., and Barrie, L.: A size-segregated particle dry deposition scheme for an atmospheric aerosol module, Atmospheric Environment, 35, 549-560, 2001.

Zhang, Y., Bocquet, M., Mallet, V., Seigneur, C., and Baklanov, A.: Real-time air quality forecasting, part I: History, techniques, and current status, Atmospheric Environment, 60, 632-655, 2012a.

Zhang, Y., Bocquet, M., Mallet, V., Seigneur, C., and Baklanov, A.: Real-time air quality forecasting, part II: State of the science, current research needs, and future prospects, Atmospheric Environment, 60, 656-676, https://doi.org/10.1016/j.atmosenv.2012.02.041, 2012b.

Zilitinkevich, S. and Mironov, D. V.: A multi-limit formulation for the equilibrium depth of a stably stratified boundary layer, Boundary-Layer Meteorology, 81, 325-351, 1996.